UNIVERSIDAD AUTÓNOMA DE MADRID
DEPARTAMENTO DE BIOLOGÍA MOLECULAR
FACULTAD DE CIENCIAS

Mechanistic studies on Protein Kinase B regulation and insights for the discovery of potential allosteric kinase inhibitors

Deborah Balzano

Madrid, 2014

UNIVERSIDAD AUTÓNOMA DE MADRID
DEPARTAMENTO DE BIOLOGÍA MOLECULAR
FACULTAD DE CIENCIAS

Mechanistic studies on Protein Kinase B regulation and insights for the discovery of potential allosteric kinase inhibitors

Doctoral thesis submitted to the Universidad Autónoma de Madrid for the degree of PhD in Molecular Biosciences

Deborah Balzano
MSc, Molecular Biology

Thesis Director
Dr Daniel Lietha

Cell Signalling and Adhesion group
Structural Biology and Biocomputing Programme
Spanish National Cancer Research Centre

Dr. Daniel Lietha, head of the Cell Signalling and Adhesion Group in the Spanish National Cancer Research Centre (CNIO),

CERTIFIES

That Deborah Balzano, Master in Molecular Biology by the University of Milan, has completed her Doctoral Thesis **"Mechanistic studies on Protein Kinase B regulation and insights for the discovery of potential allosteric kinase inhibitors"** and meets the necessary requirements to obtain the PhD Degree in Molecular Biosciences. To this purpose, she will defend her Doctoral Thesis at the Universidad Autónoma de Madrid. The Thesis has been carried out under my direction and hereby I authorize it to be defended to the appropriate Thesis Tribunal.

I hereby issue this certificate in Madrid on September the 25th 2014.

Daniel Lietha, PhD
PhD Thesis Director

Catalina Ribas Núñez,
PhD Thesis Tutor

This thesis, submitted for the degree of Doctor of Philisophy at the Universidad Autónoma de Madrid, has been completed in the Cell Signalling and Adhesion Group at the Spanish National Cancer Research Centre (CNIO), under the supervision of Dr. Daniel Lietha.

This work was supported by the following grants and fellowships:
La Caixa/CNIO International PhD Fellowship. 2010 call- Deborah Balzano
Proyecto BIPEDD2, Comunidad Autónoma de Madrid (CAM), Spain- Dr. Daniel Lietha

A MaPa

Ad Albi

Acknowledgements

First, I would like to thank Daniel to give the opportunity of being his first PhD student and give me a chance to work with him. I also thank all the present and past members of the Cell Signalling and Adhesion group.

Thank to all the members of the Structural Bases of Genome Integrity group and of the Macromolecular crystallography group for their support and advices during these four years.

Un grazie speciale ai miei genitori e ad Alberto per esserci sempre, nonostante la distanza. Senza il vostro costante sostegno, non sarei riuscita a portare a termine questa esperienza, a tratti faticosa.

Abstract

Signal transduction into the cell occurs through cell surface receptors, which specifically recognize extracellular messengers and then further transmit the signal to intracellular molecules. In the complex system of communication pathways that governs the behaviour of the cell, growth factor and cell adhesion signalling tightly and cooperatively cross talk to provide crucial stimuli for the regulation of important cellular functions, such as cell proliferation, survival and migration. Signalling proteins need to be strictly controlled to prevent the rise of pathologies, like cancer and metabolic diseases. In our studies we focused on two kinases that belong to different family: Protein Kinase B (PKB) and Focal Adhesion Kinase (FAK). They are both key signalling molecules, PKB is activated downstream of growth factor-induced PI3K signalling, and FAK downstream of integrin cell- matrix adhesion receptors; both have been reported as attractive drug targets. Based on a detailed biochemical analysis, we propose a model of how the different PKB domains modulate the signalling output. Our results suggest that PKB can follow two distinct activation pathways depending on the nature of the upstream signal. Furthermore, we propose that PKB targets specific substrates depending on the activation pathway. Such new insights on PKB regulation and substrate specificity could allow the interpretation of the effects of different classes of PKB inhibitors and enable the design of inhibitors with improved specificity. Moreover, we performed a screening of fragments-like compounds (<300 Da), interacting with allosteric pockets on the FERM domain of FAK. Crystal structures of FERM in complex with these fragments have been solved and structural data for two positive fragment hits have been obtained. The collected structural information will guide the strategy and design of extended compounds that potentially can be developed into allosteric inhibitors.

Presentación

Los factores de crecimiento y la señalización de adherencia celular se comunican estrechamente para proporcionar el estímulo necesario para la regulación de importantes funciones celulares como la proliferación, la supervivencia y la migración. Los factores de crecimiento son moléculas importantes para la transmisión de señales desde el exterior de la célula hacia su interior. Cuando los receptores transmembrana reciben una señal, la transmiten a mensajeros intracelulares. Las integrinas son receptores de adhesión que median en la interacción entre los componentes de la matriz extracelular (ECM), favoreciendo la transmisión de señales desde el espacio extracelular a la célula, a través de proteínas de señalización y proteínas adaptadoras asociadas a las integrinas. Las proteínas de señalización necesitan ser estrictamente controladas para impedir la aparición de patologías como el cáncer y las enfermedades metabólicas. En este trabajo nos hemos centrado en estudio de dos kinasas, pertenecientes a diferentes familias: Proteína Kinasa B (PKB) y Kinasa de Adhesión Focal (FAK). Se trata de dos moléculas de señalización claves, PKB se activa mediante la vía de señalización inducida por el factor de crecimiento PI3K, y FAK mediante la de los receptores de adhesión de integrinas a la matriz celular; ambas son atractivas dianas farmacológicas. Basándonos en un detallado análisis bioquímico, hemos propuesto un modelo según el cual los diferentes dominios de PKB modulan la señalización hacia abajo. Nuestros resultados sugieren que PKB puede seguir dos vías diferentes de activación, dependiendo de la naturaleza de la señal hacia arriba. Además, proponemos que PKB modula sustratos específicos dependiendo de la vía de activación. Esta novedosa información en la regulación de PKB y en su tendencia en modular de manera específica sus substratos podría facilitar la interpretación de los efectos de las diferentes clases de inhibidores disponibles para PKB y ayudar en el diseño de nuevos inhibidores de especificidad mejorada. Además, hemos examinado la interacción de compuestos de pequeño tamaño (<300 Dalton) con los bolsillos alostéricos del dominio FERM de FAK. Las estructuras cristalinas de FERM en complejo con estos fragmentos aportan datos estructurales interesantes para dos de ellos, que nos orientaran hacia la estrategia y el diseño de compuestos que podrían ser desarrollados como inhibidores alostéricos.

Table of contents

Abbreviations

ABL	Abelson oncogene
ATP	Adenosine triphosphate
BCR	Breakpoint Cluster Region
BSA	Bovin Serum Albumin
CD	Circular dicroism
DNA	Deoxyribonucleic acid
cDNA	Complementary DNA
DNA-PK	DNA Protein Kinase
dNTAPs	deoxyribonucleotide triphosphates
DTT	Dithiothreitol
E.coli	*Escherichia coli*
EDTA	Ethylenediaminetetracetic acid
ECM	Extracellular matrix
EGFR	Epidermal Growth Factor receptor
EGTA	Ethylene Glycol Tetraacetic acid
ELISA	Enzyme-linked Immunosorbent assay
FAK	Focal Adhesion Kinase
FAT	Focal adhesion targeting
FERM	4.1, ezrin, radixin, moesin homology motif
FOXO	Forkhead box transcription factor class O
FP	Fluorescent Polarization
GSK3	Glycogen synthase kinase-3
GST	Glutathione S-transferases
HM	Hydrophobic motif
ILK	Interleukin
IPTG	Isopropyl β-D-1-thiogalactopyranoside
kb	kilo bases
kDa	kilo Dalton

Km	Michaelis-Menten constant
LB	Luria- Bertani media
LDH	Lactose dehidrogenase
MW	Molecular weight
NMR	Nuclear Magnetic Resonance
OD	Optical Density
p27	Protein 27
PAGE	Polyacrylamide Gel Electrophoresis
PDB	Protein Data Base
PDK1	Phosphoinositide-dependent kinase-1
PH	Pleckstrin homology
PI3K	Phosphoinositide 3-Kinase
PIP_2	Phosphatidylinositol bisphosphate
PIP_3	Phosphatidylinositol trisphosphate
PK	Pyruvate kinase
PKB	Protein Kinase B
PTB	Phosphotyrosine binding
Rpm	Revolution per minute
RTK	Receptor tyrosine kinase
SDS	Sodium dodecyl sulfate
SPR	Surface Plasmon Resonance
TSC2	Tuberous sclerosis complex 2
wt	*wild type*

Introduction

1.1 Cell signalling: the communication network of the cell

Mechanisms enabling one cell to influence the behaviour of another have been vital already in the world of unicellular organisms as confirmed by studies of present-day unicellular eukaryotes such as yeast. In fact, yeast cells communicate with one another for mating by secreting a small number of small peptides (Gibeaux R. & Knop M, 2013). In contrast, cells in multicellular organisms communicate by means of hundreds of kind of signal molecules, including proteins, small peptides, amino acids, nucleotides, steroids, retinoids, fatty acid derivatives, and even dissolved gases such as nitric oxide and carbon monoxide (Bukoreshtliev N.V *et al*, 2013). Every aspect of cellular function within a multicellular organism, including proliferation, metabolism, gene expression, cytoskeleton organisation and cell survival, is dependent on external signalling molecules and it must be closely regulated to avoid disorders in these fundamental properties of the cell (Pawson T. *et al*, 2000).

1.1.1 The importance of specificity in signal transduction

The mechanisms by which a wide variety of messages, in form of growth factors, hormones and cytokines, are conveyed to their targets in the cytoplasm and nucleus have been an object of study over the last four decades. Regardless of the nature of the signal, this is a problem of molecular recognition between the signalling molecules and the cell surface receptors, specific proteins of the target cells. In fact, extracellular signals bind selectively to their membrane receptors, which initiate a characteristic cascade of reactions within the cell (Pawson T. *et al*, 1997). Based on their primary signal transduction mechanism, we consider three broad classes of signalling receptors: ligand ion-channel, G-protein linked receptors (GPLRs) and the protein kinase-linked receptors. The ligand-gated ion-channels transiently open or close when activated, resulting in highly selective changes in ionic flux (Shupeng L. *et al*, 2014). GPLRs are non-covalently bound to heterotrimeric GTP-binding proteins (G proteins), which mediate the interaction between the receptor and

the target protein that can be an enzyme or an ion channel. G proteins act as molecular switches by binding GTP (ON state) and then hydrolysing the terminal phosphoester bond to leave GDP (OFF state) (Hamm & Gilchrist, 1996). The protein kinase-linked receptors are a large family of cell surface receptors and play significant roles in virtually every type of cell to promote growth, proliferation, differentiation and survival. The most numerous of this type of receptors are the receptor tyrosine kinase (RTK), like the epidermal growth factor receptor (EGFR), currently one of the best characterized (Hsuan J.J & Khoon Tan S, 1997). Upon binding to their ligands, RTK molecules dimerize and undergo autophosphorylation on specific tyrosine residues. In turn, they phosphorylate intracellular proteins, inducing a cascade of intracellular pathways that trasduce a unique biological response, through the interaction of specific cytoplasmic targets (Madhani H D, 2001).

The propagation of the signal from the cell surface receptors to the cytoplasm and nucleus is guarantee by the activation of key intracellular signalling proteins, under a highly controlled integration of the signal transduction. Two major mechanisms of signal integration in eukaryotic cells are protein phosphorylation and dephosphorylation, mediated by the activity of protein kinases and protein phosphatases. Signal integration can be achieved through the phosphorylation of protein that control the levels of second messangers, through the phosphorylation of protein kinases and phosphatases themselves or through reversible phosphorylation of their substrate (Cohen P, 1992).

Signal transduction is complicated by the fact that different biochemical pathways use the same intracellular effectors to control cellular behaviour. Therefore, an evolutionary-suitable way to refine the signalling network was to use modular protein domains and recognition motifs, through which specificity is generated during signal transduction. (Schlessinger J, 2000). There are different modules that promote specific interactions of intracellular signalling proteins and transmembrane receptors with other proteins, phospholipids, or nucleic acids. The combination of one or more modular protein domains allows variations in binding interfaces to generate new specificities. Examples of modules are the Src-Homology 2 domain (SH2), which mediate the docking of

intracellular proteins at specific sites in response to tyrosine phosphorylation (Eck *et al*, 1993), and the Pleckstrin-Homology domain (PH) that bind charged headgroups of specific polyphosphoinositides, promoting the subcellular targeting of signalling proteins to specific regions of the plasma membrane (Yoon *et al*, 1994).

A molecular understanding of the signalling pathways employed by each type of cell surface receptor is therefore essential to learn about many cellular functions and, consequently, to treat efficiently diseases caused by breakdowns in the signalling process, by targeting specifically the malfunctioning signalling molecules (Hsuan J.J & Khoon Tan S, 1997).

1.2 Growth and Adhesion signalling

In the intricate network of signalling pathways inside the cell, we focused our interest on growth factor and cell adhesion induced-signals, which both provide crucial stimuli for cell proliferation, survival and migration. As already mentioned, growth factors are important molecules for signal transduction into the cell through transmembrane receptors, like the RTK, that then further mediate the signal via intracellular messengers. On the other hand, at the level of the focal adhesion, point of contact between the cell surface and extracellular matrix (ECM) components, the integrin family of adhesion receptors mediate the intracellular signal propagation of the extracellular cues. (Ridley *et al*, 2003). Integrins are heterodimeric cell-surface molecules that on one side link the actin cytoskeleton to the cell membrane and on the other side mediate cell-matrix interactions. In addition to their structural function, they mediate signalling from the extracellular space into the cell through integrin-associated signalling and adaptors like FAK, ILK and PINCH (Hanningan GE, et al, 1996). Via these molecules, integrin signalling tightly and cooperatively interacts with RTK signalling to regulate cell survival, proliferation, cell shape as well as polarity, adhesion migration and differentiation, and therefore needs to be strictly controlled. In fact, their deregulation leads to different pathologies like cancer and metabolic diseases (e.g. diabetes). Consequently, proteins associated to all the major signal

transduction pathways downstream these receptors are likely good drug target candidates in therapeutic approaches (Megison M.L *et al*, 2013). In the complex scenario of the cell-signalling transduction, we focus our interest on two protein kinases that belong to different families: Protein Kinase B (PKB) and Focal Adhesion Kinase (FAK). They are crucial effectors downstream growth factor receptors and integrin cell- matrix adhesion receptors respectively and they are both interesting drug target, since they are both protein kinases and they crucial regulator of fundamental cellular processes (Fig. 1.1).

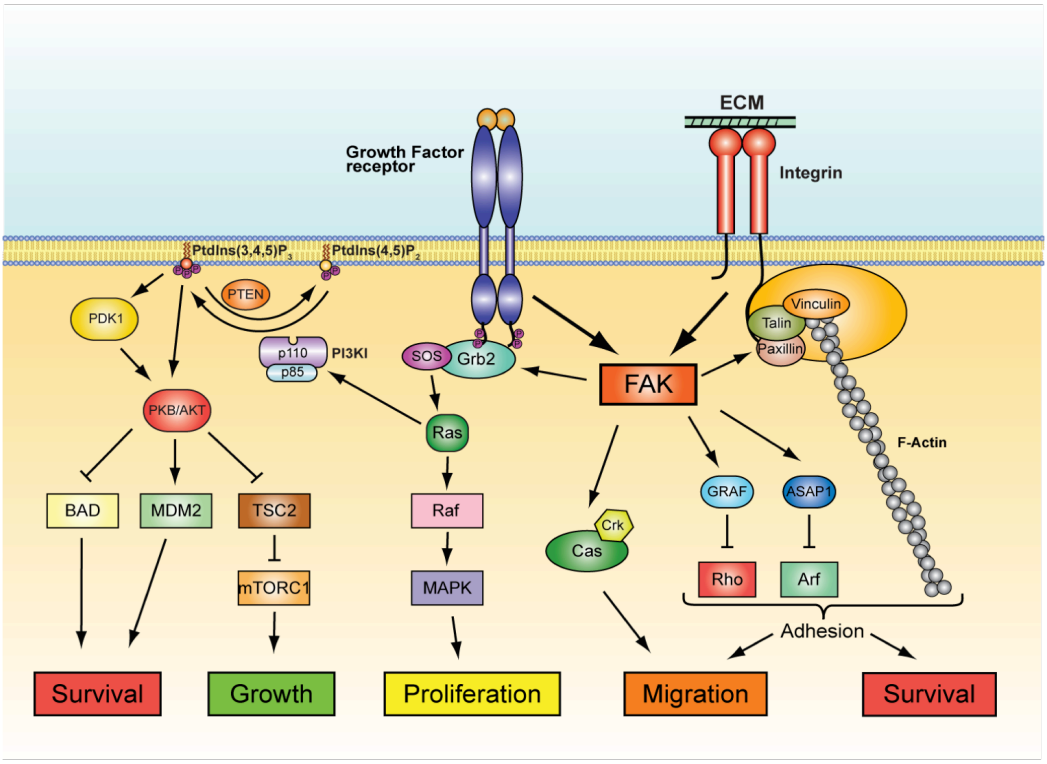

Fig.1.1- Schematic representation of the growth factor and adhesion signalling pathways. Cooperative integrin-RTK signalling determines survival, proliferation, differentiation and apoptosis of cell by a cascade of downstream signals. Kinase activity of PI3K is Ras-dependent and leads to the activation of PKB parthway by increasing the intracellular concentration of PIP_3. Upon cell attachment via integrins to the ECM, FAK is localised to focal adhesions through binding to paxillin, linking integrin receptors to intracellular signalling pathways. Furthermore FAK plays a role in connecting the integrins and growth factors receptors pathways.

1.3 Protein kinases in cell signalling

Protein phosphorylation is one of the major mechanisms of signal integration in eukaryotic cells and consists in transfer phosphate groups from donor molecules at high energy, like ATP and its derivatives. The phosphorylation of a substrate can inhibits its activity or allow its binding to other proteins, carrying domain which recognized phosphorylates residue of Ser, Thr and Tyr. In fact, phosphorylation of Ser, Thr and Tyr residues can trigger conformational changes in regulated proteins, which alter their properties and start a controlled physiological response (Adams JA & Taylor SS, 1995)

Phosphorylation process is achieved by the activity of a specific family of enzymes, the protein kinases, also known as phosphotrasferase. All kinases require a metal ion, like Mg^{2+} or Mn^{2+} in order to stabilize the high-energy bonds of the ATP, the donor molecule, and allow the phosphorylation reaction (Bossemeyer D. *et al*, 1993).

These proteins are classified in tyrosine, serine or threonine kinases, according to the substrate amino acid residue that is phosphorylated. As already mentioned, the spatial and temporal control of phosphorylation events is crucial to many cellular processes, including metabolism, transcription, cell cycle progression, cytoskeleton rearrangement, cellular movement, apoptosis and cell differentiation. Therefore, protein kinases play an important role in cell function and maintenance and this control relies on the proper regulation of protein kinases. Consequently, kinase activity in the wrong place or at the wrong time can lead to cell transformation and the rise of pathologies, such as cancer and diabetes (Rubin G M, et al, 2000).

1.3.1 The Kinome

Protein kinases represent the largest group of enzyme in nature. In fact, the human genome codes about 520 protein kinase genes (Hunter T, 1987). Although most of these genes are well characterized, a large number of genes code for proteins recognized more recently as kinases only after computational analysis. The part of the human genome that codes for protein kinases is commonly defined as the "kinome". The kinome is in continuous expansion, both for the discovery of additional genes and for potential protein variants, translated after splicing events (Milanesi L. *et al*, 2005). There are often several kinases able to phosphorylate the same substrate. Most protein kinases act in a network of kinase and other signal effectors of different nature, as their activity is modulated by autophosphorylation and phosphorylation by other kinases. (Reviewed in Manning G. *et al*, 2002). Protein kinases mutations and misregulation play a fundamental role in human pathogenesis, and their structural organisation and characteristics make them good targets in clinical therapies (Blume-Jensen P. & Hunter T, 2001).

1.3.2 Protein kinase structure and activity

Protein kinases show an extremely well conserved structural organisation among serine/threonine and tyrosine kinases, although they display high substrate specificity. In the structure of these enzymes (Fig. 1.2), we can recognize two lobes or subdomains. The smaller N-terminal lobe consists of a 5- stranded β sheet and one prominent α helix, called helix αC. On the other hand, the C-terminal lobe (C lobe) is larger and predominantly helical (Zheng *et al*, 1993). ATP is bound in a deep cleft between the two lobes and sits beneath a highly conserved loop for phosphate binding, the P loop (in yellow in Fig 1.2), connecting strands β1 and β2 (Johnson L N *et al*, 1998). The P loop contains a conserved glycine-rich sequence motif GXGXφG, where φ is usually tyrosine or phenylalanine. The glycine residues allow the loop to approach the phosphates of ATP very closely and to

coordinate them via backbone interactions, thanks to their low steric hindrance (Mohammadi et al., 1997). The glycine residues make the P loop very flexible in the absence of ATP, a fact that facilitates the binding of small molecule inhibitors. Some of these inhibitors induce large structural distortions in the loop by interacting with the conserved aromatic residue (Schindler et al., 2000).

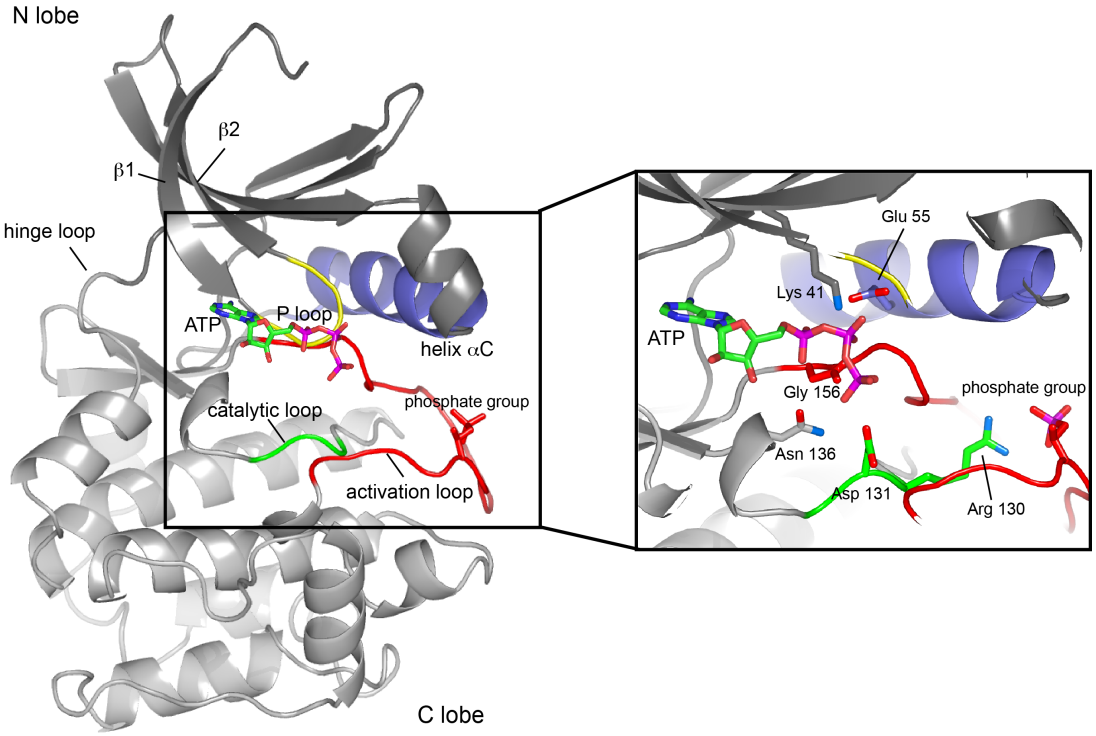

Fig.1.2- Casein Kinase 1δ (PDB code: 1CKI). Key structural elements conserved in protein kinases are highlighted. Activation loop in red, helix αC in blue, P loop in yellow, catalytic loop in green. In the zoom insert the binding pocket in complex with the ATP nucleotide and some highly conserved residues in the active site are shown. In anticlockwise there are: Gly156 of the DFG motif at the end of the activation loop; Glu55 of the helix αC; Lys41 of the N-terminal lobe; Asn136 which coordinates ATP and Mg^{2+}; Asp131 and Arg130 of the conserved HRD in the catalytic loop, where the arginine helps to coordinate ATP phosphate groups.

In the binding pocket, ATP interacts through the adenine ring, establishing hydrogen bonds with the kinase hinge, the connecting loop between the N- and the C-terminal lobe. Instead, the ATP ribose and triphosphate groups bind in a hydrophilic channel towards the binding site for the substrate, which is characterized of conserved aminoacids, essential for catalysis (review in Zhang J. *et al*, 2009). The correct transfer of the phosphate required a precise spatial disposition of some catalytic residues, conserved in all kinases (review in Huse M & Kuriyan J, 2002). Among them, there are an aspartate residue and an asparagine within the catalytic loop, a conserved structure at the bottom of the active site (Fig 1.2). The aspartate interacts with the substrate binding hydroxyl side chain, whereas the asparagine is involved in hydrogen bonds, which orient the above-mentioned aspartate (Hubbard *et al*, 1994). This asparagine residue is also required, together with another conserved residue of aspartate, for the binding with two bivalent cations (usually Mg^{2+}), involved in the recognition of the nucleotide. In the N lobe, there is a lysine residue, fundamental to place correctly the phosphate α and β groups during the catalysis. The lysine is buried in the cleft between the two lobes where it is itself stabilized and correctly oriented by ionic interactions with a glutamate residue of the helix αC (see insert in Fig 1.2). The peptide substrate binds in an extended conformation across the front end of the nucleotide-binding pocket, close to the γ-phosphate of ATP. All kinases have a centrally located and conserved loop, known as "activation loop", typically 20-30 residues in length (Fig1.2). It is an important element in kinase activity regulation and it is characterized by DFG and APE motif, respectively located at the beginning and at the end of the activation loop (reviewed in Zhang J. *et al*, 2009). The DFG motif structure, in particular the aspartic acid residue conformation, is closely connected to the phosphorylation of the activation loop, which stabilizes the loop itself in a open and extended conformation that allows the substrate binding (reviewed in Huse M et al, 2002). The localisation and the total number of the phosphorylation sites in the activation loop changes from kinase to kinase (Russo A A *et al*, 1996). Whereas the phosphorylated activation loop conformation is conserved, it can undertake a wide range of conformations in the unphosphorylated state. Protein

kinases are molecular switches that can adopt at least two extreme conformations: an "on" state that is maximally active, catalytically competent, where the activation loop is generally phosphorylated (Hubbard, 1997), and a "off" state, where the activation loop is not positioned for optimal substrate binding (Hubbard *et al*, 1994) (Fig. 1.3). An important element of the conformational changes in the catalytic site is the helix αC. This helix helps the formation of direct contacts between the activation loop and the N lobe, and its conformation is often DFG motif-dependent (Jeffrey *et al*, 1995- Xu *et al*, 1997).

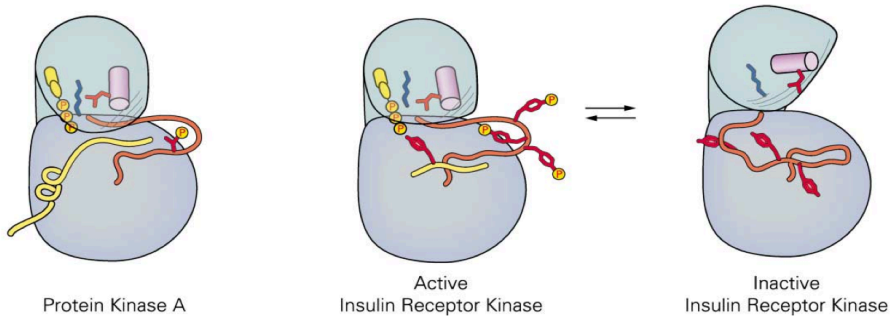

Fig.1.3- Active and Inactive conformations of the Protein Kinase Domain. The three structures schematize the conformational transitions involved in the regulation of kinase activity, with particular emphasis on the C helix and activation loop. The catalytic lysine and glutamate (Lys72 and Glu91 in PKA), which form a salt bridge in active kinase conformations, are shown in each schematic (adapted from Huse M. *et al*, 2002)

1.3.3 Protein kinase inhibitors

The ability of the protein kinase activation loop to adopt different conformational states when the enzyme is in a "off" state, has been recently used for important clinical benefits. Antitumoral drugs that target kinases, like Gleevec, are all small molecules able to bind to different kinase sites, either in the active or inactive conformation (Cohen P. 2002). The majority of the so far discovered inhibitors compete for the ATP binding and show from one to three hydrogen bonds with the amino acids residues in the hinge loop of

the target enzyme. In this way, the hydrogen bonds usually formed by the ATP adenine ring are mimicked (Traxler P *et al*, 1999). According to the inhibition mechanism followed, protein kinase inhibitors can be classified in: type I inhibitors, type II inhibitors, covalent inhibitors and allosteric inhibitors.

***Type I inhibitors*-** This type of inhibitors targets the ATP binding site in an active conformation of the kinase (Liu Y, 2006). They typically consist of a heterocyclic ring system. In active kinases, when the purine binding site assumes a "DFG-in" conformation, these inhibitors occupy the binding site at the level of the binding pocket hydrophobic regions, mimicking the ATP molecule (Fig. 1.4). By blocking the ATP binding, the activity of the enzyme is prevented (reviewed in Zhang J. *et al*, 2009).

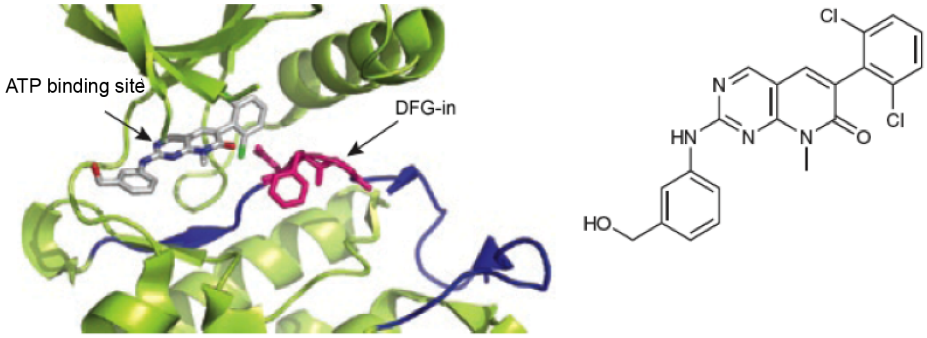

Fig.1.4- Representation of the kinase inhibition mechanism in presence of type I inhibitors. The activation loop takes a "DFG-in" conformation, in presence of PD166326 inhibitor bound to ABL1 (PDB code: 1OPK).

***Type II inhibitors*-** In this case, the inhibitors target an inactive conformation of the ATP binding site, known as "DFG-out" state, where the Asp side chain points out of the active site and the Phe blocks the access of ATP to the active site. Movement of the activation loop to the "DFG-out" conformation exposes an additional hydrophobic back-pocket, directly adjacent to the ATP binding site (Fig. 1.5). These compounds inhibit protein kinases, preventing ATP binding and stabilizing the inactive conformation of the

protein. Examples are Gleevec, Nilotinib (Manley P.W. *et al*, 2005), and Sorafenib (Wan P.T *et al*, 2004), inhibitors of ABL1, KIT, Ras and PDGFR.

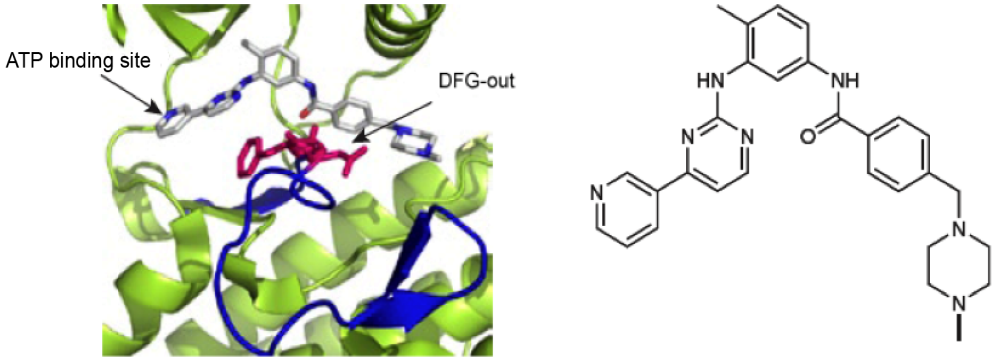

Fig.1.5- Representation of the kinase inhibition mechanism in presence of type II inhibitors. The activation looptakes a "DFG-out" conformation, in presence of Gleevec bound to ABL1 (PDB code: 1IEP).

***Covalent inhibitors*-** This type of inhibitors formsa covalent bond with the protein target, usually via cys sidechains, To date, inhibitors developed of this type occupy the ATP binding pocket like type I ones (Fig. 1.6). Covalently likned inhibitors block the ATP- kinase binding in an irreversible way, keeping the enzyme inactive (Cohen M.S. *et al*, 2005). Examples are the inhibitors 34-JAB, HKI-272 and CL-387785, specific for the Epidermal Growth Factor receptor (EGFR) (Fry D.W *et al*, 1994).

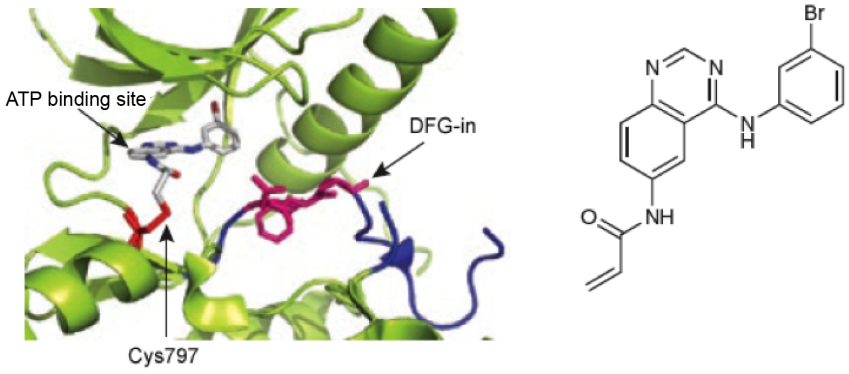

Fig.1.6- Representation of the kinase inhibition mechanism in presence of covalent inhibitors. The activation loop adopts a "DFG-in" conformation, in presence of the 6-acrylamide group of 34-JAB inhibitor in the active site of the epidermal growth factor receptor (PDB code: 2J5F).

Allosteric inhibitors- They bound outside the ATP binding site and modulate kinase activity in an allosteric manner (Fig 1.7). The best-characterized members of this class of inhibitors are CI- 1040 and PD334581, that inhibit MEK1 and MEK2 (Ohren J *et al*, 2004). Other examples are GNF2, Akti-1 and BMS-345541, respectively specific for BCR-ABL1, PKB and nuclear factor kB kinase (Adrian F.J *et al*, 2006 - Lindsley C.W *et al*, 2005- Mclntyre KW *et al*, 2003). Inhibitors that belong to this category tend to exhibit the highest degree of kinase selectivity because they exploit binding sites and regulatory mechanisms that are unique to a particular kinase. Allosteric inhibitors can bind far away from the ATP binding site or can occupy the ATP binding backpocket, if the DFG motif adopts an "out" conformation (reviewed in Zhang J. *et al*, 2009).

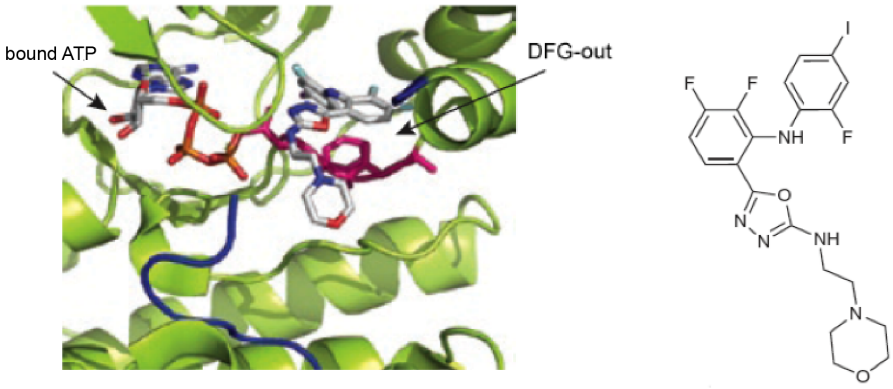

Fig.1.7- Representation of the kinase inhibition mechanism in presence of allosteric inhibitors. The activation loop undertakes a DFG "out" conformation, in presence of PD334581, bound to MEK2 (PDB code: 1S9I).

1.4 Protein Kinase B (PKB)

Protein Kinase B (PKB), also known as Akt, is a member of the serine/threonine AGC protein kinase family. Three highly homologous isoforms of PKB exist in mammals (PKB-α/Akt1, PKB-β/Akt2 and PKB-γ/Akt3), each of them containing an amino (N)-terminal pleckstrin homology (PH) domain, a kinase domain and a 21-amino acid carboxy (C)-terminal hydrophobic motif (HM) (Fig. 1.8). These three isoforms mainly differs on the tissue distribution. PKBα is widely distributed and is implicated in cell growth and survival (Chen W.S. *et al*, 2001), whereas PKBβ is highly expressed in muscle and adipocytes and contributes to insulin-mediated regulation of the glucose homeostasis (Garofalo et al, 2003). PKBγ, instead, is more restricted with expression mainly found in the testes and brain (Tschopp *et al*, 2005). PKB is a key-signalling molecule downstream of growth factor induced phosphoinositide 3-kinase (PI3K) signalling. Many growth factors and cytokines stimulate an increase in activity in the lipid enzyme PI3K, resulting in a subsequent increase in phosphatidylinositol 3,4 bisphosphate (PIP_2) and phosphatidylinositol 3,4,5 trisphosphate (PIP_3) in the cell (Bellacosa A. *et al*, 1998) Previous work has revealed that the 3-phosphoinositides interact with the PH domain of PKB, recruiting the kinase to the inner surface of the plasma membrane. Upon binding of PIP_3, PKB undergoes a conformational change where the PH domain changes the position relative to the kinase domain (Toker A & Newton A C, 2000). It has been shown that phosphoinositide-dependent kinase 1 (PDK1) directly activate PKB by phosphorylating T308 (PKBα numbering) in the activation loop (Alessi D. *et al*, 1997). To achieve full kinase activity, PKB needs to be phosphorylated at a second key residue, S473, which is located in the HM region. S473 is phoshorylated by members of the PI3K-releted kinase family, mTORC2 or DNA-PK, depending on the stimulus and the context (Sarbassov DD. *et al*, 2004). The contribution of Ser473 phosphorylation in the regulation of Thr308 phosphorylation, Akt activity and phosphorylation of downstream substrates is not yet

fully understood. Initial studies using alanine mutants showed that Akt Thr308 and Ser473 could be phosphorylated independently of each other (Alessi *et al*, 1996a).

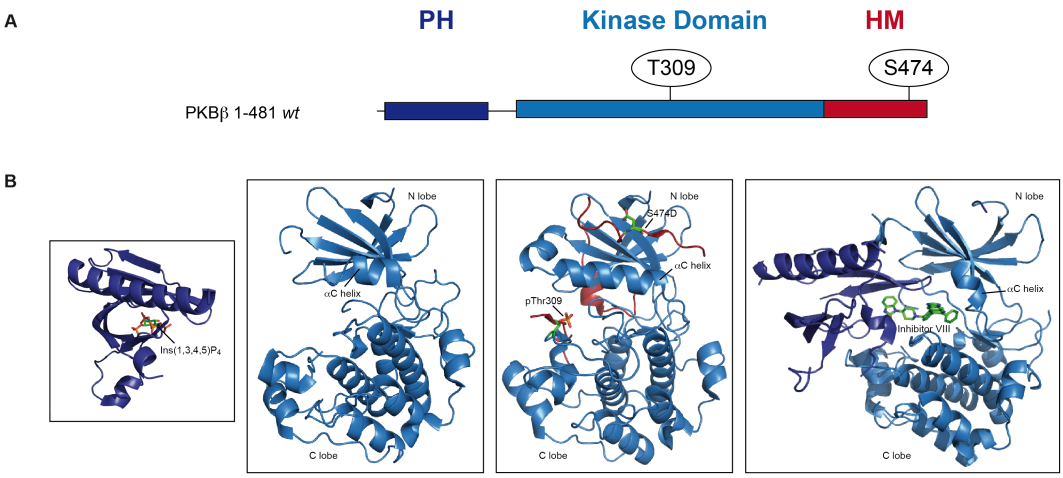

Fig.1.8- Domain structure of PKBβ isoform. A) PKBβ comprises three functional domains: an N-terminal PH domain, a central kinase domain, and a C-terminal hydrophobic motif (HM). The domain structure shown is highly conserved also in PKBα and PKBγ isoforms. B) Crystal structures available in literature for PKB are shown, adapted from Thomas C.C *et al*, 2002 (PDB code: 1H10), Yang J. *et al*, 2002a (PDB code: 1GZO), Yang J. *et al*, 2002b (PDB code: 1O6L) and Wu W. *et al*, 2010 (PDB code: 3O96).

1.4.1 PKB substrates

Upon Akt phosphorylation and activation, PKB dissociates from the membrane and translocates to the cytosol and nucleus, where it activates downstream signalling pathways through phosphorylation of a huge variety of substrates (reviewed in Hers I *et al*, 2011). In the large list of PKB cytoplasmic and nuclear targets, we include Bcl-2-associated death promoter (BAD), Forkhead box transcription factor class O (FOXO), Tuberous sclerosis complex 2 tumor suppressor (TSC2), Glycogen synthase kinase-3 (GSK3), and protein 27 (p27), also called Kip1. Phosphorylation by PKB can have various effects on protein substrates, including inhibiting or stimulating theirs activities, altering their subcellular localisation, protecting them against degradation or regulating binding to protein partners

(reviewed in Manning & Cantley, 2007). Within the different PKB targets, some can directly be related to specific cellular responses, even thought each physiological response downstream of PKB appears to be mediated by multiple targets (Fig. 1.9). For example, PKB promotes cell survival by blocking the function of proapoptotic proteins, such as BAD, and preventing the FOXO-mediated transcription of target genes that promote apoptosis and cell-cycle arrest (Brunet A, *et al* 2009). Furthermore, one of the best-conserved functions of PKB is its role in promoting cell growth through the phosphorylation-driven inhibition of TSC2, a critical negative regulator of mTORC1 signalling (Inoki K et al, 2002). Moreover, p27 phosphorylation by PKB prevents its nuclear localisation promoting cell proliferation (Liang J et al, 2002), whereas GSK3 phosphorylation inhibits GSK3, a regulatory kinase of Glycogen synthase (GS) (Cross et al, 1995).

PKB is, therefore, an important and versatile protein kinase at the core of the human physiology, due to its function in the regulation of important cellular processes, like the ones listed above. Aberrant regulation of the PKB pathway is implicated in the pathogenesis of different diseases, including several human cancers (Roy H.K *et al*, 2002), type-2 diabetes (Cho H *et al*, 2001) and cardiovascular and neurological diseases (Shiojima I *et al*, 2002- Datta S *et al*, 1997). Hence, PKB is therefore considered an important drug target and several small molecule inhibitors of PKB have been developed to date. In fact, different sites on the PKB provide functionally important regions suitable for binding ATP-competitive, allosteric, substrate competitive inhibitors as well as inhibitors of PIP_3 binding, but most of them are lacking sufficient selectivity (reviewed Lindsley *et al*, 2010).

Although, the mechanism by which PKB is activated has heavily been studied using cell biology experiments, there are still open questions, mainly about how mechanistically all the regulatory mechanisms act together to control PKB activity, membrane association, release upon full activation and how the regulatory elements of PKB can lead to substrate specificity. Therefore, new insight on PKB regulation and structure could allow the

interpretation of the effects of different classes of PKB inhibitors and enable the design of inhibitors with improved selectivity.

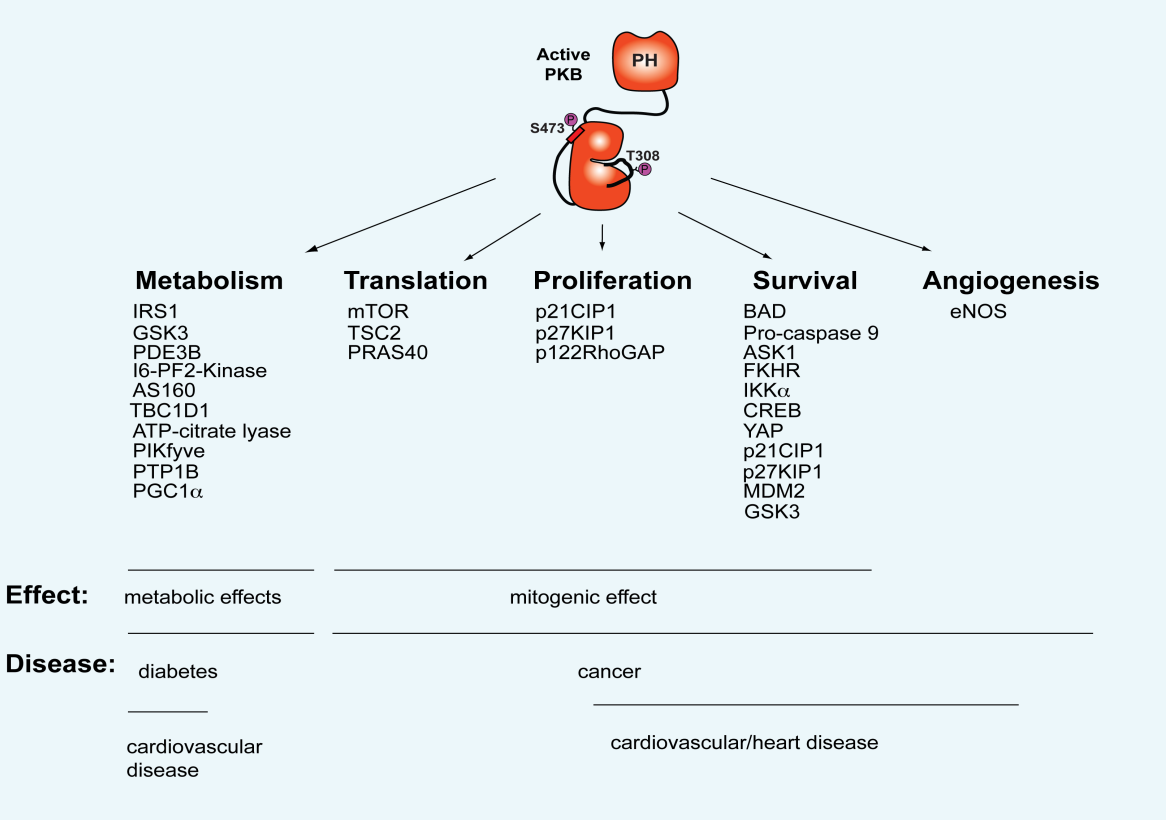

Fig.1.9- Downstream PKB effectors. PKB phosphorylation leads to the activation or inhibition of many downstream effectors. Their regulation by PKB contributes to the cellular processes and effects indicated. The deregulation of PKB downstream effectors phosphorylation may lead to diseases such as diabetes, cancer and cardiovascular/ hearth disease (adapted from Hers I. *et al*, 2011).

1.5 Focal Adhesion Kinase (FAK)

Focal Adhesion Kinase is a non-receptor tyrosine kinase (NRTK) that is localized at focal adhesion, the contact sites between cells and extracellular matrix (Ridley *et al*, 2003). FAK protein structure includes an amino (N)-terminal FERM (4.1, ezrin, radixin, moesin homology) domain, a ≈ 40 residue linker region, a central kinase domain, a ~ 220 proline-rich low complexity region, that interacts with other signalling molecules and a carboxyl (C)- terminal FAT (focal adhesion targeting) domain (Fig.1.10). The FERM domain is responsible for regulating the catalytic activity of FAK. It consists of a three-lobed protein interaction domain (F1, F2 and F3 lobes), arranged in a "clover leaf" structure. The F1 lobe adopts an ubiquitin-like fold, the F2 resembles acyl CoA binding protein and the F3 lobe exhibits the pleckstrin homology (PH) or phosphotyrosine binding (PTB) domain fold (Ceccarelli *et al*, 2006). On the other hand, the FAT domain consists of a four-helix bundle and is critical for targeting FAK to focal adhesions via binding to paxillin, but it is not thought to play a direct role in catalytic regulation of FAK (Hayashi I *et al*, 2002).

In the autoinhibited state, the FERM domain binds directly to the kinase C-lobe, impeding access to the active site and protecting FAK's activation loop from phosphorylation by Src (Cooper et al, 2003). When the FERM domain is released, FAK Tyr397 in the linker region becomes autophosphorylated, leading to exposure of a docking site for the SH2 domain of the Src kinase (Jacamo et al, 2005). The interaction between Tyr397-phosphorylated FAK and Src leads to a cascade of tyrosine phosphorylation of multiple sites on FAK by Src (Y576, Y577, Y925), as well as binding of other signalling molecules, such as p130Cas and paxillin, resulting in cytoskeletal changes and activation of other downstream signalling pathways (Lietha D, et al, 2007).

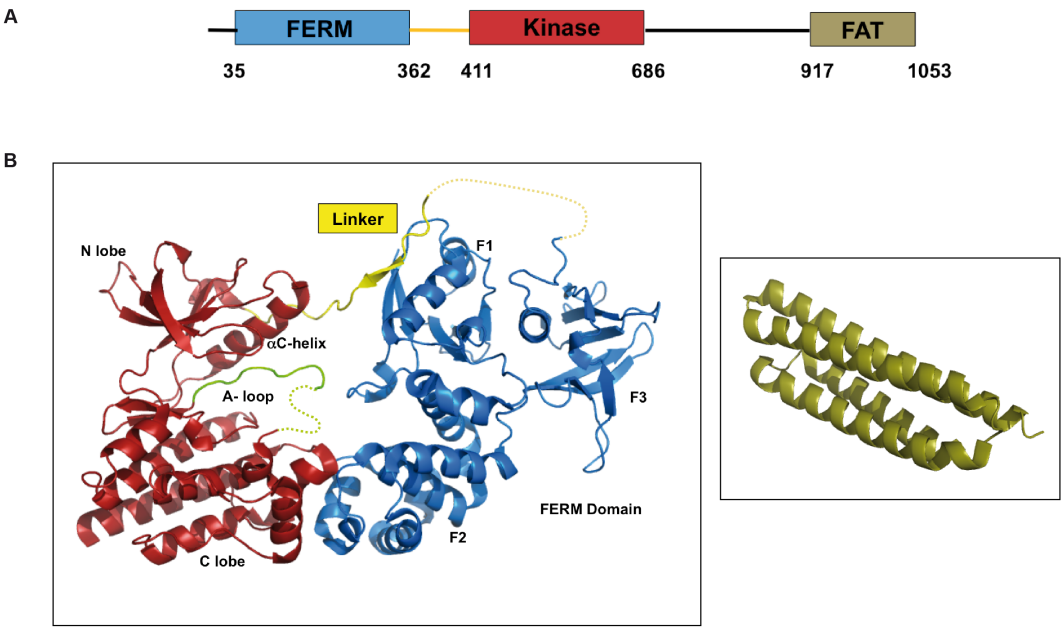

Fig.1.10- Domain structure of Focal Adhesion Kinase. A) FAK consists of a N-terminal FERM (blue), a central kinase (red) and a C-terminal FAT (focal adhesion targeting) domain (brown). B) Ribbon representation of the FERM-Kinase crystal structure adapted from Lietha D. *et al*, 2007 (PDB code: 2J0J) and of the FAT domain structure adapted from Hayashi I. *et al*, 2002 (PDB code: 1K40).

FAK becomes tyrosine phosphorylated in response to a number of stimuli, such as mitogen agents, integrin clustering or growth factor receptor signalling (Schaller MD et al, 2001). In turn, FAK is involved in the regulation of multiple cellular functions, such as proliferation, survival, invasion, metastasis, adhesion and angiogenesis (Schlaepfer DD *et al*, 1999). Indeed, FAK is frequently overexpressed in many types of tumours, including those of skin, brain, colon, breast, liver and thyroid, and it is highly correlated to invasive phenotypes in these tumours (Bonome T *et al*, 2005). Therefore, FAK is represents an important target for the development of anti- neoplastic and anti-metastatic drugs (Halder J *et al*, 2007). We previously discussed that several kinase inhibitors of different classes are currently in clinical use for the treatment of cancer and other diseases. Previous studies showed TAE226, a bis-anilino pyrimidine compound, as a potent ATP- competitive inhibitor of FAK (IC50= 5.5nM), but it also inhibits both insulin receptor (44nM) and

insulin-like growth factor I receptor (IC50 = 140nM), even though less potently (Liu TJ et al, 2007).

Since FAK is structurally and functionally well characterized, it is a suitable target to design more selective inhibitors, for example by developing inhibitors that target FAK allosterically.

Objectives

Objectives

In this thesis the following objectives have been pursued:

1. Understand the regulatory mechanism of Protein Kinase B (PKB) at atomic level and, in particular, biochemically and structurally investigate:
a) the mode of PKB autoinhibition in its basal state;
b) how the binding to PIP_3 and phosphorylation of the activation loop and of the hydrophobic motif affect the catalytic activity, accessibility of phosphorylation sites, PIP_3 binding and substrate specificity.

2. Utilize the structural information and the mechanistic insight available for FAK to identify allosteric Focal Adhesion Kinase (FAK) modulators targeting the regulatory FERM domain of FAK.

Objetivos

Objetivos

Los objetivos que se pretenden conseguir con esta tesis son:

1. Entender el mecanismo regulador de la Proteína Kinasa B a nivel atómico y, en particular, investigar a nivel bioquímico y estructural:
a) el modo de autoinhibición de PKB en su estado basal;
b) cómo la interacción con PIP_3 y la fosforilación del loop de activación y del motivo hidrofóbico (HM) afectan la actividad catalítica, la accesibilidad de sitios de fosforilación, la interacción con PIP_3 y la especificidad de sustratos.

2. Identificar moduladores alostéricos de la Kinasa de Adhesión Focal (FAK) dirigidos al dominio regulador FERM de FAK, basándose en la información estructural disponible.

Materials and Methods

3.1 Media, buffers and antibiotics

- LB (Luria-Bertani): 10g/L Casein pepton, 5g/L yeast exctract, 5g/L NaCl
- TAE (1X): 40mM Tris-acetate, 1mM EDTA
- Laemmli loading buffer (5X): 200mM Tris pH 6.8, 4% SDS, 20% Glycerol, 10% β-mercaptoethanol, 0.04% bromophenol blue
- SDS-PAGE stacking gel: 5% acrylamide, Stacking buffer pH 6.8 (125mM Tris HCl pH 6.8, 0.1% SDS), 0.1% APS, 0.1 % TEMED
- SDS-PAGE resolving gel: variable % acrylamide (8-15%), Resolving buffer pH 8.8 (378mM Tris HCl pH 8.8, 0.1% SDS), 0.1% APS, 0.1 % TEMED
- Running buffer for SDS-PAGE electrophoresis (1X): 192mM Glycin, 25mM Tris-HCl pH 6.8, 1% SDS
- Coomassie solution: 2g/L Coomassie Brilliant-blue, 10% Ethanol, 40% Acetic acid
- Destaining solution: 10% Ethanol, 40% Acetic acid
- TBS (1X): 150mM NaCl, 20mM Tris HCl pH 7.6
- TBS-Tween (TBST): 150mM NaCl, 20mM Tris HCl, 0.05% Tween (v/v), pH 7.6
- PBS (1X): 150mM NaCl, 3mM KCl, 10mM Na_2HPO4, 2mM KH_2PO_4, pH 7.6
- PBS-Tween (PBST): 150mM NaCl, 3mM KCl, 10mM Na_2HPO4, 2mM KH_2PO_4, 0.05% Tween (v/v), pH 7.6
- ELISA binding solution: 30mM Na_2CO_3, 70mM $NaHCO_3$, pH 9.6
- ELISA stop solution: 180 mM H_2SO_4, water
- Antibiotics: 100mg/ml Ampicillin, 30mg/ml Kanamicin, 33 mg/ml Chloramphenicol

3.2 Plasmid vectors

pET HisTT: modified version of T7lac promoter vector pET 32 (Novagen), that adds an N-terminal 6xHis tag, a TEV cleavage site and a thrombin site to the proteins expressed in bacteria. The expressed protein is fused to the His tag to allow the purification of the protein from the bacterial lysate. Downstream the 6xHis sequence, there are a cleavage site for the Thrombin and for the TEV protease in order to remove the affinity TAG. The plasmid carries a Kanamicin resistence. This plasmid has been used to over-express most of the human Protein Kinase B (PKB) constructs and PDK1 Kinase. Dr. Brian Hemmings at the Friedrich Miescher Institute (FMI) in Basel (Switzerland) gently provided the original pFastBac vectors containing the codifying sequences for PKB (*Homo sapiens*) and PDK1 (*Homo sapiens*). The restriction enzyme sites used for cloning are shown in Tab 3.1.

pET GST: modified version of pET 32 (Novagen) as described in pET HisTT, but in this case, an N-terminal GST tag is added to the proteins expressed in bacteria to allow the purification of the protein from the bacterial lysate. This plasmid has been used to over-express FAK 31-405 *wt*. The codifying sequence for FAK (*Gallus gallus*) was previously cloned from a pBluescript vector in Mike Eck's laboratory (Dana-Faber Cancer Institute) and gently provided. The restriction enzyme sites used for cloning are shown in Tab 3.1.

pOPIN-F: modified version of three-promoter vector pTriEx2 (Novagen), that allows the expression of recombinant proteins in *E.coli*, mammalian and insect hosts. This vector has been constructed based on the In-Fusion^{TM} cloning enzyme, which allow a ligation-independent cloning (Berrow *et al*, 2007). This plasmid includes a N-terminal 6xHis fusion tag and it contains a Prescission cleavage site, downstream the 6xHis sequence, to remove the affinity tag. The plasmid carries an Ampicillin resistance. This plasmid has been used to over-express PKB Kinase+HM S474D and zebrafish PKB FL *wt*. The original pFastBac vectors containing the codifying sequence for PKB (*Homo sapiens*) was gently provided by Dr. Brian Hemmings (FMI-Basel-CH), whereas cDNA PKB (*Danio rerio*) was bought from Source BioScience.

A

Reference	Sequence	Restriction site	T_m (°C)	Vector
hPKBa_1fw	**5'** TAT**GGATCC**ATGAGCGACGTGGCTATTGTG **3'**	BamHI	68	pET HisTT
hPKBa_434rv	**5'** TAT**CTCGAG**TTATTAGTCAGTCTCCGACGTGACC **3'**	XhoI	66	
hPKBb_1fw	**5'** TAT**GGATCC**ATGAATGAGGTGTCTGTCATCAAAG **3'**	BamHI	66	
hPKBb_435rv	**5'** TAT**CTCGAG**TTATTAGTCGACCTCGGACGTGACC **3'**	XhoI	67	
hPKBg_1fw	**5'** TAT**GATATC**ATGAGCGATGTTACCATTGTG **3'**	EcoRV	62	
hPKBg_431rv	**5'** TAT**CTCGAG**TTATTAATCTGTCTCAGATGTTACTTG **3'**	XhoI	63	
hPKBb_fl(481)rv	**5'** TAT**CTCGAG**TTATCACTCGCG **3'**	XhoI	58	
hPKBb_117rv	**5'** TAT**CTCGAG**TTATTACTCGCC **3'**	XhoI	56	
hPKBb_147fw	**5'** TAT**GGATCC**GTGACCATGAATGACTTCGAC **3'**	BamHI	66	
hPDK1_76fw	**5'** TAT**GATATC**ATGAAGAAGCGGCCTGAGGACTTC **3'**	EcoRV	67	
hPDK1_360rv	**5'** TAT**GCGGCCGC**TTATTAAGCGGTGAGCTTCG **3'**	NotI	69	
chFAK31fw	**5'** AT**GGATCC**GGGGCCATGGAGCGAGTCCTAAAG **3'**	BamHI	73	pET GST
chFAK405rv	**5'** GG**CTCGAG**ATTATTAATCTTCTTCATCTATTATCTCTGC **3'**	XhoI	64	

B

Reference	Sequence	T_m (°C)	Vector
hPKBb_pOPIN_147for	**5' AAGTTCTGTTTCAGGGCCCG**GTGACCATGAATGACTTCGACTATC **3'**	70	pOPIN-F
hPKBb_pOPIN_fl(481)rv	**5' ATGGTCTAGAAAGCTTTA**TCACTCGCGGATGCTGGC **3'**	67	
drPKBb_1fw	**5' AAGTTCTGTTTCAGGGCCCG**ATGAACGAGATCAGCGTCGTC **3'**	69	
drPKBb_479rv	**5' ATGGTCTAGAAAGCTTTA**TCACTCCCGCACACTGGC **3'**	67	

Tab. 3.1- Primers list. Primers used to amplify PKB, PDK1 and FAK constructs and to clone them in the **A)** pET family vectors and in the **B)** pOPIN-F. In bold we highlight **A)** the nucleotides of the restriction cutting site sequence for the corresponding restriction enzyme and **B)** the primer extension peculiar of the pOPIN vectors (Berrow *et al*, 2007). T_m= melting temperature of the primers. The melting temperature is calculated based on the length of the DNA and the GC ratio [$T_m = 71 + 0.41*(\%GC) – 675/length$].

3.3 *E.coli* strains

XL1-Blue: chemically competent host strain of *E.coli* suitable for routine cloning applications of plasmid or lambda vectors. This strain allows blue-white colour screening for recombinant plasmids.

BL21 (DE3): chemically competent host strain of *E.coli* suitable for transformation and protein expression.

BL21 (DE3)-pLysS: chemically competent host strain of *E.coli*, containing the pLys S plasmid which allow a tighter control of protein expression and is Chloramphenicol resistant. This host strain is therefore ideal for transformation and expression of proteins that are toxic to *E.coli* and/or exhibit high leakage of expression under uninduced condition, due to high copy numbers, as is the case for pOPIN vectors.

3.4 Cloning

To amplify the coding sequence of interest we use the polymerase chain reaction (PCR), performed in a thermocycler. The cycles of reaction are divided in three steps: initial denaturation step (2 min/ 95°C)/ 1 cycle; denaturation (30sec /95°C), primer annealing (45sec/ T_A, where $T_A = T_m - 4$°C), and extending phase (1 min/kb/ 72°C) form the second step (30cycles); final extending step (10 min/ 72°C). The 50ul of the reaction mixture contain: 100ng DNA template, 0.4uM primer 5', 0.4uM primer 3' (Tab. 3.1), 200uM dNTPs, Pfu Ultra High Fidelity DNA Polymerase (2.5U/ reaction) and the reaction buffer (10X Pfu Ultra HF buffer). Run an electrophoresis on a 1% agarose TAE 1X gel at 90V to check that the size of the amplified sequence is corrected. In the case of ligation-dependent cloning (see 3.4.1), clean the reactions to remove salts in excess using "QIAGEN PCR purification" kit according to the manufacturer protocol.

3.4.1 Ligation-dependent cloning

Both the fragment of interest and the host plasmid vector need to be digested with the chosen restriction enzymes (Tab. 3.1), in presence of BSA and the specific buffer that guarantee a high level of cutting efficiency for both restriction enzymes. Incubate the reactions at least 3 hours at 37°C (max 16 hours). Digested DNA fragments are separated on a 1% agarose TAE 1X gel at 90V. Locate bands and slice the gel with a scalpel. DNA is then extracted and purified using "Gel Extraction kit" (QIAGEN) according to the manufacturer protocol. The digested amplified DNA sequences and the digested vectors

are covalently linked in presence of a DNA ligase. The 15ul ligation mixture contains the following: ~100ng of digested plasmid vector, DNA insert (4X molar concentration of vector), T4 DNA ligase 10X buffer (New England BioLabs), 1ul of T4 DNA ligase (New England BioLabs) and water. Incubate the mixture at 16°C for 16 hours.

3.4.2 In-Fusion® ligation-independent cloning (Clontech)

To transform In-Fusion® reaction, the pOPIN-F need to be previously linearized using restriction enzymes (KpnI/HindIII) according to the manufacturer protocol of In-Fusion® HD cloning kit (Clontech). Treat unpurified PCR fragments with Cloning Enhancer (Clontech) and, then, follow the In-Fusion Cloning procedure for Cloning Enhancer-treated PCR fragments as described in the manufacturer protocol.

3.5 Transformation of competent cells

To transform chemically competent cells directly incubate 2.5-5ul of cloning DNA products with 50ul aliquot of XL1-Blue cells on ice for 10 min. Then, heat shock cells at 42°C for 45 sec without agitation and transfer directly the competent cells on ice and incubate for 30 min. So-transformed cells are then let grown in 300ul of LB and incubate at 37°C for 1h. Streak the cells on plates containing LB agar and the antibiotic of selection (see 3.1 for final concentration used). Incubate the plates overnight at 37°C.

3.6 Prep of plasmid DNA from *E.coli*

After transformation of 50ul of *E.coli* competent cells with 50ng of DNA to amplify the vectors after ligation, pick a single colony from the plate. Inoculate it in 5ml of LB and the antibiotic of selection and let it shake at 37°C for 16 hours. Afterwards, centrifuge the cells at 3300xg for 15 min, removing the supernatant and keeping the pellet. To isolate the plasmid DNA we follow the manufacturer protocol of the "QIAprep ® Spin Miniprep" kit. Elute the plasmid DNA in 30ul of water after 15min incubation and keep it at -20°C.

3.7 Clone sequencing

The DNA sequencing of the obtained clones is performed by the internal facility of the Spanish National Cancer Research Centre (CNIO). Confirmed clones are then used for protein expression.

3.8 Expression of recombinant proteins in *E.coli*

Expression constructs are transformed in *E.coli* (BL21 or BL21-pLysS) following the heat shock protocol and then streak the cells on plates containing LB agar and the antibiotic/s of selection. For all the constructs, prepare 2x50 ml of LB media with the antibiotic/s of selection. Inoculate a colony and let the cells growing in a shaker at 37°C for 16 hours. From this point the protocol of expression has to be optimized in a construct-dependent manner in order to improve the level of expression of soluble proteins.

1) *PKB PH domain*: dilute the cells grown overnights in 1 L of LB media in order to have a starting optical density (OD_{600}) ~ 0.1. Let the cultures growing at 37°C, shaking at 220rpm until they reach an OD_{600} ~ 0.6. Incubate the cultures on ice for 10 min. Add 750uM of isopropyl β-D-1-thiogalactopyranoside (IPTG) to induce the over-expression of the protein of interest. Protract the over-expression for 16 hours at 20°C.

2) *PKB PH+Kinase (ΔHM motif) constructs, PKB FL constructs, PKB Kinase and PKB Kinase+HM*: dilute the cells grown overnights in 500 ml of LB media in order to have a starting optical density (OD_{600}) ~ 0.1. Let the cultures growing at 37°C, shaking at 220rpm until they reach an OD_{600} ~ 0.6. Induce the over-expression with 500uM of IPTG. Protract the over-expression for 16 hours at 20°C, decreasing the shaking speed to 205 rpm. In the case of the *Danio rerio* PKB FL construct the temperature was decreased to 16°C.

3) *PKB Kinase+HM S474D*: dilute the cells grown overnights in 500 ml of LB media in order to have a starting optical density (OD_{600}) ~ 0.1. Let the cultures growing at 37°C, shaking at 220rpm until they reach an OD_{600} ~ 0.6. Induce the over-expression with 500uM of IPTG. Protract the over-expression for 1 hour at 37°C, 180 rpm and then 16 hours at 18°C, 205 rpm.

4) *PDK1 Kinase*: dilute the cells grown overnights in 1L of LB media in order to have a starting optical density (OD_{600}) ~ 0.1. Let the cultures growing at 37°C, shaking at 220rpm until they reach an OD_{600} ~ 0.6. Incubate the cultures on ice for 10 min. Induce the over-expression with 500uM of IPTG. Protract the over-expression for 16 hours at 18°C.

5) *FAK 31-405 wt*: dilute the cells grown overnights in 1L of LB media in order to have a starting optical density (OD_{600}) ~ 0.1. Let the cultures growing at 37°C, shaking at 220rpm until they reach an OD_{600} ~ 0.7-0.8. Incubate the cultures at RT for 30 min. Induce the over-expression with 500uM of IPTG. Protract the over-expression for 16 hours at 20°C.

Harvest the cell cultures and centrifuge them at 4000xg at 4°C for 40 min, remove the supernatant and freeze the pellet at -80°C.

3.9 Purification of recombinant proteins

Pellets obtained from protein expression (see 3.8) are resuspended in 40 ml of the corresponding LYSIS BUFFER (see Tab 3.2) and sonicated on ice for 10 min (6''on, 9''off cycles) at 37% amplitude. All the *PKB constructs* are gently resuspended at 4°C and, then, deep-frozen in liquid nitrogen and thawed three times before the sonication step. Cell lysates are centrifuged at 40K rpm at 4°C for 40 min using a rotor 45Ti (Beckman) to separate the insoluble fraction (pellet) and the soluble one (supernatant). In the following purification step, we process the soluble fraction. All *PKB constructs* and *FAK 31-405 wt* were initially purified by affinity chromatography, secondly by ion exchange chromatography and finally by a size-exclusion step, whereas *PDK1 Kinase* was purified in two-step purification, including affinity and size-exclusion chromatography. Beads, buffers and columns used along these purification steps are indicated in Tab. 3.2.

3.9.1 Affinity Chromatography

Based on the TAG fused to the expressed protein, add the indicated resin (2ml/L of protein expression) to the soluble fraction and incubate the samples 2hours max at 4°C in the case of chelating beads or for 16 hours at 4°C in the case of glutathione Sepharose beads (see Tab. 3.2). The beads are then washed as follow: 1) 3x3 column volume (CV= ml of beads) of WASH BUFFER 1; 2) 4x2 CV of WASH BUFFER 2; 3) 5x1 CV of ELUTION BUFFER (see Tab 3.2). When necessary, the TAG fused to the protein is removed by incubation of the eluted protein with TEV protease (1:20 concentration ratio protease/protein of interest) at 4°C for 16 hours. The TAG is kept in *PKB Kinase*, *PKB Kinase+HM*, *PKB Kinase+HM S474D* and *PDK1 Kinase*. Eluted protein are dialysed at 4°C for 16 hours, using Spectra/Por® membrane dialysis MW 6-8000Da, 32 mm (SpectraLabs.com) or directly diluted to reach the NaCl concentration of the corresponding BUFFER A (Tab 3.2).

3.9.2 Ion Exchange Chromatography

According to the pI predicted by ExPASy, the different constructs were further purified as follow: 1) by cathion exchange chromatography (*PKB PH domain*, *PKB PH+Kinase wt*, *PKB FL constructs*); 2) by anion exchange chromatography (*PKB PH+Kinase T309A*, *PKB PH+Kinase T309D*, *PKB Kinase*, *PKB Kinase+HM*, *PKB Kinase+HM S474D*, *FAK 31-405 wt*). SOURCE columns (GE Healthcare), indicated in Tab. 3.3, are equilibrated in the corresponding BUFFER A and then the proteins injected are eluted with different gradients of BUFFER B as indicated in Tab3.2. The eluted fractions are loaded on a 12% polyacrylamide gel (see 3.10) and then stained by Coomassie solution to discriminate the fractions containing protein bands of the correct molecular weight.

3.9.3 Size-exclusion Chromatography

As final step of purification the proteins are injected on a SUPERDEX 16/60 (GE Healthcare), previously equilibrated with the corresponding GF BUFFER (see Tab. 3.2). After running the eluted fractions on a 12% polyacrylamide gel as described, the fractions containing the protein of interest are pooled and concentrated in Amicon Ultra-4 Centrifugal Filter Units (Millipore) with a porous membrane with a molecular weight cut-off of 10000 Da, to a maximal concentration variable from protein to protein, as indicated in Tab. 3.2

A

Construct	TAG	LYSIS BUFFER	Beads	WASH 1 BUFFER	WASH 2 BUFFER	ELUTION BUFFER
PKB PH Domain	6xHis	50mM Tris-HCl pH 7.4 150mM NaCl 10mM Imidazole 10% Glycerol 2mM TCEP 1 protease inh / 40ml 3mg/ml lysozyme	Nickel Sepharose Fast flow (GE Health-care)	20mM Tris-HCl 500mM NaCl 20mM Imidazole 10% Glycerol 2mM TCEP pH 7.4	20mM Tris-HCl 150mM NaCl 50mM Imidazole 10% Glycerol 2mM TCEP pH 7.4	20mM Tris-HCl 150mM NaCl 250mM Imidazole 10% Glycerol 2mM TCEP pH 7.4
PKB PH + Kinase *wt*						
PKB PH + Kinase T309A						
PKB PH + Kinase T309D						
PKB FL *wt*						
PKB FL S474D						
PKB Kinase	6xHis	50mM Tris-HCl pH 8.0 150mM NaCl 10mM Imidazole 10% Glycerol 0.1% Tryton 2mM TCEP 1 protease inh / 40ml 3mg/ml lysozyme	Nickel Sepharose Fast flow (GE Health-care)	20mM Tris-HCl 500mM NaCl 20mM Imidazole 10% Glycerol 2mM TCEP pH 8.0	20mM Tris-HCl 150mM NaCl 50mM Imidazole 10% Glycerol 2mM TCEP pH 8.0	20mM Tris-HCl 150mM NaCl 250mM Imidazole 10% Glycerol 2mM TCEP pH 8.0
PKB Kinase +HM						
PKB Kinase +HM S474D						
PDK1 Kinase	6xHis	50mM Tris-HCl pH 7.4 150mM NaCl 10mM Imidazole 10% Glycerol 2mM TCEP 1 protease inh / 40ml 0.2mg/ml lysozyme	Nickel Sepharose Fast flow (GE Health-care)	20mM Tris-HCl 500mM NaCl 20mM Imidazole 10% Glycerol 2mM TCEP pH 7.4	20mM Tris-HCl 150mM NaCl 50mM Imidazole 10% Glycerol 2mM TCEP pH 7.4	20mM Tris-HCl 150mM NaCl 250mM Imidazole 10% Glycerol 2mM TCEP pH 7.4
FAK 31-405 *wt*	GST	50mM Tris-HCl pH 7.4 2000mM NaCl 5% Glycerol 2mM TCEP 1mM PMSF 1 protease inh / 40ml 0.2mg/ml lysozyme	Glutathione Sepharose (GE Health-care)	20mM Tris-HCl 500mM NaCl 5% Glycerol 2mM TCEP pH 8.0	20mM Tris-HCl 150mM NaCl 5% Glycerol 2mM TCEP pH 8.0	20mM Tris-HCl 150mM NaCl 5% Glycerol 1% Glutathione 2mM TCEP pH 8.0

B

Construct	pI	Column	BUFFER A	BUFFER B	Gradient
PKB PH Domain	8.66	SOURCE 15S (GE Healthcare)	20mM Hepes 30mM NaCl 5% Glycerol 5mM DTT pH 6.8	20mM Hepes 1M NaCl 5% Glycerol 5mM DTT pH 6.8	40ml of 25% BUFFER B
PKB PH + Kinase *wt*	6.44				
PKB FL *wt*	5.98				
PKB FL S474D	5.89				
PKB PH + Kinase T309A	6.44	SOURCE 15Q (GE Healthcare)	20mM Tris-HCl 30mM NaCl 5% Glycerol 5mM DTT pH 8.0	20mM Tris-HCl 1M NaCl 5% Glycerol 5mM DTT pH 8.0	40ml of 25% BUFFER B
PKB PH + Kinase T309D	6.28				
PKB Kinase	6.29				
PKB Kinase +HM	5.80				
PKB Kinase +HM S474D	5.69				
FAK 31-405 *wt*	5.72	SOURCE 15Q (GE Healthcare)	20mM Tris-HCl 30mM NaCl 5% Glycerol 2mM TCEP pH 8.2	20mM Tris-HCl 1M NaCl 5% Glycerol 2mM TCEP pH 8.2	60ml of 35% BUFFER B

C

Construct	kDa	Column	GF BUFFER	[protein]
PKB PH Domain	13.9	Superdex 16/60 (GE Healthcare)	20mM Hepes 100mM NaCl 5% Glycerol 2mM TCEP pH 7.0	2mg/ml
PKB PH + Kinase *wt*	50.5			4mg/ml
PKB FL *wt*	55.9			3mg/ml
PKB FL S474D	55.9			6mg/ml
PKB PH + Kinase T309A	50.5	Superdex 16/60 (GE Healthcare)	20mM Tris 100mM NaCl 5% Glycerol 2mM TCEP pH 7.4	2mg/ml
PKB PH + Kinase T309D	50.5			2mg/ml
PKB Kinase	33.6	Superdex 16/60 (GE Healthcare)	20mM Tris 100mM NaCl 10% Glycerol 2mM TCEP pH 8.0	1mg/ml
PKB Kinase +HM	38.9			1mg/ml
PKB Kinase +HM S474D	39.0	Superdex 16/60 (GE Healthcare)	20mM Tris 100mM NaCl 5% Glycerol 2mM TCEP pH 8.0	2mg/ml
PDK1 Kinase	35.4	Superdex 16/60 (GE Healthcare)	20mM Hepes 200mM NaCl 5% Glycerol 2mM TCEP pH 7.0	10mg/ml
FAK 31-405 *wt*	42.9	Superdex 16/60 (GE Healthcare)	20mM Tris 150mM NaCl 5% Glycerol 5mM TCEP pH 8.0	15mg/ml

Tab. 3.2- Resine beads, buffers and column used during the different steps of purification. A) Affinity chromatography. "Protease inh" refers to the Complete EDTA-free protease inhibitors (Roche). Nickel Sepharose Fast flow (GE Healtcare) and Glutathione Sepharose beads (GE Healthcare) are equilibrated according to manufacturer; **B)** Ion exchange chromatography; **B)** Size exclusion chromatography.

3.10 Electrophoresis on polyacrylamide gels

3.10.1 Denaturant conditions (SDS-PAGE)

The electrophoresis in denaturant conditions (SDS-PAGE) is performed using discontinuos polyacrylamide gels (Laemmli UK, 1970) made of a mix of acrylamide: bisacrylamide (37.5:1). SDS- PAGE gels are made of a stacking gel, constantly at 5% acrylamide in Stacking buffer (see 3.1), and a resolving gel whose acrylamide percentage can vary according to the molecular mass protein separation needed. Therefore, 15% acrylamide resolving gels are prepared for *PKB PH domain* and 12% for the rest of the

protein constructs, using Resolving buffer (see 3.1). Protein samples are diluted in 5X Laemmli loading buffer (see 3.1), and incubated at 95°C for 5min. The electrophoresis is run in MGV-402 Dual vertical mini-gel electrophoresis system (CBS Scientific) at 190V in running buffer. We used the Precision Plus Protein™ Prestained Standard Dual color (Biorad) as a protein marker. Gels are finally stained in Coomassie solution and destained in Destaining solution (see 3.1).

3.10.2 Isoelectric focusing (IEF)

The Isoelectric focusing electrophoresis (IEF) is performed using "pH 3–10 Ready Gel® IEF Gel" (Biorad) as indicated by the manufacturer. 4ug of PKB constructs were loaded and the Anode and Cathode buffers provided by the manufacturer were used. Gels are run at 4°C as follow: 1) 100V for 1 hour; 2) 200V for 1 hour; 3) 500V for 30 min. The gel is uncast and fixed in Trichloroacetic acid (TCA) for 15 min and then extensively rinsed in water. Gels are finally stained in Coomassie solution and destained in Destaining solution (see 3.1).

3.11 Western Blotting (Immunoblotting)

After separation on SDS-polyacryamide gel (see 3.10.1), proteins were transferred at 20V for 40 min onto nitrocellulose membranes (Amersham™ Hybond ECL) using a Trans-blot SD semi-dry transfer cell (Biorad). Nitrocellulose membranes are then blocked in TBS-Tween buffer, containing 5% Bovine Serum Albumine (BSA) at RT for 1 hour. Blotted membranes are washed 3x10 min with TBST and incubated at RT with the specific primary antibody as indicated in Tab 3.3. Perform 3x10 min washes with TBST and then incubate the membranes with the specific HRP-conjugated secondary antibody, as indicated in Tab 3.3. Perform again 3x10 min washes with TBST and detected using a standard chemilunimescence Western Blot protocol (ECL system, Amersham).

Antibody	Species	WB	ELISA	Manufacturer
a- AKt	Rabbit	1:1000	-	Cell Signalling
a- pAkt T308	Rabbit	1:1000	1:2500	Cell Signalling
a- pAkt S474	Rabbit	1:1000	-	Cell Signalling
a- FOXO3a	Rabbit	1:1000	-	Cell Signalling
a- pFOXO3a	Rabbit	1:1000	-	Cell Signalling
a- GSK3	Mouse	1:1000	-	Becton Dickinson
a- pGSK3 S21/9	Rabbit	1:5000	-	Cell Signalling
a- TSC2	Rabbit	1:5000	-	Cell Signalling
a- pTSC2 T1462	Rabbit	1:1000	-	Cell Signalling
a- pTSC2 S939	Rabbit	1:1000	-	Cell Signalling
a- p27	Rabbit	1:1000	-	Invitrogen
a- pp27 S10	Rabbit	1:1000	-	Invitrogen
a-rabbit--HRP	Goat	1:2000	1:500	Dako
a-rmouse-HRP	Goat	1:2000	-	Dako

Tab. 3.3- Antibodies list. "Species" refers to the source of purification of the antibody. Dilution used in immunoblotting (WB) and ELISA assays are shown.

3.12 Mass spectrometry

All reagents used for protein mass determination were of LC-MS quality when available. Samples were desalting immediately before analysis to prevent protein precipitation. Proteins were diluted 1:10 in LC-MS grade water containing 0.1% (v/v) trifuoroacetic acid. Samples were applied to a home-made Poros 20 R2 tip microcolumn (Applied Biosystems Foster City, CA) previously equilibrated with the same buffer.

Columns were washed three times with 200 uL of water containing 0.1% Acetic acid and eluted with 250 uL elution buffer consisting in a mixture of 65/35 Acetonitrile/Water (v/v) containing 2.5% Acetic acid. Desalted proteins were adjusted to a concentration of 1 ug mL^{-1} in elution buffer and analyzed by electrospray in a maXis QQ-TOF (Buker Daltonik, Bremen, Germany) Samples were infused at a flow rate of 3 uL min^{-1} and a capillary voltage of 4500V. Mass spectra were recorded from 500 to 2000 Da for 120 to 240 seconds. Spectra were analyzed using the DataAnalysis 4.0 program (Bruker Daltonic) To calculate the mass of the proteins the signals were deconvoluted by using the MaxEnt program, a charge deconvolution method based on the Maximum Entropy algorithm.

3.13 ThermoFluor assays

To assess the thermal stability of designed proteins we used the ThermoFluor assay, a quick, dye-based assay that allows the determination of melting temperatures (T_m) as an alternative to Circular Dichroism. 40ul reactions are prepared as follow: 1 uM of protein of interest, 200X SYPRO® Orange dye (Invitrogen). We used Micro-Amp™ Optical 96-well reaction plate (Applied Biosystems). The plate was heated from 20°C to 95°C and the temperature was increase with a rate of 1°C /cycle. As the temperature increases, the protein unfolds, and the increase in fluorescence is monitored using a 7300 Real Time PCR system (Applied Biosystems). Melting temperatures are determined as described in Lavinder *et al*, 2009.

3.14 In vitro PDK1-dependent PKB T309 phosphorylation assays

Fully-phosphorylation of PKB constructs at T309 is performed as follow: 20uM of PKB constructs are incubated at RT for 4 hours with 1uM of PDK1 Kinase, 2mM ATP and 4mM $MgCl_2$ in PDK1 Kinase GF BUFFER. Add 20mM EDTA to stop the reactions. Isoelectric focusing gel (IEF) and immunoblotting with anti-phosphoT309 (Cell

Signalling) are run to check the complete phosphorylation of PKB constructs (as described in 3.10.2 and in 3.11). Time courses of PKB phosphorylation are performed in 20ul reaction at RT using 400nM PKB constructs, 100nM PDK1 Kinase, 1mM ATP and 2mM $MgCl_2$. Reactions were stopped at different time points (0'-2'-10'-30') by addition of 3X Laemmli loading buffer, 20% EDTA for immunoblotting analysis or in ELISA binding solution, 20% EDTA for ELISA assays. Phosphorylation rate is monitored by immunoblotting (see 3.11) and by indirect ELISA assays (see 3.17). When phosphorylation timecourses are done in presence of soluble lipids, a final concentration of 10uM phosphatidylinositol (3,4,5)-triphosphate (PIP_3) (Echelon) is added.

3.15 In vitro λ phosphatase treatement

0.2 ug/ul PKB constructs in 30ul reaction are incubated at 30°C for 40 min with 1ul of λ protein phosphatase (New England BioLabs), 1X NEBuffer for PNP (New England BioLabs) and 1mM $MnCl_2$. Isoelectric focusing gel (IEF) of pre-treated and after-treated samples are run to check the complete dephosphorylation of the protein of interest.

3.16 Kinase activity assays

PKB constructs activity has been measured by a coupled kinase assay, where ATP hydrolysis is coupled to the transformation of pyruvate in lactate in presence of pyruvate kinase (PK) and lactose dehidrogenase (LDH). In this assay we monitor the absorbance of NADH during its oxidation to NAD^+ by UV absorption at 340nm. NADH absorbance decreases when ATP is hydrolysed to ADP. Kinase assay reaction were performed in 100ul reaction mixture, containing 1 μM of unphosphorylated PKB construct or 0.1 uM of phosphorylated PKB constructs, 20 mM HEPES pH 7.0, 100 mM NaCl, 2 mM TCEP, 10 mM $MgCl_2$, 100 mM phosphoenolpyruvate, 0.28 mM NADH, 0.08 units/μl pyruvate kinase, 0.1 units/μl lactate dehydrogenase (SIGMA), and 50 μM of peptide substrate

ARKRERTYSFGHHA (Bio-Synthesis Inc). Reactions were initiated by addition of 0.5mM ATP. Absorbance at 340 nm was monitored during 20min using a Jasko V550 spectrometer (Advanced Technology & Industrial *Co*). When kinase assays were done in presence of soluble lipids, a final concentration of 10uM phosphatidylinositol (3,4,5)-triphosphate (PIP_3) (Echelon) or 10uM of phosphatidylcoline (PC) was used. Lipids and PKB constructs were incubated 20 min at RT before the addition of the mix.

3.17 Enzyme linked immunosorbent assay (ELISA)

We quantified the phosphorylation by PDK1 of different PKB constructs by ELISA. Samples from PDK1 phosphorylation reactions were diluted 15 times to a final volume of 300uL of ELISA binding buffer to a concentration of 27nM. 50uL of this final dilution is added to Nunc Maxisorp 96-well Clear Plates wells in duplicate or triplicate. Each plate contains as a standard 2-fold serial diluted PKB FL, previously fully phosphorylated by PDK1, in the concentration range 0-27nM. Allow the incubation of the diluted reaction and standards at RT for 2 hours on a plate shaker at 300rpm. Wash with 2x200ul/well of PBS and shake dry. To block wells incubate with 200ul/well of TBS- 5% BSA at RT for 1 hours on a shaker. Wash with 2x200uL/well of PBS-T and shake dry. Incubate at RT for 1 hour on a shaker with 100ul/well of anti phospho-AKT (Thr308) (Cell Signalling), diluted as indicated in Tab 3.3. Wash with 2x200uL/well of PBST and shake dry. Incubate at RT for 1 hour on a shaker with 100ul/well of HRP-conjugated anti-Rabbit antibody (Dako) diluted as indicated in Tab 3.3. Wash 4x200uL/well of PBST, allowing last wash to run on plate shaker while set-up for detection is done. Add 100uL/well of TMB Solution (Calbiochem) and allow shake on plate shaker. Once colour development of the standard wells is in an appropriate range (20sec-1min), add 100uL/well of ELISA stop solution. Read the absorbance of all wells at 450 nm wavelength, using Varian Carey 50 Bio UV/Visible spectrophotometer (McKinley Scientific). Optical density (OD) values are converted to concentration of phospho-protein using a non-linear fit of phosphorylation standards, using the program Prism (GraphPad Software Inc.). Results are displayed as

Arbitrary Units (AU), or fold-change relative to the values of the full-length WT construct at 30 minutes.

3.18 Fluorescence polarization

To perform protein-lipid interaction studies we used Fluorescence Polarization (FP). This technique exploits the fact that when a fluorescently labeled molecule is excited by polarized light, it emits light with a degree of polarization that is inversely proportional to the rate of molecular rotation. Increasing concentration of PKB constructs (18.5nM, 39nM, 78.1nM, 312.5nM, 625nM, 1.25uM) were added to 12.5nM of fluorescence phosphoinositide in buffer 20mM Hepes pH7.5, 150mM NaCl, 1mM TCEP and incubated 20 min at RT. C_6-PIP_3 (Echelon) is labelled by a BODIPY®-TMR probe (544/570nm), whereas C_6-phosphatydilinositol (4,5)-bisphosphate (C_6-PIP_2) (Echelon) is labelled by a BODIPY®-FL probe (505/513nm). Anisotropy measurements were taken at RT using an EnVision® Multilabel Reader (Perkin Elmer) in presence of C_6-PIP_3 and using a VICTOR^2 Multilabel Counter (Perkin Elmer) in presence of C_6-PIP_2. Binding curves and dissociation constants were determined using the program Prism (GraphPad Software Inc.).

3.19 Cell lysate substrate specificity assay

Hela cells were cultured in serum free media, Dulbecco's Modified Eagle Media (DMEM) (Solmeglas) for 16 hours. Cell were centrifuged at 1500 rpm for 5 min and then cell pellets were washed twice with ice cold 1X PBS. Cell pellets were resuspended in 300µl of kinase lysis buffer (20 mM Hepes pH 7.4, 5 mM $MgCl_2$ and 0.5 mM EGTA, 100 µM ATP, 1 mM DTT) and in 300ul of kinase lysis buffer in presence of 0.1mM orthovanadate, inhibitor of protein tyrosine phosphatase. 1/3 volume of glass beads (particle size 425-600µm) (Sigma) was added to the resuspended pellets. Samples were vortexed at maximum speed for 30 sec and then transfer on ice. This step was performed twice to completely break the cells. Cells were then centrifuged for 10 min at 4°C at

13000rpm and then the supernatant was collected. Cell lysate were aliquoted to have 500ug/tube in a final volume of ~30ul. Then, 1µg of unphosphorylated or phosphorylated PKB constructs was incubated with cell lysate at 30°C for different time points (0, 5, 20 min) and stopped by addition of Laemli 5X Sample buffer. Following SDS-PAGE gels were processed for immunoblotting with the indicated proteins to detect the phosphorylation level of PKB substrates using specific antibodies (see Tab 3.3).

3.20 Screening of fluorinated compounds

3.20.1 Primary ^{19}F-NMR screening

The CNIO library of fluorinated compounds, a small fragment-oriented library of 371 chemically diverse fluorinated compounds, was used for the primary screening. The collection of fluorinated molecules for fragment-based screening using ^{19}F-NMR was assembled using three different sources (Garavís, M. et al., 2014): 1) 113 compounds were selected using the LEF (Local Environment of Fluorine) approach (Vulpetti, A. et al., 2009) and purchased individually from different vendors (Maybridge, Sigma-Aldrich, ChemDiv, Enamine, Asinex); 2) 210 compounds available in house at CNIO and 3) 53 selected compounds from commercially available collections.

The fluorinated fragments have been grouped in two categories, those having a trifluoromethly group (CF3) and those having a fluorine atom only (CF) because of the different resonances of the fluorine atom, from -9.9 ppm to 26.6 ppm and from -64.0 ppm to -19.1 ppm for CF3 and CF containing fragments, respectively. Compounds were grouped therefore in 34 cocktails of CF3 fragments (244 CF3 fragments) and in 17 cocktails of CF compounds (127 CF fragments). A cocktail stock contains typically between 8 and 10 fragments at 10 mM each in deuterated dimethylsulfoxide (d6-dmso) and each fluorine signal is unambiguously assigned to an individual fragment. The primary screening consists in the acquisition of two ^{19}F-NMR spectra of the cocktail samples at 20 µM each (for CF3 fragments) or 50 µM (for CF fragments) in PBS-1x, 10% D_2O, a regular

1D, and a 1D with a CMPG T_2 relaxation filter of 200/400ms (for CF/CF3) that results in a further decrease of signal intensity due to relaxation during this time. Consecutive protein additions at fragment:protein ratios of 100:1 and 50:1 result in a increase of line width and a decrease of intensity for the fluorine signals of binders whereas fluorine signals from nonbinding compounds remain unmodified. The primary screening of the fluorinated fragment library can be performed in less than two days with samples exchanged automatically by an automated sample exchanger with capacity of 120 samples.

3.20.2 Validation of FERM primary hits

Validation of the primary hits was performed by using three independent techniques: 1) ^{19}F and ^{1}H-NMR and 2) Surface Plasmon Resonance (see 3.21). Samples of the individual hits were prepared at 100 μM in PBS-1x, 10% D_2O for NMR experiments. As in the primary screening, two 1D ^{19}F-NMR experiments (without and with relaxation T_2 filter) were recorded for the individual hits and they were used as reference for the successive additions of protein (typically five consecutive protein additions from a 100:1 hit:protein ratio up to a final 20:1 hit:protein ratio were done). The interactions were confirmed by independent ^{1}H-RMN experiments, both Saturation-Transfer Difference (STD) (Mayer, M., Meyer, B., 1990) and WaterLOGSY (Dalvit, C. *et al*., 2001) experiments were measured at the highest protein:hit ratio (1:20). STD NMR measures the decay of the intensity of the signals of a protein bound compound after selective saturation of protein protons. WaterLOGSY measures the selective intermolecular magnetization transfer from water via protein (protein-bound water, exchanging protons) to temporarily binding ligands. Protons of binding ligands have the same sign as protein signals whereas non-binding compounds give signals of opposite sign.

3.21 Surface Plasmon Resonance

3.21.1 Fragment screening

Surface Plasmon Resonance (SPR) monitors molecular interactions between molecules in real time by measuring changes in the concentration of the molecules at the sensor surface as molecules bind to or dissociate from the surface. One binding partner is therefore immobilized over the sensor surface and the other passed over the surface in a continuous flow of sample buffer. All biosensor data was recorded on a Biacore X100. FERM was immobilized on a CM5 sensor chip using standard amine-coupling chemistry at 20 °C. PBS-P+ (20 mM phosphate, 2.7 mM KCl, 137 mM NaCl, 0.05% Surfactant P20, pH 7.4) was using as running buffer. First, the carboxyl groups from the dextran matrix were activated by a 1:1 mixture of 0.4 M 1-ethyl-3-(3-dimethylaminopropyl)-carbodiimide hydrochloride (EDC)/0.1 M N-hydroxy succinimide (NHS) and then coupled to the amine groups of FERM. FERM was diluted at 50 µg/ml in 10 mM sodium acetate (pH 5.52) for the coupling reaction. Then, 1 M ethanolamine-HCl (pH 8.5) was flown over the surface to block the unreactive activated carboxyl groups. FERM was immobilized at density of ~ 8000 RUs using 4 µg of protein in total.

Once, the protein is immobilized over the chip, a procedure called solvent correction should be done to adjust measured SPR responses for the effects of varying concentrations of dmso. A series of blank buffer injections with different percentages of dmso (in a range that includes the percentage of dmso used to solubilize the fragments) are passed over the surface and a solvent calibration curve is obtained. Finally, fragments at 50 µM in PBS-P+ buffer supplemented with 2% dmso were flown over the surface. Biosensor data for the fragments were collected at 20 °C and a flow rate of 10 µl/min. Each fragment was injected for 60 s association and 300 s dissociation. Positive and negative controls (hit10 or hit17 at 50 µM and running buffer) were injected throughout each experiment to assess stability and reproducibility of the assay. All SPR data were solvent corrected and double-referenced for blank injections and reference surface. SPR responses at equilibrium

normalized by the molecular weight of the fragments were used as a metrics for the interaction.

3.21.2 Affinity Measurements

The affinity constant for the interaction between Hit17 and FERM was measured by SPR. Increasing concentrations of Hit17 (from 31.25 μM up to 2 mM) were passed over FERM immobilized on the surface. The average steady-state responses (over 5s, 10 s before the end of the hit injection) were plotted against the ligand concentration and the data fitted to a 1:1 steady-state affinity model.

3.22 Crystallization

Crystallization screening of PKB constructs (see Results) were performed with a Cartesian MicroSys robot (Genomic Solutions) using the sitting- drop method in 96 wells MRC plates (Molecular Dimensions) with nanodrops of protein and reservoir solution. The PKB constructs and the conditions tested are explained in Results.

Crystallization of *FAK 31-405 wt* was performed using the hanging-drop method in 24-wells VDXm greased- plates (Hampton Research). Reservoir solution contains 100mM Tris HCl pH 8.5, 10mM TCEP, increasing concentration of PEG-4000 (from 16.5% to 19% with 0.5% increments) and of $MgCl_2$ (from 250mM 325mM with 25mM increments). 500ul of reservoir volume was used. 0.75ul of reservoir solution was added to 0.75ul of 8mg/ml protein on a plastic coverlid (Molecular Dimensions, sealed on top of the reservoir solution and incubated at 18°C. Crystals grow in appr 2-3 days.

3.23 Soaking and Fishing of crystals

To soak *FAK 31-405 wt* crystals with the chosen inhibitor (see Results), single crystals were transfered in a drop of a cryo-protecting buffer, corresponding to the buffer of the crystal growing condition, supplemented with 15% Ethylene glycol and 10mM of

fluorinated compound at 20°C for 5 hours. Then crystals were flash-frozen in liquid nitrogen.

3.24 Data collection and integration

Data were collected at beamline XO6SA at the Swiss Light Source (SLS) at the Paul Scherrer Institut (PSI- Villigen, CH) to a resolution of 2.6-3.4 Ångström (Å). For each crystal 400 images were collected with a oscillation ($\Delta\phi$) of 0.5° at 1.0 Å. Integration of the data was performed with iMOSFLM 7.0.9 (Leslie, A.G.W, 1992- Battye *et al*, 2011) and scaled with SCALA (Evans, 2006), as implemented in CCP4 Suite 6.4.0.

3.25 Structure determination and refinement

Phases were obtained using the FAK FERM structure (pdb code: 2AEH; Ceccarelli et al., 2006), which was solved from isomorphous crystals. Refinement was performed using the program Refmac (Murshudov et al., 1997) and manual rebuilding using the molecular graphic program Coot (Emsley and Cowtan, 2004). When new density was observed, the fluorinated compound used previously in the soaking (see 3.23) was manually placed into the density, using Coot and the resulting model was further subjected to refinement. For a complete summary of data collection and refinement parameters see Tab. 4.4 in Results.

Results

4.1 PKB

4.1.1 PKB β isoform is more soluble in E. *coli* than the α and γ isoforms

Since the regulatory elements we study are conserved among the PKB isoforms, we started working in parallel with the three PKB isoforms (α, β and γ) to investigate which of them was the most suitable to obtain soluble protein for our studies. For each of them we cloned a construct lacking the C-terminal HM motif, named PH+Kinase, into a pET HisTT vector (see 3.2). The original codifying sequences for PKB were provided by Dr. Brian Hemmings (FMI-Basel-CH) in a pFastBac vector, used for high-level expression of proteins in insect cells using the baculovirus system. In fact, PKB is traditionally expressed in insect cells as reported in previous work (Yang *et al*. 2002a). However, we decided to initially test the possibility of expressing PKB constructs in *E.coli*. Bacterial expression has the advantages of fast and cheap production of potentially large amounts of protein, as required for X-ray crystallisation experiments. However, multi-domain eukaryotic proteins expressed in bacteria often are non-functional and frequently are not folded correctly resulting in insoluble protein (Baneyx 1999). We transformed *E. coli* cells (BL21-DE3) with the PH+Kinase constructs of the different PKB isoforms. The γ isoform appears to be toxic for bacterial cells, therefore we performed a preliminary small-scale expression test of only of PH+Kinase α and β. A large amount of α isoform turned out to be insoluble, whereas the overexpressed PKB β appears to be mostly soluble (Fig. 4.1A). Then we purified both isoforms by affinity chromatography, using a N-terminal His tag that was appended during the cloning step in the pET vector (see Materials and Methods). As shown in Fig. 4.1A, the yield of eluted protein after Nickel pull down is higher for PKBβ, so we decided to work with this isoform. PKBβ PH+Kinase (residues 1- 435) expression was scaled up and purified firstly by affinity chromatography. This construct is easily overexpressed in *E.coli* and most of the protein is soluble, allowing us to have enough protein for our studies. On the other hand the level of purity obtained was not sufficient for

our goal, therefore the eluted His-tagged PH+Kinase was secondly purified by size exclusion chromatography, to obtain a higher level of purity (Fig. 4.1B).

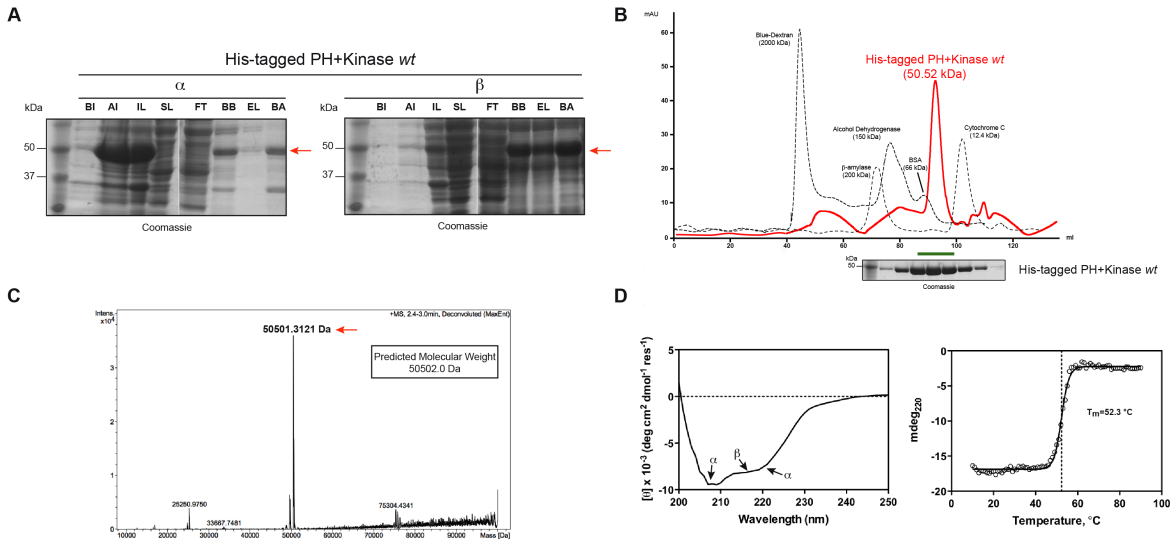

Fig. 4.1 Purification and biophysical characterization of His-tagged PKB PH+Kinase. A) Comparison of small-scale Nickel pull-down of α and β isoform of His-tagged PKB PH+Kinase by SDS-PAGE. BI, before induction; AI, after induction; IL, insoluble lysate; SL, soluble lysate; FT, flow-through; BB bead before elution, EL elution, BA, beads after elution. The red arrow points to the bands corresponding to the molecular weight expected for His-tagged PKB PH+Kinase. **B)** Size-exclusion elution profile of His-tagged PKB β PH+Kinase wt (red trace) compared to the elution of different standards (dashed traces). The chromatographic profiles (Superdex200) are monitored by absorption at 280nm. Peak fractions (green line) were analysed by polyacrylamide gel electrophoresis (SDS-PAGE), shown in the insert below. **C)** Intact-mass spectrum of His-tagged PKBβ PH+Kinase wt. The major peak, highlighted by a red arrow, corresponds to the predicted molecular weight for His-tagged PH+Kinase wt. **D)** Circular dicroism experiments (left) suggest folded protein with mixed α/β content. The melting temperature (T_m) was measured by monitoring thermal unfolding at 220 nm in the CD spectrum (right).

In order to check whether the purified protein contains any modification or degradation we carried out intact mass spectrometry and observed that the molecular weight corresponding to the major peak firs with the predicted molecular weight for His-tagged PH+Kinase (Fig. 4.1C). Moreover, we performed circular dichroism spectroscopy

analysis (CD) to validate the secondary structure properties of the protein sample that, as expected, showed a mix composition of alpha helix and β sheet conformation. Thermal unfolding experiments confirmed that the purified His-tagged PH+Kinase is stably folded with a T_m of 52.3°C (Fig. 4.1D).

4.1.2 Expression and purification of PKB β constructs from *E.coli*

In order to study the role of the different PKB domains we designed several constructs of the β isoform of PKB. Besides the full-length constructs, we cloned shorter versions of PKB in order to cover the different combination of domains as shown in Fig. 4.2. In addition we wanted to control the phosphorylation state of the two main phosphorylation sites of PKB, Thr309 and Ser474. Therefore, we generated mutant PKB forms where Thr309 and Ser474 are substituted by alanine (T309A) to prevent the phosphorylation or aspartate (T309D and S474D), to mimic phosphorylation. All the constructs were cloned in pET His TT, transformed in *E.coli* (BL21-DE3) and initially purified by a two-step purification composed of His tag- affinity and size-exclusion chromatography as previously described for PH+Kinase. Subsequently, we decided to optimize the purification procedure, because the resulting proteins contained impurities and failed to crystallize (see 4.1.5). To this end, we cleaved the 6xHis tag in the protein eluted by affinity chromatography and we introduced an ion exchange chromatography step before the size-exclusion one. All the constructs purified behaved similarly, even if the PH+kinase constructs are generally more soluble compared to full-length and ΔPH domain constructs. Also the presence of the phospho-mimetic mutation S474D increases the yield both for full-length and ΔPH domain constructs. To minimize degradation, all purification steps were performed at 4°C in the shortest time window possible. For ΔPH domain constructs it was most difficult to obtain sufficient amounts of soluble protein for our studies. In order to improve the solubility of these constructs we added low concentrations of Tryton (0.1%) to the lysis buffer. Furthermore, these constructs were very prone to degradation especially after removing the His tag, therefore we decided to

keep the tag in these constructs, after verifying that it had no affect in our assays. Further, after testing various lysis conditions, we increased the pH and Glycerol concentration to further help the protein stabilisation. Unfortunately, we were not able to get soluble FL T309D protein therefore we use the FL *wt* construct after phosphorylation of the Thr309 by PDK1 Kinase.

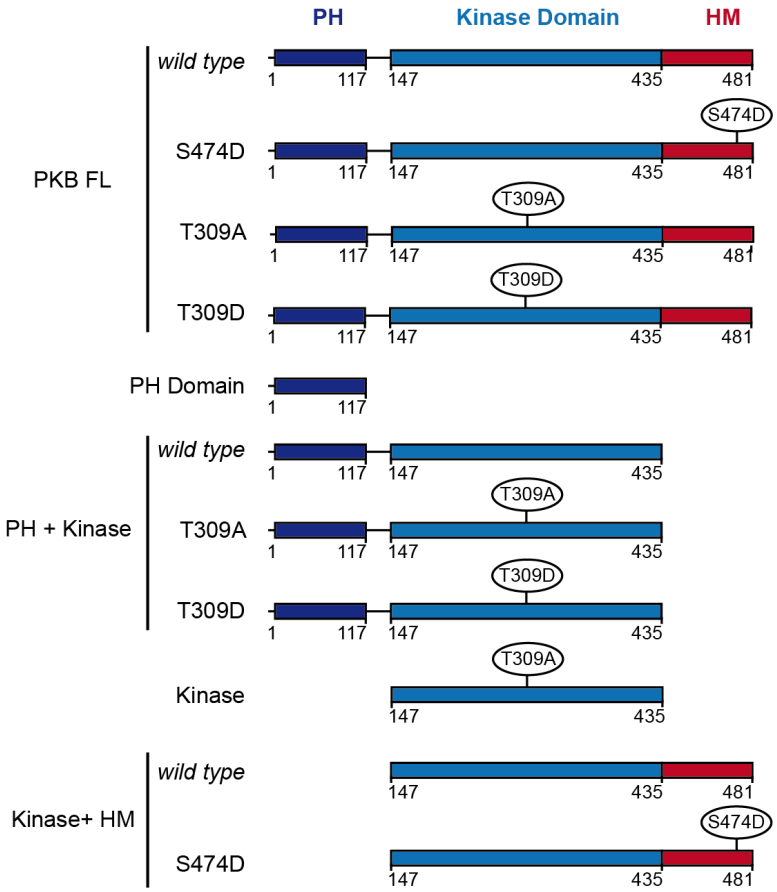

Fig. 4.2 hPKBβ constructs. Summary of the different hPKBβ constructs cloned. PKBβ comprises three functional domains: an N-terminal PH domain (**dark blue**), a central kinase domain (**light blue**), and a C-terminal Hydrophobic Motif (HM) (**magenta**). T309 and S474 are the two main phosphorylation sites in PKB.

4.1.3 Optimization of PDK1-dependent T309 phosphorylation

In order to obtain T309-phosphorylated PKBβ constructs, we decided to optimize in vitro phosphorylation reactions of PKB T309 by the PDK1 kinase. PDK1 is known to be the kinase responsible for T309 phosphorylation. PDK1 is a member of the AGC protein kinase family and it comprises an N-terminal kinase domain and a C-terminal plecktrin homology domain (PH). For our purpose we decided to clone the kinase domain of PDK1, sufficient to correctly phosphorylate PKB, into pET His TT. PDK1 kinase was purified as His-tagged protein by affinity chromatography followed by size exclusion chromatography. PDK1 kinase overexpression in bacteria appeared to be good and enabled a yield and purity suitable to set up phosphorylation reactions of PKB. The two kinases were mixed and incubated at RT as described in Material and Methods.

Phosphorylation trials at 30°C resulted in protein degradation. We checked the level of T309 phosphorylation by western blotting using a specific antibody (Fig. 4.3A). Since western blotting does not provide quantitative information about the completeness of the phosphorylation reaction, we analyzed the unphosphorylated and phosphorylated samples by mass spectrometry analysis (Fig 4.3B). Moreover, we monitored the completeness of PKB phosphorylation by isolelectric focusing where the proteins separate according to their pI (Fig. 4.3C), which is affected by negatively charged phosphates. In further experiments we only used IEF analysis to monitor T309 phosphorylation by PDK1.

Before starting the optimisation of the phosphorylation reaction, all the constructs were incubated in presence of λ phosphatase and then run on IEF gels, in order to check whether the purified proteins were already in a phosphorylated state. Phosphatase-treated samples showed the same pI as the untreated ones, suggesting that the original proteins are not in a phosphorylated state. To check whether autophosphorylation of PKB occurs, we incubate the constructs in presence of ATP. No shift was observed by IEF, indicating no autophosphorylation (Fig. 4.4A).

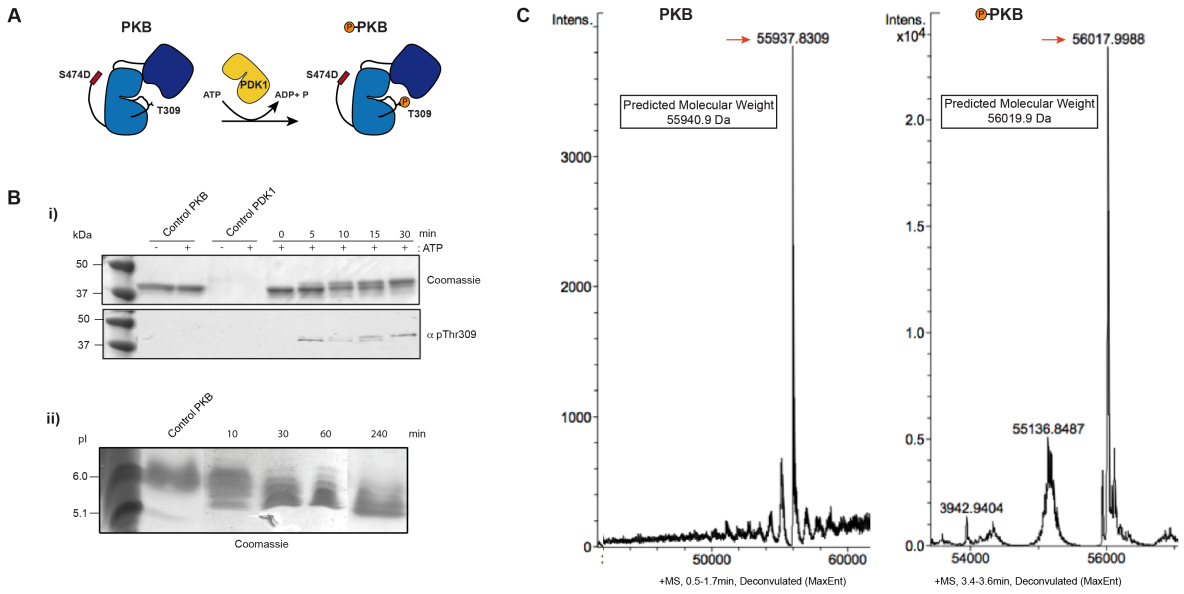

Fig. 4.3 ***In vitro*** **PDK1-dependent T309 phosphorylation of PKB FL S474D.** **A)** Schematic of the phosphorylation reaction. **B) i)** Different time points of phosphorylation reaction were analysed by SDS-PAGE (upper panel) and by western blotting (bottom panel)**,** using a specific phospho antibody for PKB T309 (α pThr309). Control PKB and Control PDK1 contain only PKB or PDK1 kinase respectively. **ii)** IEF gel of different time point of phosphorylation reaction. Control PKB refers to the FL S47D in presence of 2mM ATP and 4mM $MgCl_2$, but in absence of PDK1. **C)** Comparison of intact-mass spectra of unphosphorylated (left) and phosphorylated PKBβ FL S47D after 4 hours reaction. The major peak, highlighted by a red arrow, corresponds to the predicted molecular weight for the two forms.

All the constructs were initially phosphorylated at different time points and run on IEF in order to define the reaction time required for complete phosphorylation of the different samples. As shown in Fig. 4.3C for FL S474D, phosphorylation shifts the migration in SDS-PAGE and IEF analysis. Since phosphorylated samples exhibit low stability, we always generated freshly phosphorylated samples for their use in our assays. Within the different constructs, PH+kinase *wt* and PKB Kinase showed slow phosphorylation and we had to increase the time up to 4 hours to achieve complete phosphorylation for all constructs.

Interestingly, while we were running phosphorylated samples in SDS-PAGE gel, we noticed that the migration of PKB constructs was affected, but only when the HM motif is present in the construct (Fig. 4.3A and Fig. 4.4B). Althought in denaturant conditions a single phosphorylation should not significantly affect the migration of a protein on SDS-PAGE, in some specific cases the migration properties has been reported to be affected by covalent modification (Kovacs *et al*, 2003). Indeed, the most common covalent modification that induce mobility shift in SDS-PAGE is phosphorylation, when it is responsible for strong conformational changes.

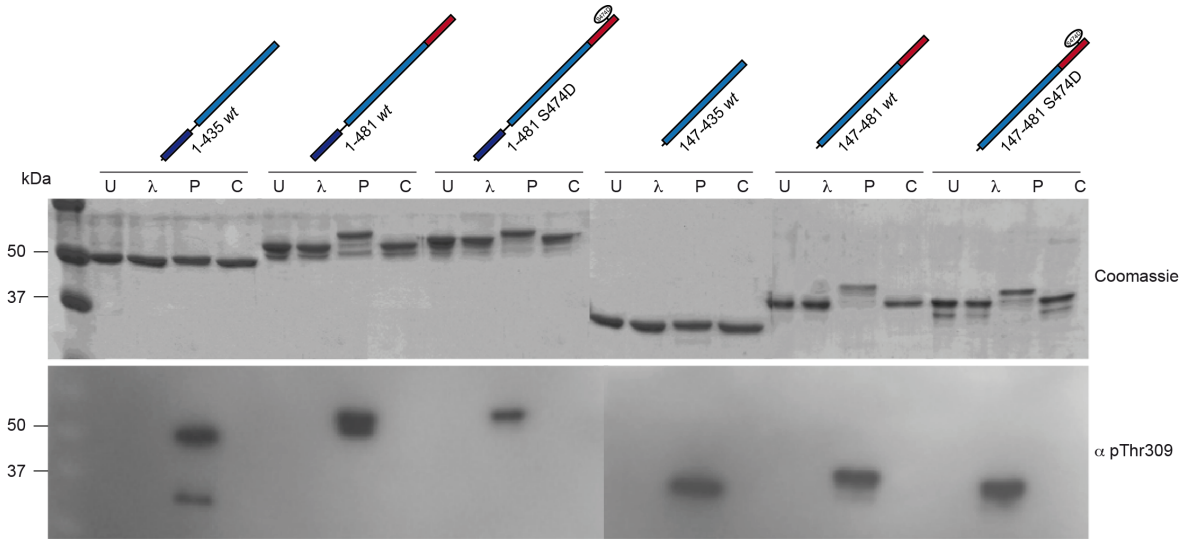

Fig. 4.4 PKBβ constructs phosphorylated *in vitro* on Thr309 by PDK1 Kinase or treated with lambda phosphatase sre analysed by SDS-PAGE gel (Coomassie) and by western blotting (α pThr309). U: untreated; λ: lambda phosphatase treated; P: phosphorylated, C: incubation with 2mM ATP and 4mM $MgCl_2$.

4.1.4 Stability of PKB constructs

In order to compare the stability of the purified PKB constructs, we performed thermofluor experiments to obtain melting temperatures (summarized in Fig. 4.5A).

A

Construct	Residues	T_m (°C)
FL *wt*	1-481	51.8
FL T309A	1-481	50.8
FL S474D	1-481	51.8
PH + Kinase *wt*	1-435	48.7
PH + Kinase T309A	1-435	50.4
PH + Kinase T309D	1-435	48.4
Kinase	147-435	45.8
Kinase+HM *wt*	147-481	49.8
Kinase+HM S474D	147-481	49.8

B

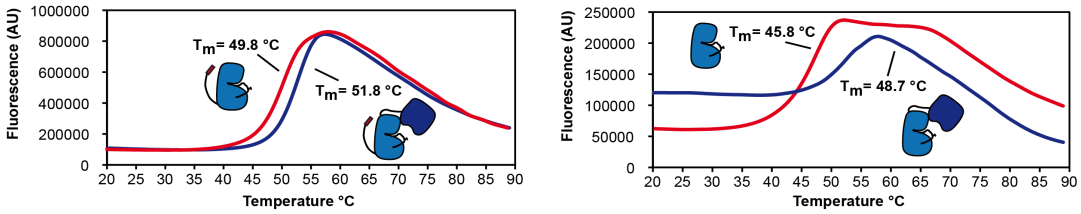

Fig. 4.5 A) Table summarizing the melting temperatures (Tm) for PKBβ constructs, measured by thermofluor analysis. **B)** Comparison of thermofluor transition curves to show the domain-dependent change of the Tm. On the left, overlay of Kinase+HM *wt* (red) and FL *wt* (blue) transition curves. On the right, comparison of Kinase (red) and PH+Kinase *wt* (blue) transition curves.

The thermofluor results outlined a clear transition for all the constructs. Both the addition of the PH domain and the HM motif to the PKB kinase noticeably leads to an increase in the melting temperature (Fig. 4.5A, B). Moreover, the highest melting temperature is reached in the FL constructs, highlighting a additive effect of PH domain and HM in the stabilisation of the protein. These considerations about protein stability based on the melting temperature values perfectly reflect our observations during the protein purification experiments in terms of solubility and propensity to degrade (see 4.1.2).

4.1.5 Crystallization attempts of PKB constructs

To gain an atomic resolution understanding of the mechanisms that regulate PKB, we tried to obtain crystals of inactive and active forms of PKBβ.

We set up different crystallization trays using the vapour diffusion method. Firstly, we explored conditions that had previously been reported to yield PKBα crystals in presence of a stabilizing inhibitor (Wu W *et al*, 2010). Initially, we prepared hanging drops of the His-tagged PKBβ PH+Kinase wt and T309A by mixing equal volumes of the protein with precipitants, consisting of a range of Na-acetate, Na-citrate (from 30mM to 300mM) and PEG MME 2000 (from 10% to 30%) at 20ºC. Since we did not obtain crystals, we decided to cleave the affinity tag and to introduce an additional ion exchange chromatography step (see 4.1) to obtain higher purity of the proteins. Meanwhile, we performed thermofluor experiments in order to identify the most suitable buffer composition, able to confer a better stability of the protein sample. We used this information to change the buffer used in the last step of size exclusion chromatography in the purification step, replacing Tris pH 7.5 with Hepes pH 7.0.

Then, we performed extensive crystallization screening of PH+kinase constructs, using a robotic nanodrop dispenser of sitting drops. We tested over 2000 conditions, setting up a wide number of commercial sparse matrix screens from Hampton and Qiagen Research. We further attempted to vary the parameters tested as summarized in Tab. 4.2. As shown, we set up screening at different temperatures (20ºC and 4ºC) and protein concentrations. We also prepared drops of the protein incubated in presence of ATP analogous (AMP-PNP) and $MgCl_2$, and in complex with a specific PKB inhibitor (Inhibitor VIII), to see if this could help the formation of protein crystals.

The only promising result obtained was the formation micro crystals for PH+Kinase T309A in a condition of the Index screen (0.1 M Hepes pH 7.0, 10% PEG MME 5000, 5% Tacsimate, 0.01 M TCEP). We tried to optimized this hit both extending the range of the precipitants concentration and applying Additive screen (Hampton) to the condition of the

good hit. Unfortunately, we did not improve either the size or the shape of the micro crystals (Fig. 4.6).

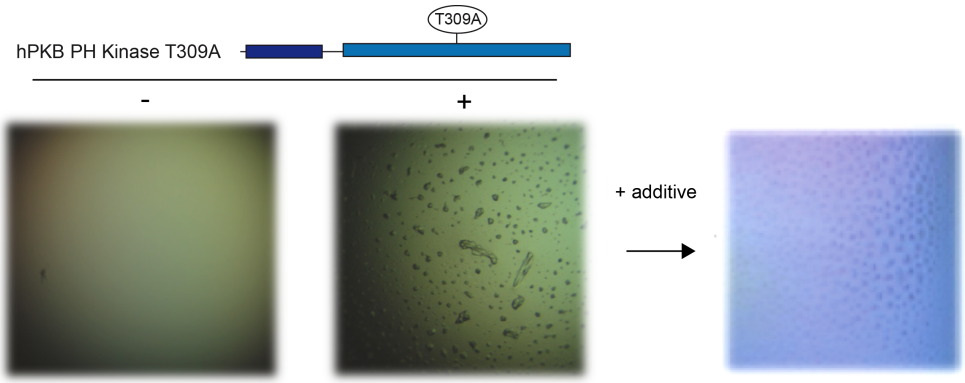

Fig. 4.6 Micro crystals of PH+Kinase T309A. On the left, we show the micro crystals of PH+Kinase T309A (+) in comparison with a control drop where we replace the proteín with gel filtration buffer (-). On the right, we show the same condition in presence of additive.

We also set up crystallization trails of the PH+Kinase T309D, FL T309A and FL S474D without any success. Chemical conditions and parameters tested are summarized in Tab. 4.2. We also decided to explore if changing the protein organism could improve the crystallization attempt. We cloned express and purify PKB FL wt of *Bos taurus*, *Danio rerio* and *Xenopus tropicalis*, the only cDNAs available for PKB in addition to the *Homo sapiens*. We only managed to produce suitable amount of soluble protein for the zebrafish (*D. Rerio*). However, crystallization trays were set up without leading to crystal hits.

At this point we decide to focus our effort more on functional studies to deepen our knowledge on our target behaviour and take advantage from our understanding to improve our crystallization efforts in a more rational way.

Construct	Length	Hampton	Index HT	PEG Ion HT	JCSG Suite	PACT Suite	pH Clear I	pH Clear II	Morpheus	Kinase	Silver bullets	Additive
hPKB wt	 1-435	+/- AMP-PNP 20°C	+/- AMP-PNP 20°C	+/- AMP-PNP 20°C								
hPKB T309A	 1-435	+/- AMP-PNP +/- Inhib VIII 20°C/ 4°C	+/- AMP-PNP +/- Inhib VIII 20°C/ 4°C	+/- AMP-PNP +/- Inhib VIII 20°C/ 4°C	+/- AMP-PNP +/- Inhib VIII 20°C/ 4°C	+/- AMP-PNP +/- Inhib VIII 20°C/ 4°C	+/- AMP-PNP +/- Inhib VIII 20°C/ 4°C	+/- AMP-PNP +/- Inhib VIII 20°C/ 4°C	+/- AMP-PNP +/- Inhib VIII 20°C/ 4°C		+/- AMP-PNP +/- Inhib VIII 20°C/ 4°C	+/- AMP-PNP +/- Inhib VIII 20°C
hPKB T309D	 1-435	+/- AMP-PNP 20°C	+/- AMP-PNP 20°C	+/- AMP-PNP 20°C	+/- AMP-PNP 20°C	+/- AMP-PNP 20°C	+/- AMP-PNP 20°C	+/- AMP-PNP 20°C	+/- AMP-PNP 20°C		+/- AMP-PNP 20°C	
hPKB T309A	 1-481	20°C		20°C	20°C	20°C						
hPKB S474D	 1-481	20°C	20°C	20°C	20°C	20°C	20°C	20°C	20°C			
drPKB wt	 1-479	20°C		4°C	4°C	20°C			4°C	4°C		

Tab. 4.2 Summary of crystallisation screening and parameters tested for the indicated PKB constructs.
h: Homo sapiens; dr: *Danio rerio* (zebrafish).

4.1.6 Efficiency of PDK1- dependent PKB phosphorylation in presence and in absence of PIP_3

To determine how the different PKB domains and of PIP_3 regulate the efficiently of the PDK1-dependent T309 phosphorylation, we performed time course of phosphorylation reactions of the different constructs of PKB in presence and in absence of PIP_3, as explained in Material and Methods. In our immunoblotting experiments (Fig. 4.7A), we observed that the PH domain reduces the efficiency of T309 phosphorylation, as we can clearly see comparing the FL constructs with their respective ΔPH mutants. This observation implies that the PH domain plays an inhibitory role. Furthermore, the constructs carrying the phospho- mimetic mutation S474D show a higher level of phosphorylation than the *wild type*, suggesting that S474D mutation accelerates T309 phosphorylation. On the other hand, removing the HM results in much lower rates of T309

phosphorylation. When PIP_3 is added during the time course reactions, the phosphorylation reaction is accelerated in the FL constructs. To obtain more quantitative results, we measured T309 phosphorylation by ELISA assays in triplicates and we quantified the phosphorylation rate of each construct in presence and in absence of PIP_3 as a fold-change of T309 phosphorylation for PKB FL wt after 30 minutes of reaction and in absence of lipids (Fig. 4.7B).

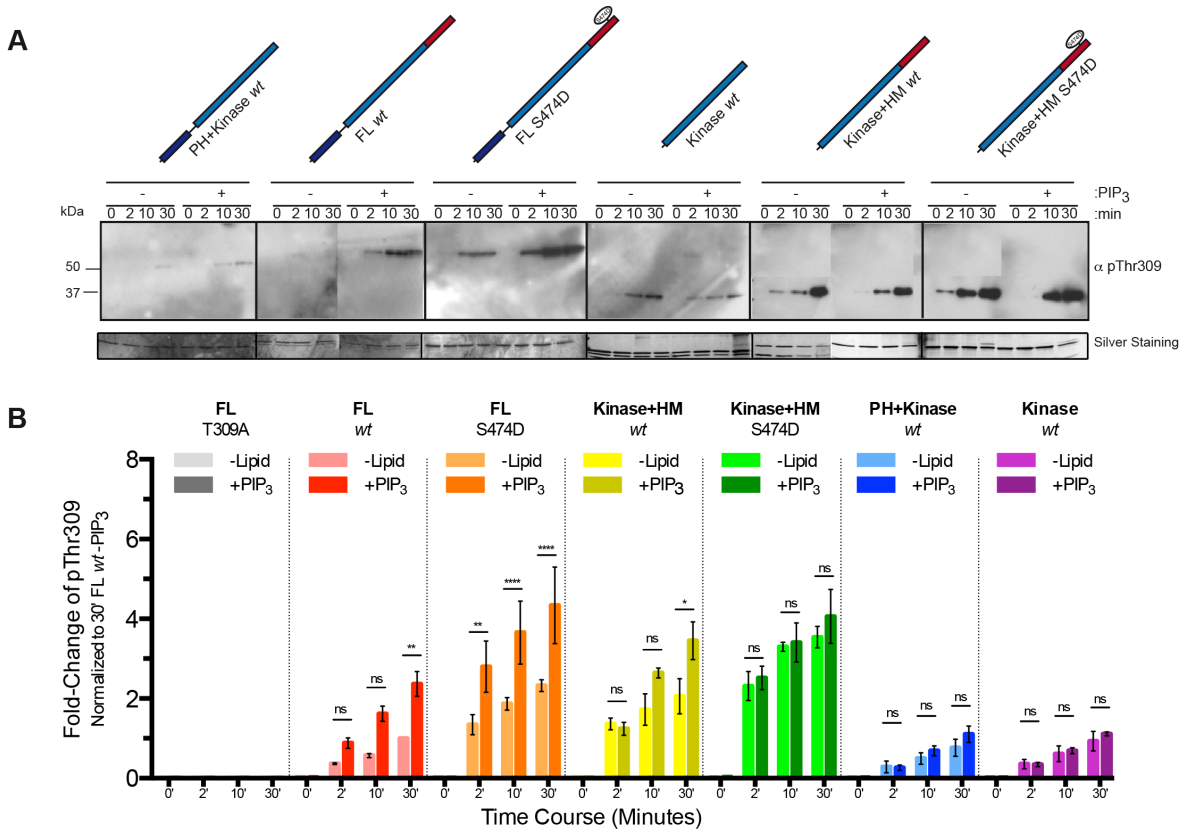

Fig. 4.7 A) Phosphorylation time course of the different PKBβ constructs in absence or in presence of $PI(3,4,5)P_3$ was monitored by western blotting, using a specific antibody recognizing PKB phosphorylation at Thr309 (α pThr309). The bottom panels are loading controls run in SDS-PAGE and dyed by silver staining. B) Quantification of phosphorylation time course of the different PKBβ constructs by ELISA assays. Observed signals are normalized to time 30 minutes of FL wt in absence of PIP_3.

ELISA assays confirmed the conclusions from western blotting experiments. As expected, the negative control FL T309A shows no signals. Interestingly, for constructs containing the HM motif, the reduced phosphorylation rate caused by the PH domain is recovered in presence of PIP3, indicating the removal of the inhibitory effect of the PH domain upon PIP3 binding. The other clear observation is that the HM motif is required for efficient T309 phosphorylation by PDK1 and this effect is further increased if the HM motif contains the S474D phosphomimetic mutation.

4.1.7 Activity assays of PKB

To measure the catalytic steady state activity of unphosphorylated and phosphorylated PKBβ constructs, we used a coupled kinase assay, where the release of ADP, driven by the kinase activity, is directly proportional to the consumption of NADH (see Material and Methods). In Fig. 4.8A, the activities of unphosphorylated and phosphorylated PKB constructs is shown. The first observation is that phosphorylation on T309 by PDK1 is required for any significant activity. The activity of freshly phosphorylated samples is measured without PDK1 removal. To test whether the presence of PDK1 Kinase affects the measurement, we included a control where PDK1 Kinase in a concentration equal to the one present in 0.1uM phosphorylated PKB samples is present. No effect was observed. As expected, the T309A mutation in PKB prevents a PDK1-induced activation. On the other hand, the T309D appears to poorly mimic the phosphorylated state of T309. A further important observation is that the HM motif is essential for PKB activity, given that ΔHM constructs show no activity (Fig. 4.8A). On the other hand, the S474D phosphomimetic mutation is not essential, but increases activity. In contrast, the PH domain has an inhibitory effect on the activity, and this is more evident in the phosphorylated PKB constructs. Possibly, this inhibition is released by the phosphomimetic mutation S474D. In fact, the activities of FL S474D and Kinase+HM *wt* are equal, suggesting that the mutation is responsible of the release of the PH domain.

However, since the Kinase+HM S474D exhibits higher activity than Kinase+HM wt, the S474D mutation appears also to have a PH indipendent activating effect.

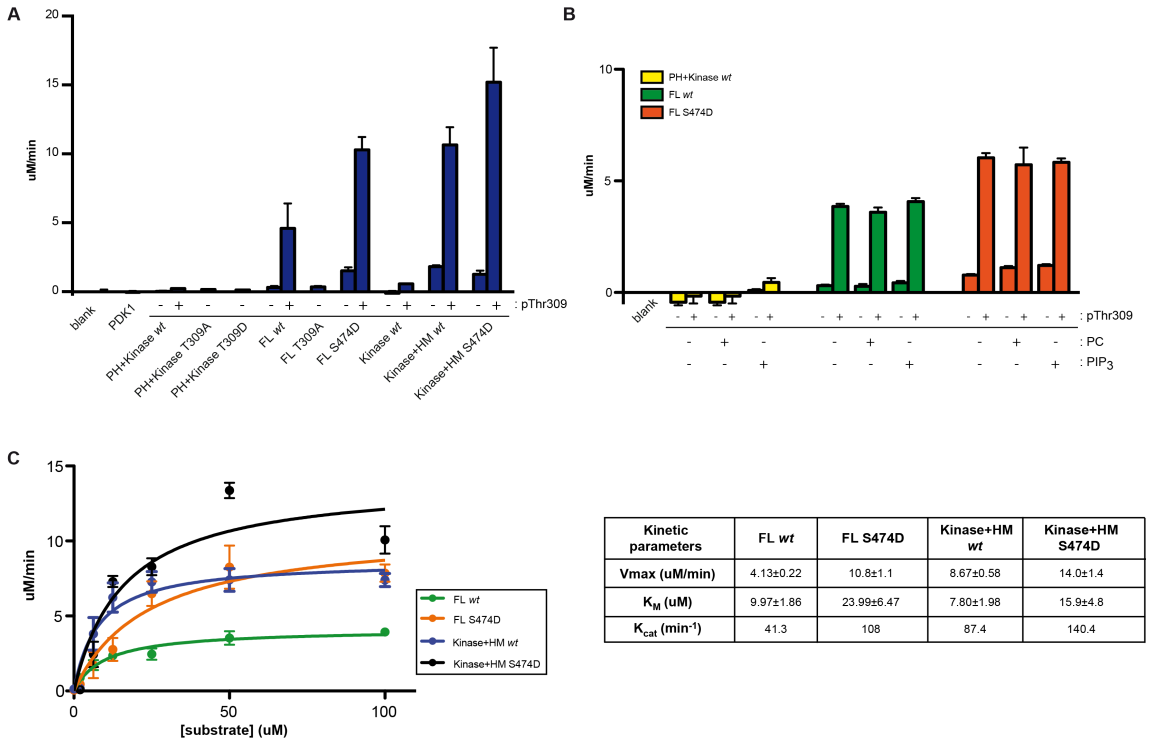

Kinetic parameters	FL *wt*	FL S474D	Kinase+HM *wt*	Kinase+HM S474D
Vmax (uM/min)	4.13±0.22	10.8±1.1	8.67±0.58	14.0±1.4
K_M (uM)	9.97±1.86	23.99±6.47	7.80±1.98	15.9±4.8
K_{cat} (min^{-1})	41.3	108	87.4	140.4

Fig. 4.8 Activity state of PKBβ constructs. The catalytic activity of PKB constructs was determined by coupled kinase assays. Error bars represent standard deviation from three experiments. **A)** Comparison between unphosphorylated PKBβ constructs (at 1uM) and PKBβ constructs phosphorylated on T309 (pThr309)(at 0.1uM). Blank: reaction mix without PKB; PDK1: measurement of catalytic activity of 5nM PDK1, concentration present in phosphorylated PKB samples. **B)** Activity comparison of the PKBβ constructs containing PH domain, in different phosphorylation states and in presence or absence of 10uM C8-PI (3,4,5)P_3 or C8-PC. **C)** Activity of PKBβ constructs phosphorylated at T309 (at 0.1uM), at increasing concentration of the substrate peptide (0uM, 2uM, 6.25uM, 12.5uM, 25uM, 50uM, 100uM). The data is fitted to Michaelis- Menten Kinetics to derive Km and Vmax, shown in the table on the right.

We also tested whether the activities changed after 20 minutes incubation with 10uM of soluble PIP_3. For these assays we tested only the constructs containing the PH domain,

since it is responsible for PIP_3 binding (see 4.1.8). As a non-specificlipid control we used phopshoatidyl choline (PC). Surprisingly, the addition of soluble PIP_3 had no effect on PKB activity (Fig. 4.8B).

Finally we also measured the activity of T309 phosphorylated PKBβ constructs at increasing concentration of the substrate peptide and we fitted the data to Michaelis-Menten kinetics to derive Km and Kcat (Fig. 4.8 C). As already suggested from Fig. 4.8A, the S474D mutation increases and the PH domain decreases Kcat. Surprisingly, the S474D mutation increases the Km for the substrate used, suggesting that perhaps S474D could play a role in substrate specificity. On the other hand the PH domain has little effect on Km.

4.1.8 Interaction studies in presence of lipids

We pursued protein-lipid interaction studies, using Fluorescence Polarization (FP). This technique exploits the fact that when a fluorescently labeled molecule is excited by polarized light, it emits light with a degree of polarization that is inversely proportional to the rate of molecular rotation. In our studies, we use this property to measure how the different states of PKBβ interact with PIP_3, labeled with a fluorescent BODIPY-TMR probe. We compared both unphosphorylated and T309-phosphorylated PKBβ constructs with PKB PH domain alone (Fig. 4.9). Surprisingly, the PKB PH domain shows an approximately 2-fold lower PIP_3 binding affinity compared to the constructs that have also the kinase domain. Perhaps, the interaction between the PH domain and the kinase stabilizes the PH domain in a conformation, which is more competent for PIP_3 binding. On the other hand, we found that the phosphorylation state (pT309 or S474D) and the presence of the HM do not affect the affinity. As expected, we did not observe a significant PIP_3 binding affinity for ΔPH constructs.

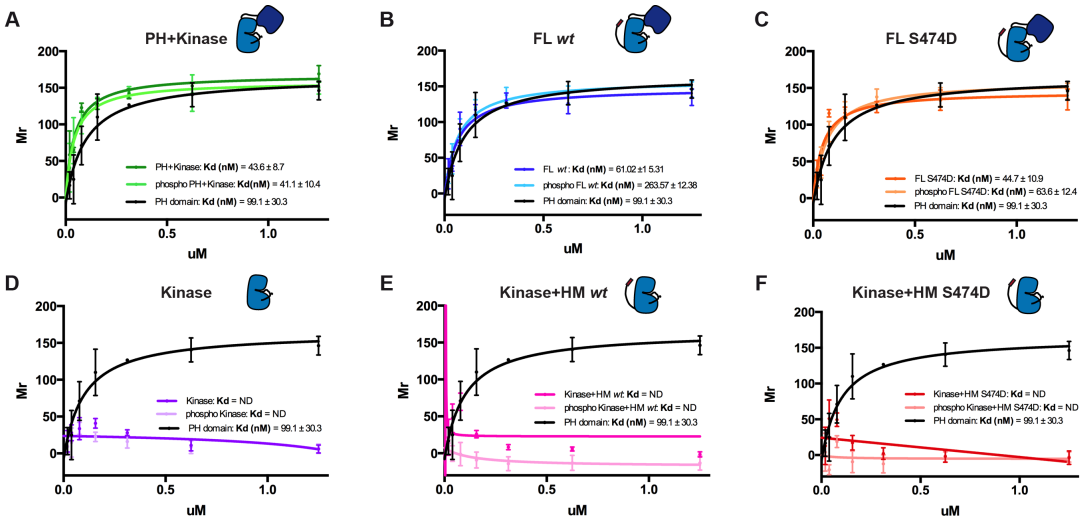

Fig. 4.9 PIP_3 affinity of hPKBβ constructs. The binding affinity of PKBβ constructs to PIP_3 was determined by fluorescence polarization assays, using increasing concentrations of PKBβ constructs (25nM, 50nM, 100nM, 250nM, 500nM, 1uM). PIP_3 (12.5nM) is labelled by a BODIPY-TMR probe (Excitation/Emission wavelenghts = 544/570nm). The binding of the isolated PH domain is compared with unphosphorylated and T309- phosphorylated hPKBβ constructs: **A)** PH+Kinase *wt*, **B)** FL *wt*, **C)** FL S474D, **D)** Kinase, **E)** Kinase+HM *wt*, **F)** Kinase+HM S474D. A one-site binding model was used to fit curves and determine Kds.

4.1.9 Role of PKB regulatory elements on substrate specificity in cell lysates

PKB is known to have a large number of cellular substrates. An important unanswered question is how PKB is regulated to select specific substrates for phosphorylation. In order to answer this question, we designed an *in vitro* assay in collaboration with Dr Mohamad-Ali Fawal and Dr Nabil Djouder, head of the Growth Factors, Nutrients and Cancer group (CNIO, Madrid). We prepared soluble cell extracts of unstimulated (starved) human HeLa cells. The starvation of the cells is required to downregulate the activity of all the growth factor receptor downstream effectors, including PKB and its substrates. We then added the different PKB constructs containing or lacking the different regulatory elements and monitored PKB-dependent phosphorylation of several known substrates, using phospho-specific antibodies.

In order to explore the main cellular processes that PKB regulates we chose the following four substrates: FOXO for survival, GSK3 for metabolism, p27 for proliferation and TCS2 for cell growth (Fig. 4.10).

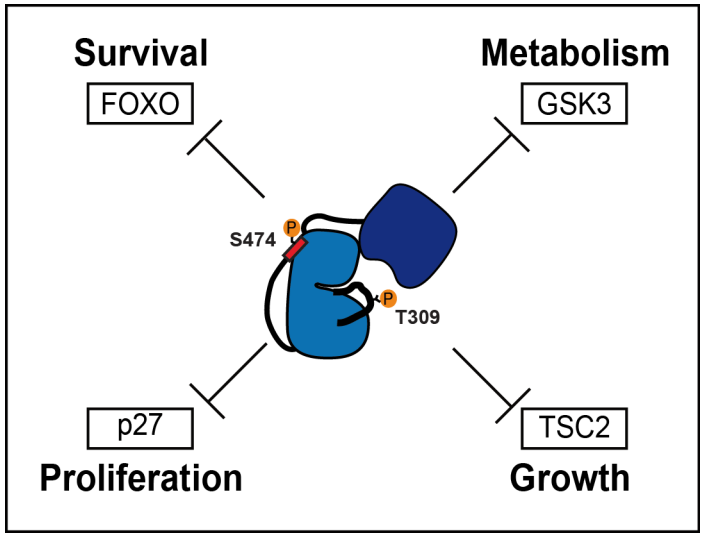

Fig. 4.10 PKB substrates chosen for substrate specificity experiments. Blocking arrows indicate that PKB-mediated phosphorylation of these proteins leads to their inhibition. By their PKB-mediated regulation, each substrate is involved in the activation of specific cellular processes here highlighted.

Interestingly, we observed that some of the regulatory elements of PKB have distinct effects on different substrates. In line with our activity studies presented above (section 4.1.9), we find no significant phosphorylation of substrates in absence of T309 phosphorylation (Fig. 4.11). On the other hand for FL PKB the S474D mutation is required to phosphorylate FOXO3a, but is essential for phosphorylation of GSK3. Strikingly, in absence of the PH domain, the S474D mutation is no longer required for GSK3 phosphorylation. Furthermore, TSC2 phosphorylation is only observed in absence of the PH domain. On the other hand, p27 required the simultaneous removal of the PH domain and the phospho mimetic mutation S474D (Fig. 4.11A). We also performed the same experiments with unphosphorylated and phosphorylated PKB FL constructs in presence of orthovanadate, a phosphatases inhibitor, to preserve the phosphorylation of the PKB substrates by inhibiting endogenous phosphatases present in cell lysate mixture. In these conditions, we monitored only the phosphorylation level of FOXO and GSK3 and, surprisingly, the substrate specificity phosphorylation is lost. In fact, in presence of pT309 FL wt and pT309 FL S474D, FOXO is not anymore phosphorylated, whereas GSK3 show phosphorylation (Fig.4.11B).

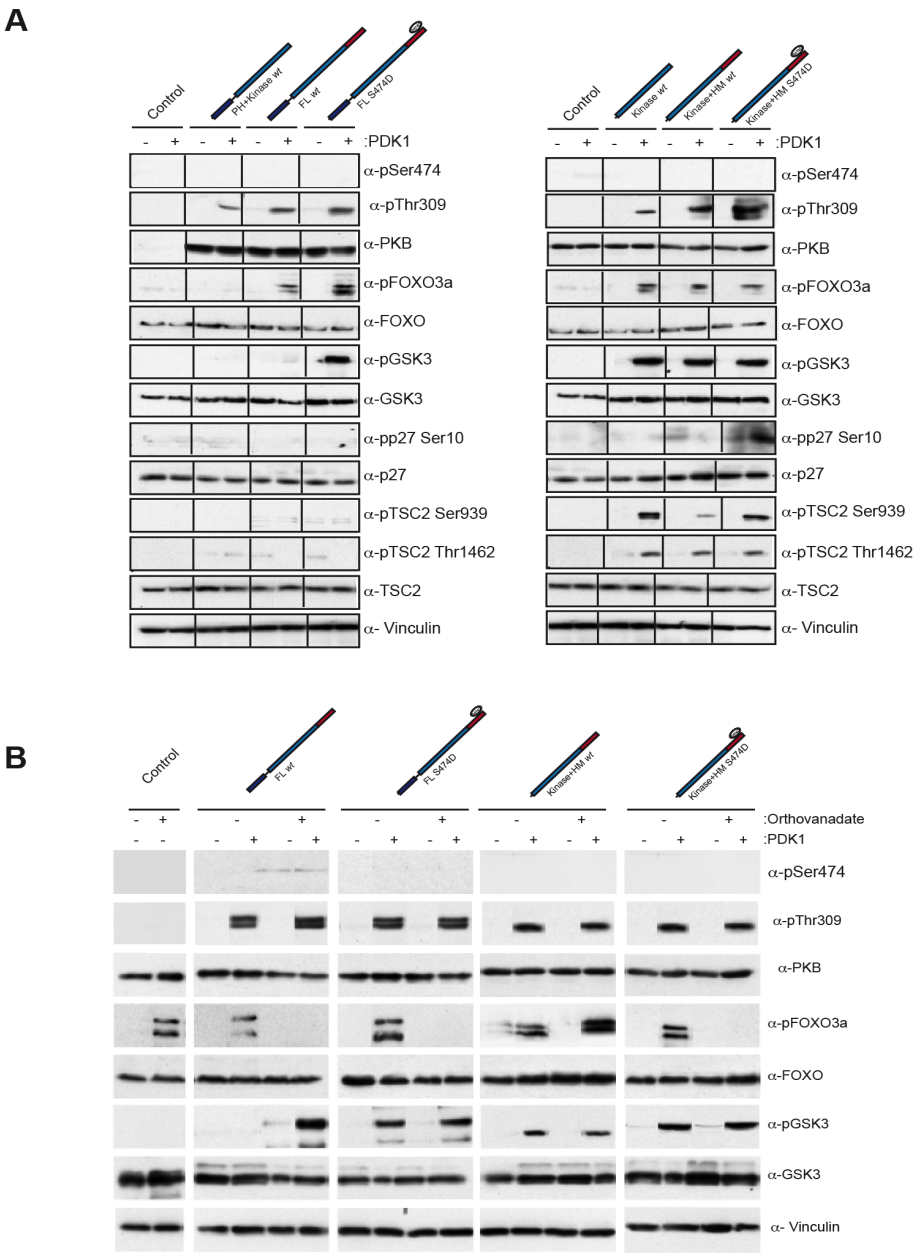

Fig. 4.11 hPKBβ substate specificity in cell lysates. A) PKB- mediated phosphorylation level of FOXO, GSK3, p27 and TSC2 are measured in presence of PKB constructs, which differ for the length and for their phosphorylation state (+/- PDK1). **B)** Phosphorylation level of FOXO, GSK3 and TCS2 in presence of orthovanadate. In all the experiments the level of phosphorylation is detected by western blotting using specific anti-phospho antibodies (α-p). Specificy antibodies (α) for each substrate and PKB are used to control the relative loaded amount. α-Vinculin= loading control of cell extracts.

4.2 FAK

4.2.1 Screening of a fluorinated compound library by NMR

In collaboration with Ramón Campos and Blanca López of the Spectroscopy and NMR unit at the CNIO, we performed ^{19}F-NMR based screening to detect binding of low molecular weight compounds (referred to as fragments: Mw < 300 Da) to FAK 31-405 *wt*, corresponding to the FERM domain of Focal Adhesion Kinase. The Spectroscopy and NMR Unit has assembled a collection of 371 fluorinated fragments with good solubility in aqueous buffer. The fragment-library is screened in pools eight compounds with well-separated 19-F signals.

Hits FERM	Chemical structures
1:	
2:	
3:	
4:	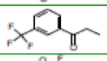
5:	
6:	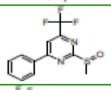
7:	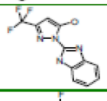
8:	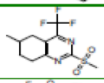
10:	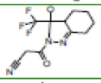
11:	

Hits FERM	Chemical structures
12:	
14:	
15:	
16:	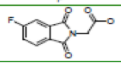
17:	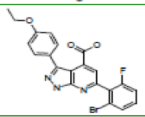
18:	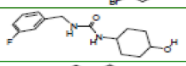
19:	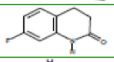
TAH:	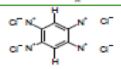
TP-160:	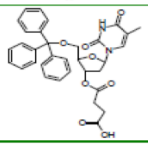

Tab 4.3 Summary of the compounds tested by SPR to measure the binding to FERM domain. Red numbering refears to hits from 19F-NMR screening. Blue numbering refears to compounds identified by computer modelling screening and remarked in literature.

Using 1D ^{19}F NMR spectroscopy we were able to monitor the binding of the compounds present in each cocktail to the FERM domain by consecutive additions of protein (at fragment:protein ratios of 100:1, 50:1 respectively) to each of the cocktails and following-up the decrease of intensity of the fluorine signal for the potential binders. 17 hits for the FERM domain (5.1%) were identified in the fluorine primary screening.

Thereafter, the individual positive hits were prepared at 100 µM each in PBS-1x, 10% D_2O and two independent NMR experiments were run for hit confirmation: a) ^{19}F-NMR spectrum (1D and 1D with a CMPG T_2 relaxation filter of 200/400ms (for CF/CF3) that allows a further decrease of signal intensity due to relaxation during this time) at successive additions of protein (typically five consecutive protein additions from a 100:1 hit:protein ratio up to a final 20:1 hit:protein ratio were done) (Fig.4.11A) and b) ^{1}H detected NMR spectrum such as STD and WaterLOGSY at the highest protein:fragment ratio (1:20) (Fig.4.11B).

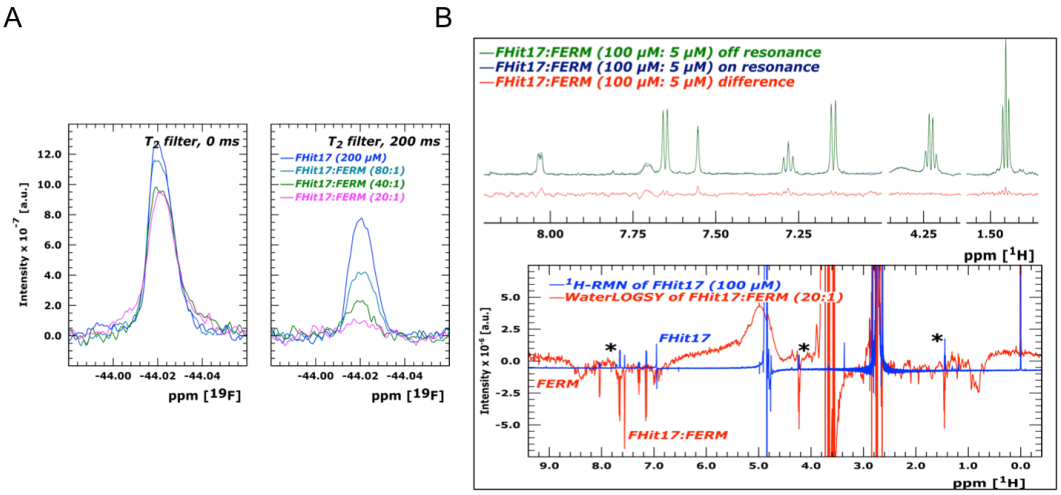

Fig.4.12 A) ^{19}F-NMR signal of Hit17 (blue) recorded without (left) and with (right) a 200 ms T_2 filter. Consecutive additions of FERM (with a protein:fragment ratio of 1:80 up to 1:20) result in a decrease of the intensity of the fragment fluorine signal. The decrease of the intensity is more clearly observed with the T_2 filter. **B)** 1H-NMR spectrum of Hit17 and FERM at a 20:1 fragment:protein ratio. STD NMR (upper panel) and WaterLOGSY (lower panel). STD NMR measures the decay of the intensity of the signals of a protein bound compound after selective saturation of protein protons. WaterLOGSY measures the selective intermolecular magnetization transfer from water via protein (protein-bound water, exchanging protons) to temporarily binding ligands. Protons of binding ligands are of the same sign as protein signals whereas non-binding compounds give signals of opposite sign.

4.2.2 Validation of hits by Surface Plamon Resonance

Surface plasmon resonance (SPR) has been used to monitor the binding of the hits summarized in Tab 4.3 to the FERM domain. In addition to the hits confirmed by titration NMR experiments, we included two compounds reported to bind the FERM domain: 1,2,4,5-Benzenetetraamine Tetrahydrochloride (TAH) (Golubovska V. M *et al*, 2008) and 5'-O-Tritylthymidine 160 (TP-160) (Golubovskaya V. *et al*, 2013). Both compounds were identified by virtual screening. They are predicted to target the autophosphorylation site Y397 (TAH) or the N- terminal FERM domain. FERM was immobilized onto a CM5 sensor chip using standard amine coupling chemistry, as described in Materials and Methods. Individual fragments were tested at 50 μM. The SPR data was solvent corrected and the steady-state responses normalized by the molecular weight of the fragments (Fig. 4.13A). Only four hits showed a response higher than 4RU/MW, corresponding to Hit17, Hit18, TAH and TP160 (Fig. 4.13A). Hit 17 showed the highest SPR response; therefore we determine the dissociation constant by SPR by passing increasing concentrations of hit 17 (from 31.25μM up to 2mM) over the immobilized FERM. The fit of the average steady-state responses (over 5s, 10 s before the end of the hit injection) to a 1:1 steady-state affinity model results in Kd of 66.7 μM (Fig. 4.13B).

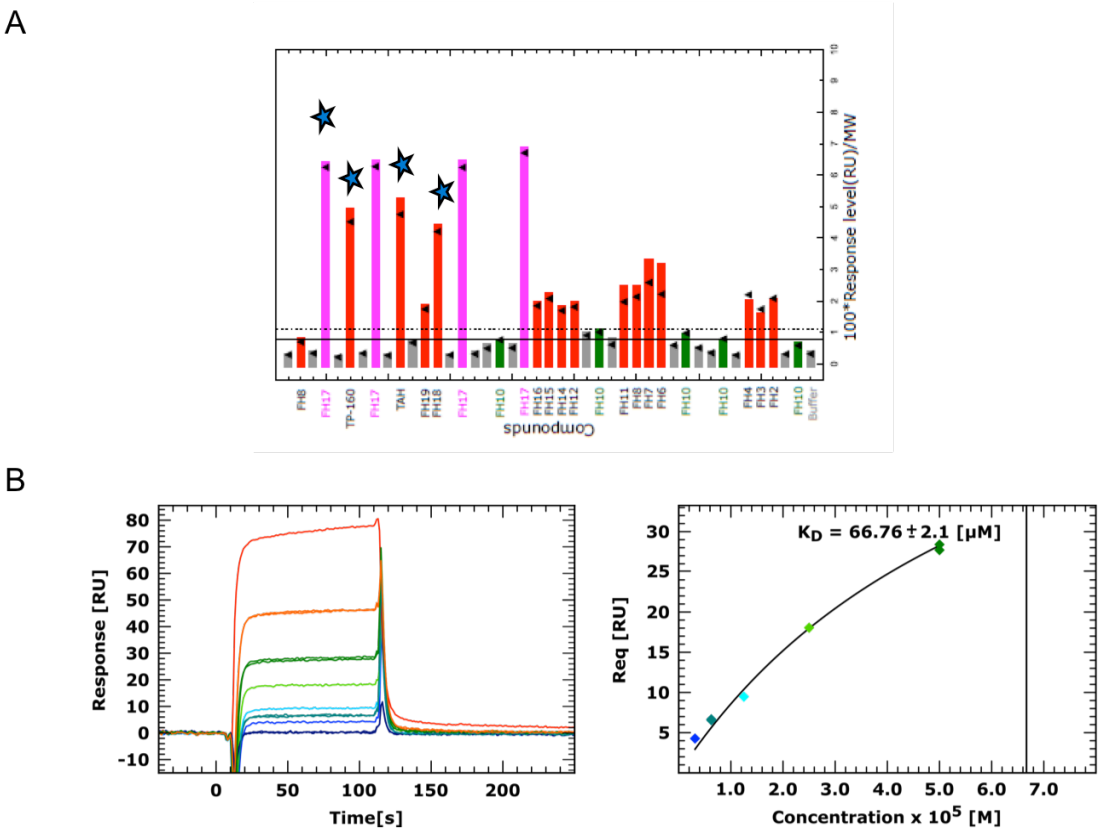

Fig. 4.13 A) SPR responses for the hits analyzed. The SPR signal was normalized to the molecular mass of each compound. Red bars correspond to the hits chosen for soaking of FERM crystals. **B)** Sensorgrams for the hit17:FERM interaction (left panel). Steady-state responses versus the hit17 concentration (right panel) and fitting to the 1:1 steady-state affinity model (continuous curve), indicating a Kd of 66.76 µM.

4.2.3 Crystallization of the FERM domain and soaking with fragments identified by NMR

We crystallised the FAK FERM domain as explained in Materials and Methods. Crystals grew after two days. We optimised the PEG4000 and $MgCl_2$ concentration and found optimal crystallization at 19% PEG4000 and 325mM $MgCl_2$ (Fig. 4.14).

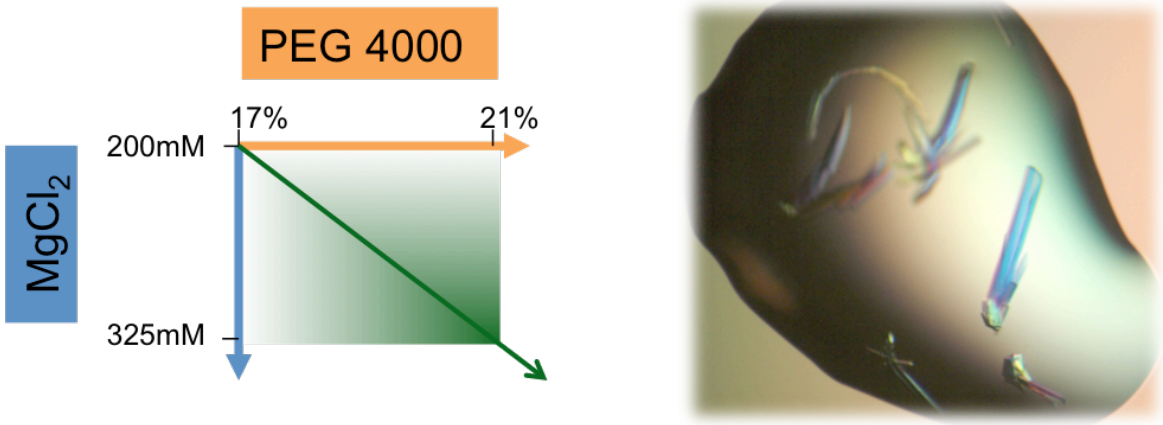

Fig. 4.14 FAK 31-405 *wt* crystals. Bigger size crystals were obtained at higher concentration of precipitant and salt (green arrow) after 2-3 days after drops setting.

For soaking experiments of FERM crystals we selected fragments hits that showed a response higher than 4RU/MW in the SPR measurements. For soaking, single crystals were transferred to a drop contianing a cryo-protecting buffer in addition to the crystallisation components (see Materials and Methods) and 10mM of fluorinated compound, and incubated at 20°C for 5 hours. Soaked crystals were flash-frozen in liquid nitrogen. TP160 displayed low solubility in the crystal buffer condition, and the precipitation observed affected the freezing step. Therefore, for this compound, we had to wash the soaked crystal in a drop of a cryo-protecting buffer containing only 1mM compound, which was the highest concentration where precipitation was not observed.

4.2.4 Identification of electron density for positive hits

Diffraction data was collected at beamline XO6SA (SLS) as described in Material and Methods. Data was processed using iMOSFLM 7.0.9 (Battye *et al*, 2011) and scaled using SCALA (Evans, 2006). Crystals belong to the P21 spacegroup with approximate cell dimensions illustrated in Tab. 4.4. Structure refinement was performed with iterative cycles of computational refinement using Refmac5 (Murshudov *et al*, 1997) and manual rebuilding using Coot (Emsley and Cowtan, 2004). For details on data processing and refinement, see Tab. 4.4.

The refined structures were inspected for the presence of large peaks in the Fo-Fc difference electron density maps as well as unmodelled peaks in the 2Fo-Fc electron density maps. Significant electron density peaks were only observed for crystals that were soaked with Hit17 and TAH.

Hit 17- The resolution of the FERM structure in presence of Hit 17 was of 2.6Å (Tab. 4.4). We attempted to place the fluorinated compound manually into the density, using Coot. As shown in Fig. 4.15, the density for the compound is not very clear and we could not conclusively define the orientation of Hit17. Therefore, we consider two potential binding modes (Fig. 4.15). The first consists in the Hit 17 binding into the pocket through the methoxy ethane group (Pose 1), whereas the second one through the 1-fluoro-5-bromobenzene ring (Pose 2). Comparing the chemical interactions that we can observe in the different binding modes, does not clearly favour one of the poses. In the Pose 1, the methoxy ethane group establishes hydrophobic interactions with Leu197, Met183, Val 196 and Tyr180. In addition, a salt bridge between the acidic group of the compound and the nitrogen of the carboxamide from the Asn193 takes place. In the Pose 2, hydrophobic interactions with Asn193, Met 183 and Val196 are established by the 1-fluoro-5-bromobenzene group, which also forms π-π stacking interactions between the phenyl ring of the fluorobrominebenzene and Tyr180. Moreover, the carboxylic group of the compound interacts with the nitrogen of the backbone of Arg184 (Fig 4.15).

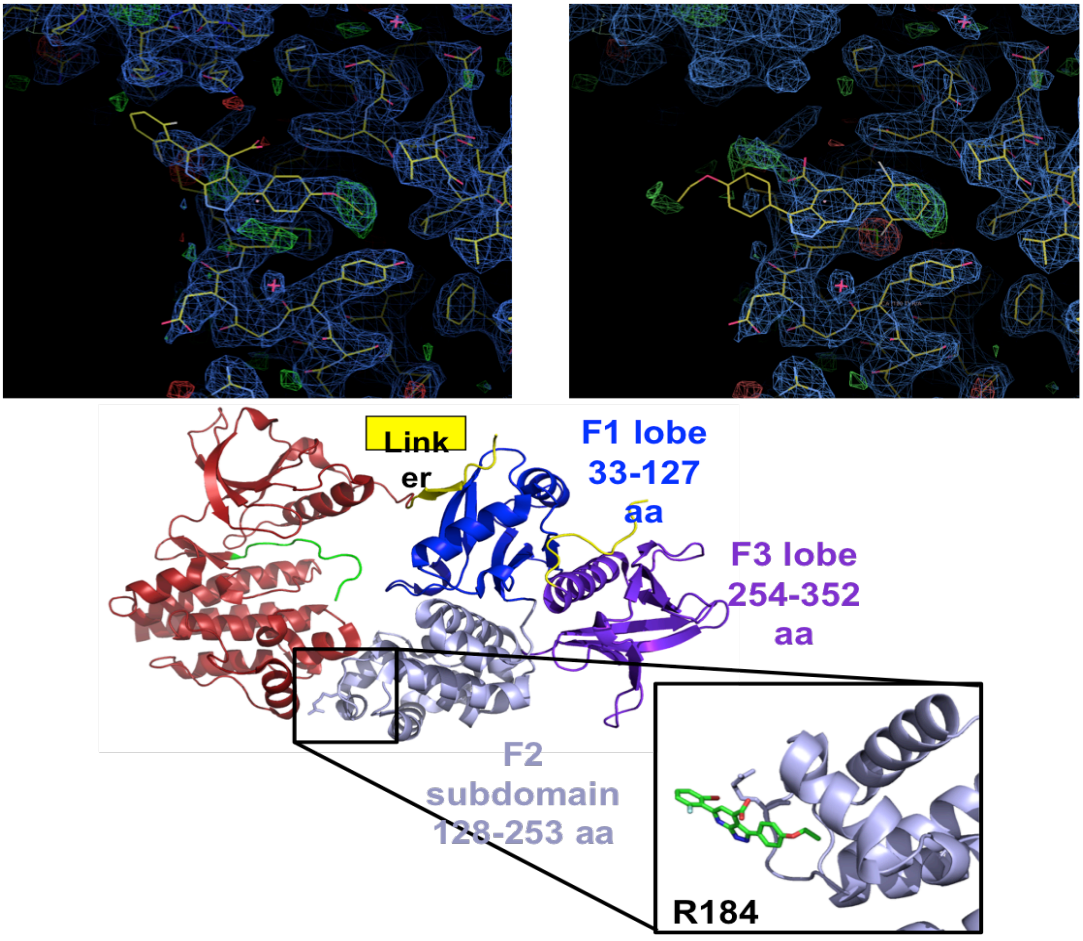

Fig. 4.15 FERM: Hit17 complex. In the upper panel, we compare the two potential poses of binding for Hit17. The 2Fo-Fc (blue) at 1 sigma and the Fo-Fc at 2.8 sigma (green for positive and red for negative density) maps are shown after refinement with the compound in the respective pose. Water molecules are labelled with a red cross. In the bottom panel, the location of Hit17 with the respect to the autoinhibited FERM+kinase structure (pdb code: 2J0J) is shown.

TAH- The density was observed in two different crystals. The resolution of the FERM structure in presence of TAH was 3.1Å and 3.4 Å respectively (Tab. 4.4). TAH electron density is located at the F1 lobe of the FERM domain, close to the site that interacts with linker residues containing the autophosphorylation site Y397. TAH closely

interacts with Cys74 and also contacts linker residue Ile400. FERM crystallizes as a dimer and interestingly TAH is present only in the dimer where the linker of the protein is well ordered, suggesting that the linker is increasing the binding affinity (Fig 4.16).

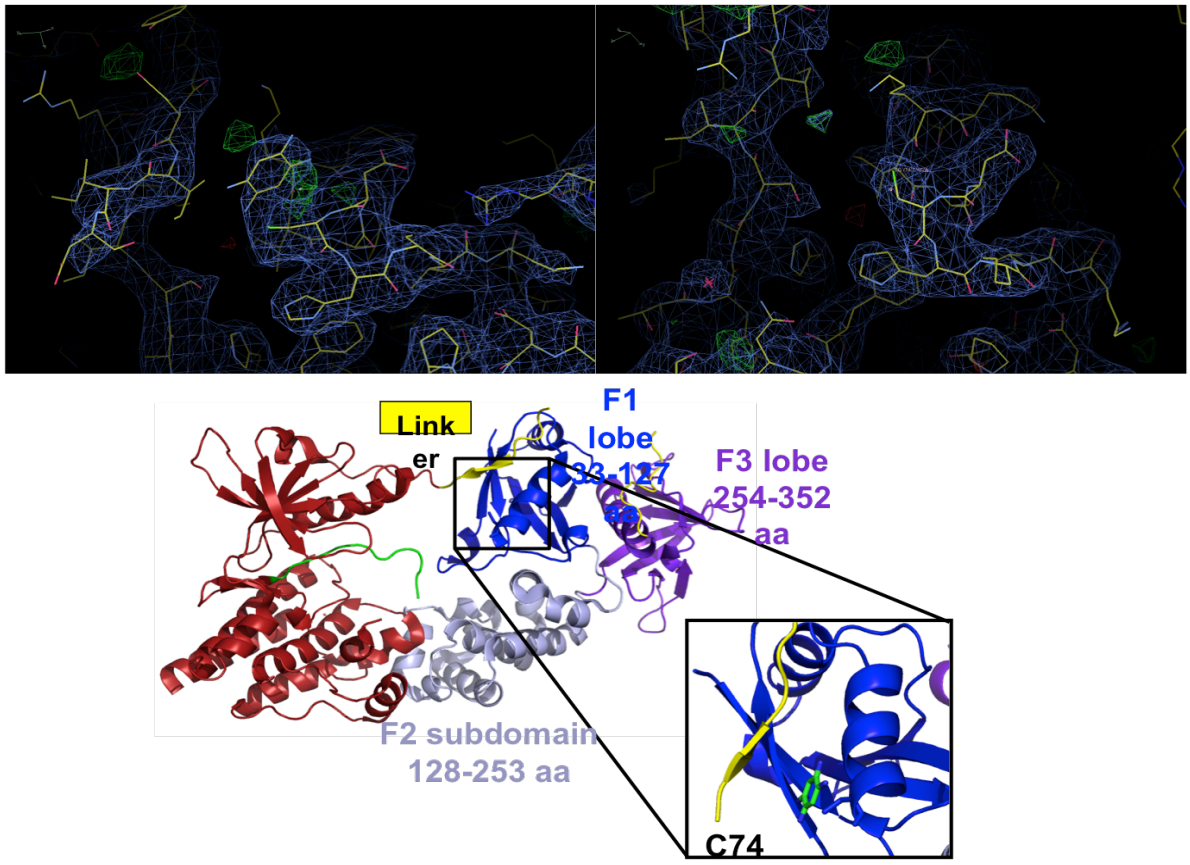

Fig. 4.16 FERM:TAH complex representation. In the upper panel, we compare the TAH interaction in the two FERM molecules in the asymmetric unit, where the linker is present (left) or absent (right). The 2Fo-Fc (blue) at 1 sigma and the Fo-Fc at 2.8 sigma (green for positive and red for negative density) maps are shown. The density corresponding to TAH is present only when the linker is well ordered (upper left panel). In the bottom, we show where TAH binds with respect to the autoinhibited FERM+kinase structure of FAK.

	FERM + compound 17	FERM + TAH
Data set name	**2A1 w1**	**2C5**
Space group	$P2_1$	$P2_1$
Cell dimensions *a, b, c* (Å) α, β, γ (°)	 45.0, 147.5, 69.0 90.00, 96.6, 90.00	 46.0, 148.9, 69.8 90.00, 94.6, 90.00
Wavelength (Å)	1.0	1.0
Resolution (Å)[a]	73.75-2.48 (2.74-2.6)	74.63-3.63 (3.63-3.44)
Completeness (%)[a]	99.7 (99.7)	99.4 (99.4)
R_{sym} (%)[a]	7.2 (41.0)	7.6 (24.6)
I/σI[a]	6.9 (1.8)	4.9 (1.9)
Redundancy	3.4 (3.4)	3.4 (3.4)
Refinement	**Run 7**	**Run 4**
Resolution (Å)	2.6	3.44
No. of reflections	92257	92257
Rwork/Rfree (%)	19.58/25.46	19.58/25.46
R.m.s. deviations Bond lengths (Å) Bond angles (°)	 0.0139 1.6570	 0.0139 1.6570

Tab 4.4 Data collection and refinement statistics for FERM: Hit17 and FERM:TAH. The dataset was collected on one single crystal. Highest resolution shell is shown in parentheses.

Discussion

5.1 PKB

5.1.1 Multiple levels of PKB regulation

As a member of the AGC kinase family, PKB possesses functional domains other than the kinase core, which are involved in regulating kinase activity and localization. In fact, activation of PKB is regulated at different levels and it involves phosphorylation of two highly conserved regulatory motifs: the activation loop (also known as T-loop) in the catalytic domain and the HM motif. In PKB, the PDK1 dependent- phosphorylation of the T309 in the T loop leads to a partial activation, and phosphorylation of S474 in the HM motif by mTORC2 is required for maximal activity (Sarbassov *et al*, 2005).

The presence of a PH domain with high affinity for PIP_3, induces a PKB conformational change and enables an easier accessibility of the T309 for PDK1 phosphorylation (Calleja *et al*, 2007). On the other hand, S6K and SGK do not possess a PH domain, but their regulation is still mediated by PIP_3, which triggers a signalling cascade, leading to the phosphorylation of the HM motif. Nevertheless, this phosphorylation alone is not sufficient for their activation, but it stimulates phosphorylation of the activation loop by PDK1 (Biondi *et al*, 2001). Uniquely among the AGC kinases, PDK1 lacks a C-terminal HM motif, although its N- term lobe hydrophobic groove possesses a region named PDK1-interacting fragment (PIF) pocket in its catalytic domain, which directly interacts with phosphorylated hydrophobic motifs, including those of S6K and SGK (Biondi *et al*, 2000). In the case of atypical PKC and PKN isoforms, the presence of an acidic phospho-mimetic Asp or Glu residue in the HM motif instead of a phosphorylatable Ser or Thr residue, seems still to interact with the PIF pocket of PDK1, promoting phosphorylation and activation and thereby bypassing the need for the phosphorylation of the hydrophobic motif (Biondi *et al*, 2000).

Moreover, it has been shown that in tissues from mice expressing a mutant form of PDK1 that cannot bind PIP_3, PKB is still phosphorylated at the activation segment (Bayascas et al, 2008). Therefore, other mechanisms might operate to enable PKB and

PDK1 to interact at the membrane or there might be other mechanisms that do not require membrane association.

5.1.2 Role of the PH domain in PKB activity and regulation

Our data suggests a regulatory role for the PH domain on different levels. On the one hand, the PH domain reduces the rate of the PDK1-driven T309 phosphorylation and secondly, it has a direct inhibitory effect on PKB catalytic activity. Interestingly, we find that binding of PIP_3 to the PH domain is able to restore T309 phosphorylation efficiency.

Therefore, PKB PH domain would have, then, a dual function on PKB activation inhibitory, by the interaction with the Kinase domain, and stimulatory after binding with PIP_3. This feature has been reported also in previous work, where they also found active PKB both in cytosol and at the membrane (Andjelkovic M, et al, 1999).

Based on dynamic model (Calleja V *et al*, 2007), it was observed a PH-induced cavity in the same region of the PKB hydrophobic pocket. The location of this cavity appeared to be in the same region as the PKB hydrophobic pocket (binding site for PKB HM) described in the crystal structure of the isolated PKB kinase domain (Yang *et al*, 2002). Through this PH-induced cavity, the Trp 80 residue, located at its centre, was accessible from outside, whereas PKB remained in its inactive conformation. To explore the importance of the positioning of the Trp 80 in the PH-induced cavity, Calleja and colleagues took advantage of a specific PKB inhibitor, AKT inhibitor VIII. By docking of AKT inhibitor VIII in the PH-induced cavity, they saw that the association of the PH domain residue Trp 80 to AKT inhibitor VIII would block PKB in the inactive conformation, preventing Thr 308 accessibility for phosphorylation. This was confirmed by the crystal structure of PH+Kinase in complex with Inhibitor VIII, obtained in 2010 by Wu *et al*, 2010.

Moreover a dynamic model done using PKB Kinase+HM S474D crystal structure by Yang et al. (PDB code: 1O6K) showed that the HM passed right across the PH-induced cavity. Actually Phe 470 and Phe 473 were positioned at a binding distance from Trp80.

This result showed that the binding of the inhibitor was not dependent on the C- terminal part of PKB and indicated further that the HM and AKT inhibitor VIII could potentially be competing for a common or close binding site on the kinase domain. These interactions suggested a role for the HM motif in the regulation of PKB prior to its traslocation and S474 phosphorylation. To conclude, also the HM motif plays a dual role in the regulation of PKB activity. On one hand, it helps in maintaining the inactive conformation of PKB by locking the conformation and on the other hand would activate allosterically the kinase by rearranging the catalytic site (as reviewed in Calleja V et al 2009).

5.1.3 Role of the HM motif in PKB activity and regulation

From comparison between the inactive and the active structures of PKB kinase domain (Yang *et al*, 2002a- Yang *et al*, 2002b) the authors concluded that the role of Ser474 phosphorylation is to promote the engagement of the HM with the hydrophobic pocket in the N lobe of the kinase domain, promoting a disorder-to-order transition of the α B and αC-helix and that the αC-helix, in turn, by interacting with pThr309 restructures and orders the activation segment, generating an active kinase conformation. The view that the phosphorylated HM is the critical factor was supported by the observation that the sole T309 phosphorylation was insufficient to allow the reorganization of the catalytic site. Our data suggests that both the HM and T309 phosphorylation are essential in stabilizing an active PKB conformation (Fig. 4.8A). Moreover, previous work confirmed that the combination of pT309 and S474D mutation was at least 2 fold more active than the single pT309, like in our kinase assays (Huang X *et al*., 2003). However, we show that the unphosphorylated HM in conjunction with pT309 is sufficient for a substantial level of activity and that the HM phosphorylation further increases Kcat of PKB. This suggests that the unphosphorylated HM is able to interact with the hydrophobic pocket, albeit with lower affinity. This is in fact supported by comparison of PKA structure and PKB Kinase+HM structure (Fig.5.1). Most importantly, structural analysis shows that two conserved phenylalanine residues (F347 and F350 in the case of PKA) in this motif

participate in the anchoring to the core of the C-terminal end, interacting interact extensively with the hydrophobic pocket in PKB (Etchebehere L *et al,* 1997). The FXXF motif, where X are usually non- hydrophobic amino acids is conserved in PKA, which does not require HM phosphorylation for activation (Biondi *et al*, 2000).

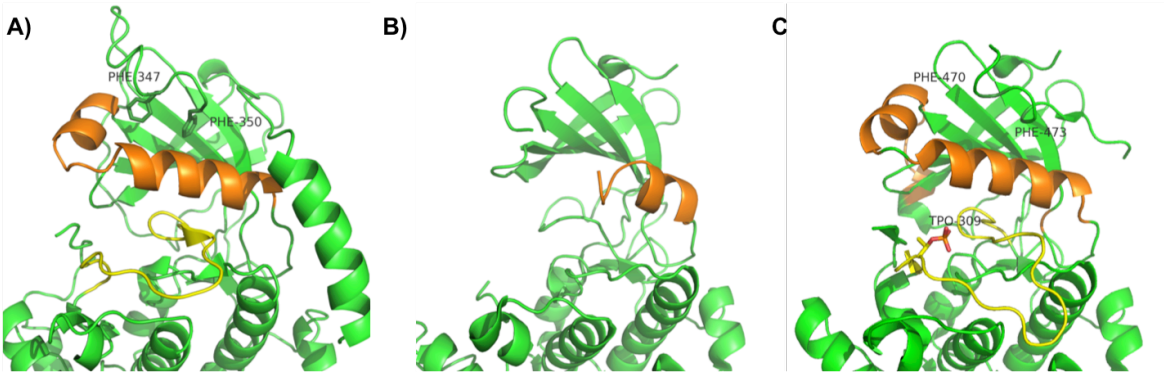

Fig. 5.1 Comparison between the N lobe structure of A) PKA, B)PKB Kinase+HM and C) PKB Kinase+HM S474D. In contrast with PKA structure, the crystal structures of PKB show that the residues corresponding to the region of the αB and αC helices (orange) are disordered in absence of Ser phosphorylation. This is correlated with weaker affinity of PKB unphosphorylated HM motif for the N lobe. In fact, in presence of a phospho-mimetic mutation S474D, the helices are ordered (from Yang *et al* 2002a). The activation loop is coloured in yellow.

5.1.4 PKB phosphorylation on substrate specificity

Our purified PKB proteins are able to phosphorylate cellular targets in soluble HeLa cell extracts. Our results fit with our in vitro studies, in that pT309 and the presence of the HM (for PH containing PKB) are essential for PKB activity. We find that the phosphorylation state of S474 and the PH domain affect the substrate selectivity of PKB. A role of S474 phosphorylation in substrate specificity is also supported by our finding that the S474D mutation lowers the affinity for the peptide substrate we used for data shown in Fig.4.8C. Such an effect could be amplified for an intact protein substrate. The role of S474 phosphorylation in substrate specificity has been investigated previously by studying

insulin stimulated cells that are unable to phosphorylate S474D, due to the lack of SIN1 in TORC2 (Jacinto E. *et al*, 2006). Jacinto and colleagues find that phosphorylation on S474 enhances FOXO phosphorylation but has no significant effect on GSK3 or TSC2. They conclude that S474 phosphorylation is not essential for GSK3 or TSC2, which mirrors our result for PKB lacking the PH domain. Since insulin stimulation triggers PI3K activity and generation of PIP_3, it is tempting to speculate that our results with ΔPH-PKB mimics a state of PKB bound to PIP_3 membranes. On the other hand, their finding that pS474 is required for efficient FOXO phosphorylation contrasts with our results. It is possible that the pS474 requirement for FOXO phosphorylation is further determined by secondary events that are not monitored in either of the two studies. In support of this, we find no FOXO phosphorylation if we perform our experiments in presence of the phosphatase inhibitor orthovanadate (Fig. 4.11B). This indicates the presence of an inhibitory phosphorylation event that prevents FOXO phosphorylation. Possibly the SIN1 deficiency in the Jacinto *et al* study, affects, through secondary effects, the phosphorylation state of that inhibitory site, however further studies will be required to fully explain these conflicting results. Importantly, our results support a view, where S474 phosphorylation and PH binding to PIP_3 membranes could determine the subset of PKB substrates that are phosphorylated, which could allow PKB to differentially trigger different cellular responses (see section 4.1.9).

Our results in Fig 4.11A further indicate that several cellular substrates can be phosphorylated by the isolated kinase of PKB (ΔPH, ΔHM). This contrasts our in vitro results that indicate no significant activity on a substrate peptide (Fig.4.8A). Possibly, in absence of the PH domain other cellular factors could aid the stabilisation of the αC helix, such as HM motifs of natively expressed PKB or other AGC kinases in HeLa cells.

5.1.5 PKB structure

Short after starting our study, a crystal structure of PKB PH+Kinase α in complex with an allosteric Inhibitor VIII was reported (Wu W. *et al*, 2010). From the analysis of the position assumed in this inhibited structure by Trp80, we pursue the idea of being able to crystallize the inactive form of PH+Kinase in absence of the inhibitor. In fact, comparing the position assumed by Trp80 in presence of Inhibitor VIII and the one assumed in the PH domain structure bound to Ins(1,3,4,5)P4 (IP_4) (Thomas C. *et al*, 2002), it is clearly visible that the side chain of the Trp80 changes significantly orientation. This suggests that the variable loop 3 (VL3) shifts in different ways to accommodate various ligands. Based on this, we wonder whether the Wu W. *et al* structure represent a native state of the protein and we thought that that without any ligand the indole group of Trp80 was able to establish stable hydrophobic interactions with the neighbouring residues, stabilizing the interactions between PH domain and Kinase domain in the N lobe adjacent to the ATP binding cleft. Unfortunately, this hypothesis turns out to be wrong, since despite all the crystallization conditions we tried, we did not manage to obtained crystals of PKB. An explanation can be that probably the PH without inhibitor is much more flexible on the loop and this does not allow to reach a stable state in the crystallization process. Another reason why we did not obtained crystals can sit in the homogeneity of the purified protein. In fact, the foundation for a successful crystallization experiment is laid at the purification stage. The purity, homogeneity and monodispersity of the protein sample are important parameters prior crystallization. Proteins should be as pure, homogeneous and free from structural and charge heterogeneity as possible, to aim the growth and the production of crystals suitable for x-ray structural analysis (Benvenuti M, et al, 2007). During the optimisation of PKB constructs purification protocol, we run the fractions of the main ion exchange chromatography peak in an IsoElectric Focusing gel (IEF) to check the heterogeneity of the samples. In this way, we clearly observed that the pure protein band seen in a SDS-PAGE gel hide a mixture of different isoelectric forms of the same protein. For most of the constructs we identified two main pools. These two species could be separated on ion

exchange and finally purified separately by a size-exlcusion step. A better separation of the different species can be obtained using isofocusing chromatography, were proteins are separated based on their pI. It would be interesting to try more crystallization screening, using the proteins with improved purity.

5.1.6 Suggested model of regulation

From previous work, the scenario of PKB activation is not easily disclosed, but several data suggest that different conformational states of PKB exist at various stages of PKB activation in vitro. Due to the fundamental role of PKB in many biological processes, the need for extensive safety levels has been established in order to prevent unwanted activation of the kinase. Canonically, under stimulation of PI3K and production of PIP_3, PKB is recruited to the inner surface of the plasma membrane by binding with the PH domain. Here, PKB is efficiently phosphorylated by PDK1 on T309, resulting in kinase activation (Bellacosa et al, 1998). On the other hand, the role of S474 phosphorylation has always been controversial. Previous work demonstrated not only the important role of S474 in fully activating PKB, but also that prior S474 phosphorylation boosted subsequent T309 phosphorylation by PDK1 (Dos D. Sarbassov et al 2005- Huang X et al, 2003). Our ELISA data (Fig. 4.7B) agree with this conclusion, confirming that S to D mutant is a better substrate for T308 phosphorylation. The two phosphorylation steps are tightly connected and interdependent, due to conformational changes in PKB induced by phosphorylation as already mentioned (Yang et al 2002)

Moreover, PH domain mutations that reduce significantly the interaction with PIP_3, did not preclude the full activation, meaning that the access of the activation loop is maintained open by other destabilisation of the interface between the PH domain and the kinase domain (Thomas CC, et al, 2002). There is, indeed, an emerging view that S474 precedes the phosphorylation of T309 and it is important for the recognition and activation of PKB by PDK1.

Based on our data we propose a model where PKB can follow two distinct pathways, one under the growth factor induced PI3K pathway, and the other under the mTORC2/DNA-PK one (Fig. 5.2). The first pathway follows mainly the canonical activation of PKB, where the PH domain binds to PIP_3 and PKB colocalizes with PDK1 to the plasma membrane and can be phosphorylated on T309 by PDK1. In this activation state, PKB leads to the phosphorylation of cellular substrates, for which the single T309 phosphorylation and the spatial removal of the PH domain is enough. On the same pathway, S474 can be also phosphorylated and specifically activate p27. Our lipid binding assays did not show a change in affinity once PKB is phosphorylated on both T309 and S474, therefore we do not embrace the theory of a release from the membrane under this state. In addition, in our model mTORC2/DNA-PK pathway triggers a membrane association-independent PKB activation. PDK1 is recruited to PKB after its phosphorylation on Ser474 via the PIF-pocket, hydrophobic docking motif on the PDK1 kinase. In this case, we speculate that phosphorylated S474 binds to the PIF pocket of PDK1 forming a complex of high binding affinity. In this state PDK1 can phosphorylate T309 in a membrane independent manner. In this state PKB is able to specifically activate GSK3. This was showed, at some extent also in other works, in which PKB T309 phosphorylation and GSK3 phosphorylation were comparable with/without PI3K inhibitors treatments (Bozulic et al, 2008).

In contrast with our model, it had been previously showed that the PIF-binding pocket in PDK1 was essential for activation of S6K and SGK, but it did not appear to be a rate limiting for PDK1-mediated activation of PKB (Biondi et al, 2001). Moreover, knock in mutations that disrupt the PIF-pocket either in ES (embryonic stem) cells (Collins et al, 2003) or in mouse muscle (Bajascas et al, 2008), were able to abolish the activation of S6K and SGK, but did not markedly affected PKB. Consistent with this conclusion, the ablation of S474 phosphorylation and, therefore of the ability of PKB to bind PDK1 PIF-pocket, had little impact on PDK1-mediated PKB Thr309 phosphorylation. This was true in different mouse model knockout of the mTORC2 components Rictor (rapamycin-

insensitive companion of mTOR) (Shiota et al, 2006) Sin1 (stress-activated protein kinase-interacting 1) (Jacinto et al, 2006) or mLST8 (mTOR-associated protein, LST8 homologue) (Guertin et al, 2006). On the other hand, the physical association of PDK1 with PKB induced by reconstituted IFP (intensely fluorescent protein) was showed to be sufficient to produce T309 phosphorylation and activation of PKB independent of PI3K activation or membrane localisation. Moreover, that complex formation stabilized by reconstituted IFP also promoted PKB S474 phosphorylation (Ding Z et al, 2010). More recently, PKB resulted to be resistant to PDK1 inhibitors whereas ablation of mTORC2 rendered PKB more susceptible to inhibition by PDK1 inhibitors (Najafov A et al, 2012. These data suggest that phosphorylation of Ser474 plays indeed a role in regulating Thr309 phosphorylation, and they highly support our suggested model. On the other hand, in vitro studies undertaken in the presence of lipid vesicles containing PIP_3 indicated that mutation of Ser474 to alanine had no effect on phosphorylation of Thr309 and activation of PKB (Biondi et al, 2001).

In the scenario, we still support the idea of this model where the activity of PKB is under the control of two different pathways, because this can allow maintenance of all the functions of PKB also when one of the pathway stops to work properly. For instance when the PI3K route is defective, the mTORC2/DNA-PK pathway can trigger the membrane association-independent PKB activation. In this respect, it was shown that PKB is specifically activated by DNA-PK –dependent S474 phosphorylation, after induction of double strands breaks (Bozulic et al, 2008). Further *in vitro* interactions studies between PDK1 and PKB in different states need to be done to add more evidences in support of this model.

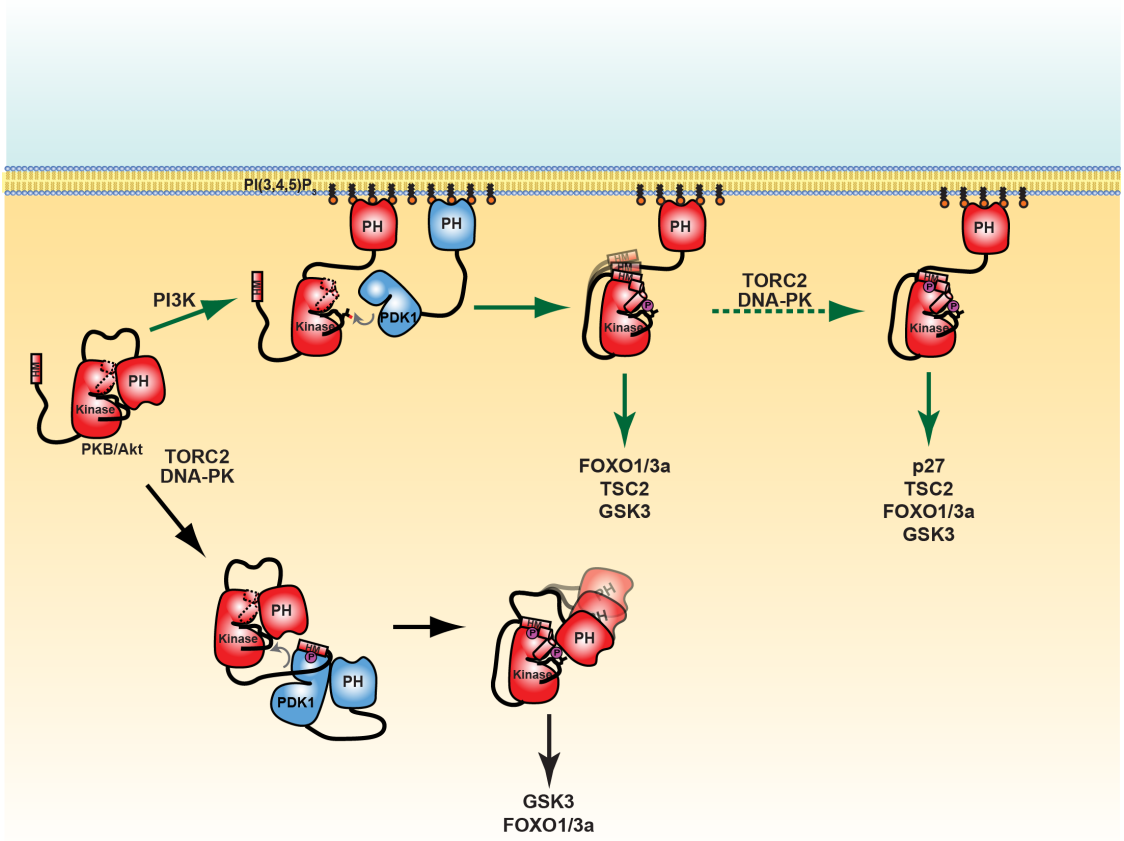

Fig. 5.2 Model for PKB regulation and activation. PKB can undertake two possible activation pathways, differencing by which regulatory site, T309 and S474, is phosphorylated first. According to the phosphorylation succession followed, PKB can specifically phosphorylate downstream cellular substrates.

5.2 FAK

5.2.1 Fragment-based drug discovery: a key contribution of structural biology

Fragment-based screening has rapidly become a proven technique to identify novel chemical starting points in drug discovery programs as an alternative to more traditional approaches based on chemical derived from high throughput screening (Erlanson D *et al*, 2004). The success of the fragment-based approach is buried, first, in the concept that chemical space can be more efficiently probed by screening collections of small fragments

rather than libraries of larger molecules. Fragments are low molecular weight compounds (typically 100-250Da) that can more easily find binding modes than larger druglike molecules (Congreve M. *et al*, 2008). Unalike druglike molecules, fragment hits show low binding affinities to their target protein (micromolar to millimolar range), as the Kd measurement of Hit17 confirmed (Fig. 4.13). Once a small molecule positive hit with affinity at uM levels has been found, more focused libraries can be rapidly improve by the introduction of chemical groups, which simultaneously improve affinity, and the pharmacokinetic properties of these molecules (Teague S *et al,* 1999). Furthermore, the rapid optimisation of fragment hits using structure-based design has established fragment-based drug discovery (FBDD) as a valuable strategy in the search for new drug molecules. Structural biology has been increasingly employed as a tool in the screening of fragments because it allows facing one of the main problems of the fragment-base drug discovery, consisting in the necessity of physical properties information of the ligand binding. In fact the structural information can be addressed to optimize efficiently the fragments hits (Harsthshorn M *et al*, 2005). Using this approach, four representative hits were selected and further optimise based on structure data, leading to the formulation of a novel cyclin dependent kinase inhibitor (CDK) (Wyatt P *et al*, 2008). Subsequently a structure-based approach using CDK2 crystallography resulted in the identification of analogous with good activity and ligand efficiency also for Aurora A. Optimization by crystallography screening lead to the formulation of an inhibitor against Aurora A (Howard S *et al*, 2009). Moreover, after a library screening of 20000 fragments, multiple fragments that bound to Heat shock protein 90 (Hsp90) were identified. Promising hits were submitted to co-crystallisation and soaking experiments and the fragment hits were rapidly optimised using a combination of in silico commercial analogue selection and structure-based design (Barker J *et al*, 2009).

5.2.2 Pose 1 *versus* Pose 2, which is the winner?

As shown in Results, the electron density for Hit 17 does not conclusively define the orientation of the Hit17 compound. Therefore, we consider two potential binding modes, and the chemical interactions that we can observe in the two poses, does also not clearly favour one or the other (Fig. 5.3). The best way to discriminate between the two binding modes would be to obtain better define electron density for Hit17. Since the affinity of Hit17 should be sufficient to obtain high occupancy of the bound compound, it is possible that the soaking protocol we applied does not allow efficient diffusion of the compound through the solvent channels in the crystal. Hence, co-crystallization could potentially result in improved electron density for Hit17. The resolution of 2.6 Å further limits a conclusive interpretation of the density: improvements in the crystallization condition to yield higher diffracting crystals could greatly facilitate the interpretation. As a potential aid to distinguish between the two possible modes we consider the anomalous signal of the bromine in Hit17. To approach this, data will be collected at 0.92 Å, instead of 1.0 Å, in order to hit the K absorption edge of bromine and be able to improve the calculation of phases by single-wavelength anomalous diffraction (SAD).

In an alternative approach, we plan to test fragments analogous of the hit17, available in the ETP library of CNIO, which either contain the ethoxy-benzene and central part or the 1-fluoro-5-bromobenzene ring with the central part of Hit17. Surface plasmon resonance analysis of these analogues should indicate which part of Hit17 is essential for binding. Once the binding pose is identified, the structural information should allow the design of modifications that increase the binding affinity. Strategy that could be followed includes replacement of displacement of a nearby water molecule interacting by hydrogen bonds with the backbone of the Glu 182 and Met183. The synthesis will be performed at the Experimental Therapeutic Programme in CNIO (headed by Joaquin Pastor).

Interestingly we observe that the allosteric pocket, where Hit17 interacts with FERM, lays on the contact interface between FERM and Kinase domain when the protein

is in the autoinhibited state (bottom panel of the Fig 4.15). This observation indicates that Hit17 could have an activating effect on Focal Adhesion Kinase instead of inhibitory. In order to turn Hit17 into an inhibitory compound it would have to be expanded to include also an anchor for the kinase domain. Such a bivalent compound could be expected to stabilize a closed and autoinhibited FAK conformation.

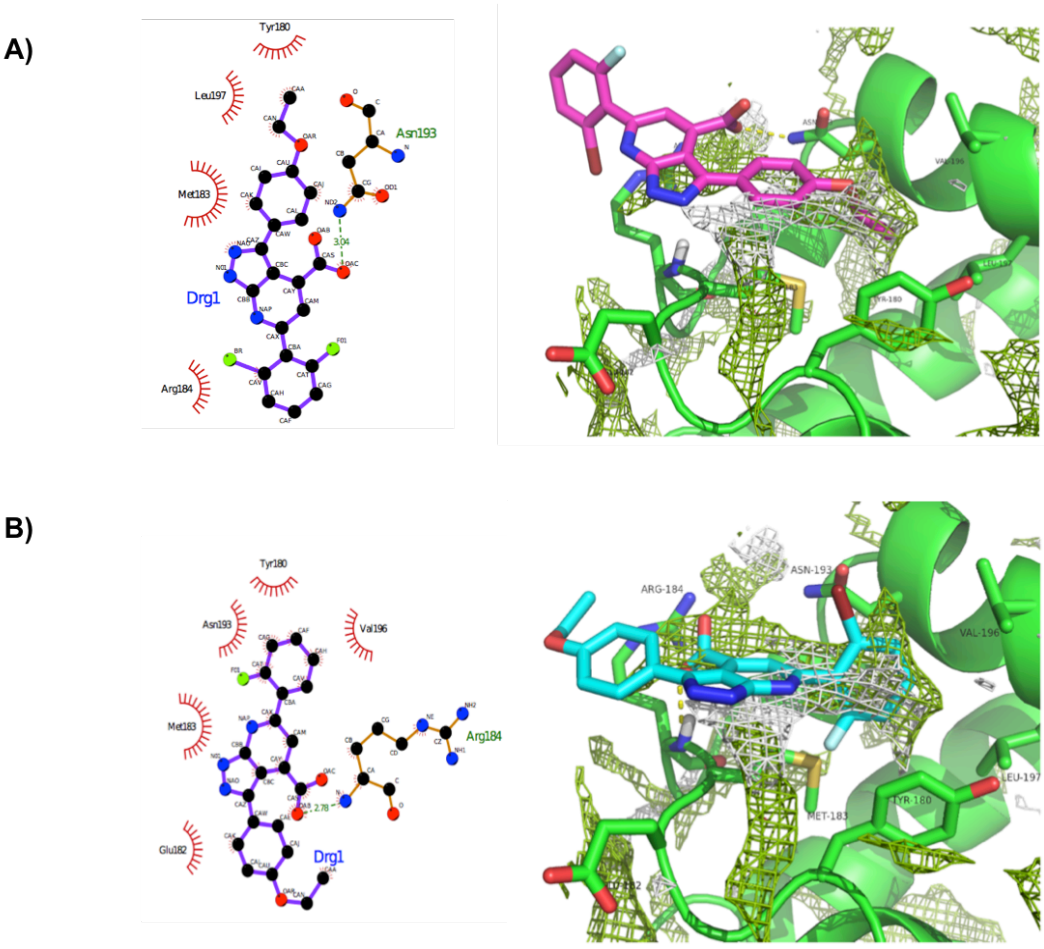

Fig. 5.2 Comparison of chemical interactions in the two binding modes of Hit17. A) Pose 1; B) pose 2. In the left panel, Ligplot+ analysis are shown, whereas in the right panel cGRILL analysis of the interactions.

Conclusions

1. PKBβ constructs expressed and purified in *E. coli* are well folded and catalytically active. The PH and HM regions stabilise PKB.
2. T309 phosphorylation and the presence of the HM are essential for PKB activity.
3. The S474D phosphomimetic mutation increases and the PH domain reduces catalytic turnover (Kcat) of PKB.
4. The S474D mutation affects Km of PKB.
5. The HM motif is essential for efficient PDK1 mediated T309 phosphorylation of PKB and the S474D mutation in the HM further enhances it.
6. The PH domain reduces the rate of the PDK1-driven T309 phosphorylation; PIP_3 binding to the PH domain restores efficient T309 phosphorylation.
7. T309 phosphorylation in PKB is essential for phosphorylation of all tested cellular substrates. The S474 phosphorylation state and the PH domain are involved in substrate specificity.
8. Our data fits a model where PKB can follow two distinct pathways, which potentially can result in activation of different substrates. In the first, PKB is initially phosphorylated on T309, after PKB binding to PIP_3 at the inner surface of cell membrane. In the second, PKB is firstly phosphorylated on S474 and therefore the HM preferably interacts to PDK1 PIF pocket, promoting T309 phosphorylation
9. The FERM domain of FAK can be targeted with small molecule fragment compounds.
10. We structurally characterise two positive fragment hits interacting with the FERM domain of FAK in specific pockets. Compounds with improved binding affinity can be designed on the structural information collected in this work.

Conclusiones

1. Las construcciones de PKBβ, expresadas y purificadas en *E. coli*, están bien plegadas y son activas a nivel catalítico. Las regiones del dominio PH y del motivo HM estabilizan PKB.
2. La fosforilación de la T309 y la presencia del motivo HM son esenciales para la actividad de PKB.
3. La mutación S474D, fosfomimética, aumenta la constante catalítica (Kcat) de PKB, mientras el dominio PH la reduce.
4. La mutación S474D influye sobre la Km de PKB.
5. El motivo HM es esencial para que la fosforilación de la T309 por PDK1 sea eficaz. En presencia de la mutación S474D, la eficacia es aun más significativa.
6. El dominio PH reduce la velocidad de la fosforilación de la T309 catalizada por PDK1; después de la interacción del dominio PH con PIP_3, se recupera la eficacia de fosforilación de la T309 .
7. La fosforilación de la T309 en PKB es esencial para la fosforilación de todos los sustratos de PKB examinados. El estado de fosforilación de la S474 junto con el dominio PH están involucrados en determinar la fosforilación de estos sustratos de manera específica.
8. Nuestros resultados sugieren un modelo donde PKB puede seguir dos rutas distintas, que potencialmente pueden dar lugar a la activación de diferentes sustratos. En la primera, PKB es fosforilada inicialmente en la T309, después de interaccionar con PIP_3 en la superficie interna de la membrana celular. En la segunda, PKB es fosforilada en primer lugar en la S474 y, por lo tanto, HM interactúa preferentemente con el bolsillo hidrofobico PIF de PDK1, promoviendo la fosforilación de la T309.
9. El dominio FERM de FAK puede ser diana para compuestos de pequeño tamaño.
10. Hemos obtenido resultados estructurales interesantes para dos fragmentos que interaccionan con el dominio FERM de FAK a nivel de bolsillos específicos. Se podrían diseñar compuestos más afines basándose en la información estructural recopilada en este trabajo.

References

Adams, J. a, McGlone, M. L., Gibson, R., & Taylor, S. S. (1995). Phosphorylation modulates catalytic function and regulation in the cAMP-dependent protein kinase. *Biochemistry*, *34*(8), 2447–54.

Alessi, D. R., Caudwell, F. B., Andjelkovic, M., Hemmings, B. a, & Cohen, P. (1996). Molecular basis for the substrate specificity of protein kinase B; comparison with MAPKAP kinase-1 and p70 S6 kinase. *FEBS Letters*, *399*(3), 333–8.

Andjelkovic, M., Jakubowicz, T., Cron, P., Ming, X., & Han, J. (1996). pleckstrin homology, *93*(June), 5699–5704.

Balendran, a, Casamayor, a, Deak, M., Paterson, a, Gaffney, P., Currie, R., … Alessi, D. R. (1999). PDK1 acquires PDK2 activity in the presence of a synthetic peptide derived from the carboxyl terminus of PRK2. *Current Biology : CB*, *9*(8), 393–404.

Baneyx, F. (1999). Recombinant protein expression in Escherichia coli. *Current Opinion in Biotechnology*, *10*, 411–421.

Barnett, S. F., Defeo-Jones, D., Fu, S., Hancock, P. J., Haskell, K. M., Jones, R. E., … Huber, H. E. (2005). Identification and characterization of pleckstrin-homology-domain-dependent and isoenzyme-specific Akt inhibitors. *The Biochemical Journal*, *385*(Pt 2), 399–408. doi:10.1042/BJ20041140

Benvenuti, M., & Mangani, S. (2007). Crystallization of soluble proteins in vapor diffusion for x-ray crystallography. *Nature Protocols*, *2*(7), 1633–51. doi:10.1038/nprot.2007.198

Biondi, R. M., Cheung, P. C., Casamayor, a, Deak, M., Currie, R. a, & Alessi, D. R. (2000). Identification of a pocket in the PDK1 kinase domain that interacts with PIF and the

C-terminal residues of PKA. *The EMBO Journal*, *19*(5), 979–88. doi:10.1093/emboj/19.5.979

Biondi, R. M., Kieloch, a, Currie, R. a, Deak, M., & Alessi, D. R. (2001). The PIF-binding pocket in PDK1 is essential for activation of S6K and SGK, but not PKB. *The EMBO Journal*, *20*(16), 4380–90. doi:10.1093/emboj/20.16.4380

Bobkova, E. V, Weber, M. J., Xu, Z., Zhang, Y.-L., Jung, J., Blume-Jensen, P., … Kariv, I. (2010). Discovery of PDK1 kinase inhibitors with a novel mechanism of action by ultrahigh throughput screening. *The Journal of Biological Chemistry*, *285*(24), 18838–46. doi:10.1074/jbc.M109.089946

Bozulic, L., Surucu, B., Hynx, D., & Hemmings, B. a. (2008). PKBalpha/Akt1 acts downstream of DNA-PK in the DNA double-strand break response and promotes survival. *Molecular Cell*, *30*(2), 203–13. doi:10.1016/j.molcel.2008.02.024

Brunet, A., Bonni, A., Zigmond, M. J., Lin, M. Z., Juo, P., Hu, L. S., … Greenberg, M. E. (1999). Akt Promotes Cell Survival by Phosphorylating and Inhibiting a Forkhead Transcription Factor University of California at San Diego, *96*, 857–868.

Calleja, V., Alcor, D., Laguerre, M., Park, J., Vojnovic, B., Hemmings, B. a., … Larijani, B. (2007). Intramolecular and intermolecular interactions of protein kinase B define its activation in vivo. *PLoS Biology*, *5*(4), e95. doi:10.1371/journal.pbio.0050095

Calleja, V., Laguerre, M., & Larijani, B. (2009). 3-D structure and dynamics of protein kinase B-new mechanism for the allosteric regulation of an AGC kinase. *Journal of Chemical Biology*, *2*(1), 11–25. doi:10.1007/s12154-009-0016-8

Calleja, V., Laguerre, M., Parker, P. J., & Larijani, B. (2009). Role of a novel PH-kinase domain interface in PKB/Akt regulation: Structural mechanism for allosteric inhibition. *PLoS Biology*, *7*(1), e17. doi:10.1371/journal.pbio.1000017

Carpten, J. D., Faber, A. L., Horn, C., Donoho, G. P., Briggs, S. L., Robbins, C. M., … Thomas, J. E. (2007). A transforming mutation in the pleckstrin homology domain of AKT1 in cancer. *Nature*, *448*(7152), 439–44. doi:10.1038/nature05933

Chan, T. O., Zhang, J., Rodeck, U., Pascal, J. M., Armen, R. S., Spring, M., … Feldman, A. M. (2011). Resistance of Akt kinases to dephosphorylation through ATP-dependent conformational plasticity. *Proceedings of the National Academy of Sciences of the United States of America*, *108*(46), E1120–7. doi:10.1073/pnas.1109879108

Cohen, P. (1992). Signal Integration at the level of protein kinases, protein phosphatases and their substrates. *Trends in Biochemical Sciences*.

Cohen, P. (1999). The Croonian Lecture 1998 . Identi ® cation of a protein kinase cascade of major importance in insulin signal transduction.

Currie, R. A., Walker, K. S., Gray, A., Deak, M., Casamayor, A., Downes, C. P., … Lucocq, J. (1999). and localization of 3-phosphoinositide-dependent protein kinase-1, *583*, 575–583.

Datta, S. R., Brunet, A., & Greenberg, M. E. (1999). Cellular survival : a play in three Akts Cellular survival : a play in three Akts, 2905–2927.

Ding, Z., Liang, J., Li, J., Lu, Y., Ariyaratna, V., Lu, Z., … Mills, G. B. (2010). Physical association of PDK1 with AKT1 is sufficient for pathway activation independent of membrane localization and phosphatidylinositol 3 kinase. *PloS One*, *5*(3), e9910. doi:10.1371/journal.pone.0009910

Frech, M., Andjelkovic, M., Ingley, E., Reddy, K. K., Falck, J. R., & Hemmings, B. a. (1997). High Affinity Binding of Inositol Phosphates and Phosphoinositides to the Pleckstrin Homology Domain of RAC/Protein Kinase B and Their Influence on Kinase Activity. *Journal of Biological Chemistry*, *272*(13), 8474–8481. doi:10.1074/jbc.272.13.8474

Frödin, M., Antal, T. L., Dümmler, B. a, Jensen, C. J., Deak, M., Gammeltoft, S., & Biondi, R. M. (2002). A phosphoserine/threonine-binding pocket in AGC kinases and PDK1 mediates activation by hydrophobic motif phosphorylation. *The EMBO Journal*, *21*(20),

Gabarra-Niecko, V., Schaller, M. D., & Dunty, J. M. (2003). FAK regulates biological processes important for the pathogenesis of cancer. *Cancer Metastasis Reviews*, *22*(4), 359–74. Retrieved from http://www.ncbi.nlm.nih.gov/pubmed/12884911

Gibeaux, R., & Knop, M. (2013). when yeast cells meet, karyogamy! *Nucleus*, *4*(3), 182–188.

Golubovskaya, V., Palma, N. L., Zheng, M., Ho, B., Magis, A., Ostrov, D., & Cance, W. G. (2013). A Small-Molecule Inhibitor, 5′-O-Tritylthymidine, Targets FAK And Mdm-2 Interaction, And Blocks Breast And Colon Tumorigenesis In Vivo. *Anti-Cancer Agents in …*, *13*(4), 532–545.

Grädler, U., Bomke, J., Musil, D., Dresing, V., Lehmann, M., Hölzemann, G., … Heinrich, T. (2013). Fragment-based discovery of focal adhesion kinase inhibitors. *Bioorganic & Medicinal Chemistry Letters*, *23*(19), 5401–9. doi:10.1016/j.bmcl.2013.07.050

Greenfield, N. (2007). Using circular dichroism spectra to estimate protein secondary structure. *Nature Protocols*, *1*(6), 2876–2890. doi:10.1038/nprot.2006.202.Using

Hannigan, G. E., Leung-Hagesteijn, C., Fitz-Gibbon, L., Coppolino, M. G., Radeva, G., Filmus, J., … Dedhar, S. (1996). Regulation of cell adhesion and anchorage-dependent growth by a new beta 1-integrin-linked protein kinase. *Nature*, *379*(6560), 91–6. doi:10.1038/379091a0

Harris, T. K. (2003). PDK1 and PKB/Akt: ideal targets for development of new strategies to structure-based drug design. *IUBMB Life*, *55*(3), 117–26. doi:10.1080/1521654031000115951

Hehlgans, S., Haase, M., & Cordes, N. (2007). Signalling via integrins: implications for cell survival and anticancer strategies. *Biochimica et Biophysica Acta*, *1775*(1), 163–80. doi:10.1016/j.bbcan.2006.09.001

Hers, I., Vincent, E. E., & Tavaré, J. M. (2011). Akt signalling in health and disease. *Cellular Signalling*, *23*(10), 1515–27. doi:10.1016/j.cellsig.2011.05.004

Hietakangas, V., & Cohen, S. M. (2007). Re-evaluating AKT regulation: role of TOR complex 2 in tissue growth. *Genes & Development*, *21*(6), 632–7. doi:10.1101/gad.416307

Hsuan, J. J., & Tan, S. H. (1997). Growth factor-dependent phosphoinositide signalling. *The International Journal of Biochemistry & Cell Biology*, *29*(3), 415–35. Retrieved from http://www.ncbi.nlm.nih.gov/pubmed/9202421

Huang, X., Begley, M., Morgenstern, K. a., Gu, Y., Rose, P., Zhao, H., & Zhu, X. (2003). Crystal structure of an inactive Akt2 kinase domain. *Structure*, *11*(1), 21–30.

Hunter, T. (1987). and One Protein Kinases Review, *50*(January), 823–829.

Hunter, T. (2000). Signaling--2000 and beyond. *Cell*, *100*(1), 113–27. Retrieved from http://www.ncbi.nlm.nih.gov/pubmed/10647936

Huse, M., & Kuriyan, J. (2002). The conformational plasticity of protein kinases. *Cell*, *109*(3), 275–82. Retrieved from http://www.ncbi.nlm.nih.gov/pubmed/12015977

Inoki, K., Li, Y., Zhu, T., Wu, J., & Guan, K.-L. (2002). TSC2 is phosphorylated and inhibited by Akt and suppresses mTOR signalling. *Nature Cell Biology*, *4*(9), 648–57. doi:10.1038/ncb839

Jacinto, E., Facchinetti, V., Liu, D., Soto, N., Wei, S., Jung, S. Y., … Su, B. (2006). SIN1/MIP1 maintains rictor-mTOR complex integrity and regulates Akt phosphorylation and substrate specificity. *Cell*, *127*(1), 125–37. doi:10.1016/j.cell.2006.08.033

Jo, H., Lo, P.-K., Li, Y., Loison, F., Green, S., Wang, J., … Luo, H. R. (2011). Deactivation of Akt by a small molecule inhibitor targeting pleckstrin homology domain and facilitating Akt ubiquitination. *Proceedings of the National Academy of Sciences of the United States of America*, *108*(16), 6486–91. doi:10.1073/pnas.1019062108

Kit, K. A. (2005). Supplemental Data SIN1 / MIP1 Maintains rictor-mTOR Complex Integrity and Regulates Akt Phosphorylation and Substrate Specificity, *126*, 1–3.

Klein, S., Geiger, T., Linchevski, I., Lebendiker, M., Itkin, A., Assayag, K., & Levitzki, A. (2005). Expression and purification of active PKB kinase from Escherichia coli. *Protein Expression and Purification*, *41*(1), 162–9. doi:10.1016/j.pep.2005.01.003

Kopec, A. M., & Carew, T. J. (2013). Growth factor signaling and memory formation: temporal and spatial integration of a molecular network. *Learning & Memory (Cold Spring Harbor, N.Y.)*, *20*(10), 531–9. doi:10.1101/lm.031377.113

Leevers, S. J., Vanhaesebroeck, B., & Waterfield, M. D. (1999). Signalling through phosphoinositide 3-kinases: the lipids take centre stage. *Current Opinion in Cell Biology*, *11*(2), 219–25.

Lehmann, O. J., Sowden, J. C., Carlsson, P., Jordan, T., & Bhattacharya, S. S. (2003). Fox's in development and disease. *Trends in Genetics : TIG*, *19*(6), 339–44. doi:10.1016/S0168-9525(03)00111-2

Lemmon, M. a, & Schlessinger, J. (2010). Cell signaling by receptor tyrosine kinases. *Cell*, *141*(7), 1117–34. doi:10.1016/j.cell.2010.06.011

Liang, J., Zubovitz, J., Petrocelli, T., Kotchetkov, R., Connor, M. K., Han, K., … Slingerland, J. M. (2002). PKB/Akt phosphorylates p27, impairs nuclear import of p27 and opposes p27-mediated G1 arrest. *Nature Medicine*, *8*(10), 1153–60. doi:10.1038/nm761

Lietha, D., Cai, X., Ceccarelli, D. F. J., Li, Y., Schaller, M. D., & Eck, M. J. (2007). Structural basis for the autoinhibition of focal adhesion kinase. *Cell*, *129*(6), 1177–87. doi:10.1016/j.cell.2007.05.041

Lindsley, C. W. (2010). The Akt/PKB family of protein kinases: a review of small molecule inhibitors and progress towards target validation: a 2009 update. *Current Topics in Medicinal Chemistry*, *10*(4), 458–77.

Manning, B., & Cantley, L. (2007). AKT/PKB Signaling: Navigating Downstream. *Cell*, *129*(7), 1261–1274. doi:10.1016/j.cell.2007.06.009.AKT/PKB

Manning, G., Whyte, D. B., Martinez, R., Hunter, T., & Sudarsanam, S. (2002). The protein kinase complement of the human genome. *Science (New York, N.Y.)*, *298*(5600), 1912–34. doi:10.1126/science.1075762

Najafov, A., Shpiro, N., & Alessi, D. R. (2012). Akt is efficiently activated by PIF-pocket- and PtdIns(3,4,5)P3-dependent mechanisms leading to resistance to PDK1 inhibitors. *The Biochemical Journal*, *448*(2), 285–95. doi:10.1042/BJ20121287

Najafov, A., Sommer, E. M., Axten, J. M., Deyoung, M. P., & Alessi, D. R. (2011). Characterization of GSK2334470, a novel and highly specific inhibitor of PDK1. *The Biochemical Journal*, *433*(2), 357–69. doi:10.1042/BJ20101732

Nicholson, K. M., & Anderson, N. G. (2002). The protein kinase B/Akt signalling pathway in human malignancy. *Cellular Signalling*, *14*(5), 381–95. Retrieved from http://www.ncbi.nlm.nih.gov/pubmed/11882383

Nolen, B., Taylor, S., & Ghosh, G. (2004). Regulation of protein kinases; controlling activity through activation segment conformation. *Molecular Cell*, *15*(5), 661–75. doi:10.1016/j.molcel.2004.08.024

Ohren, J. F., Chen, H., Pavlovsky, A., Whitehead, C., Zhang, E., Kuffa, P., … Hasemann, C. a. (2004). Structures of human MAP kinase kinase 1 (MEK1) and MEK2 describe novel noncompetitive kinase inhibition. *Nature Structural & Molecular Biology*, *11*(12), 1192–7. doi:10.1038/nsmb859

Pawson, T. (1997). Signaling Through Scaffold, Anchoring, and Adaptor Proteins. *Science*, *278*(5346), 2075–2080. doi:10.1126/science.278.5346.2075

Pawson, T., & Nash, P. (2000). Protein – protein interactions define specificity in signal transduction Protein – protein interactions define specificity in signal transduction, 1027–1047. doi:10.1101/gad.14.9.1027

Potter, C. J., Pedraza, L. G., & Xu, T. (2002). Akt regulates growth by directly phosphorylating Tsc2. *Nature Cell Biology*, *4*(9), 658–65. doi:10.1038/ncb840

Scheid, M. P., Marignani, P. A., James, R., & Woodgett, J. R. (2002). Multiple Phosphoinositide 3-Kinase-Dependent Steps in Activation of Protein Kinase B Multiple Phosphoinositide 3-Kinase-Dependent Steps in Activation of Protein Kinase B. doi:10.1128/MCB.22.17.6247

Schlaepfer, D. D., Hauck, C. R., & Sieg, D. J. (1999). Signaling through focal adhesion kinase. *Progress in Biophysics and Molecular Biology*, *71*(3-4), 435–78.

Steeg, P., & Abrams, J. (1997). Cancer prognostics: Past, present and p27. *Nature Medicine*, *3*, 222–234.

Toker, a. (2000). Akt/Protein Kinase B Is Regulated by Autophosphorylation at the Hypothetical PDK-2 Site. *Journal of Biological Chemistry*, *275*(12), 8271–8274. doi:10.1074/jbc.275.12.8271

Van Weeren, P. C., de Bruyn, K. M. T., de Vries-Smits, a. M. M., van Lint, J., & Burgering, B. M. T. (1998). Essential Role for Protein Kinase B (PKB) in Insulin-induced Glycogen Synthase Kinase 3 Inactivation: CHARACTERIZATION OF DOMINANT-NEGATIVE MUTANT OF PKB. *Journal of Biological Chemistry*, *273*(21), 13150–13156. doi:10.1074/jbc.273.21.13150

Watton, S. J., & Downward, J. (1999). A k t / P K B Iocalisation and 3' phosphoinositide generation at sites of epithelial cell-matrix and cell-cell interaction Sandra J. Watton and Julian Downward, 433–436.

Wu, W.-I., Voegtli, W. C., Sturgis, H. L., Dizon, F. P., Vigers, G. P. a, & Brandhuber, B. J. (2010). Crystal structure of human AKT1 with an allosteric inhibitor reveals a new mode of kinase inhibition. *PloS One*, *5*(9), e12913. doi:10.1371/journal.pone.0012913

Yang, J., Cron, P., Good, V. M., Thompson, V., Hemmings, B. a, & Barford, D. (2002). Crystal structure of an activated Akt/protein kinase B ternary complex with GSK3-peptide and AMP-PNP. *Nature Structural Biology*, *9*(12), 940–4. doi:10.1038/nsb870

Yang, J., Cron, P., Thompson, V., Good, V. M., Hess, D., Hemmings, B. a, & Barford, D. (2002). Molecular mechanism for the regulation of protein kinase B/Akt by hydrophobic motif phosphorylation. *Molecular Cell*, *9*(6), 1227–40.

Zhang, J., Yang, P. L., & Gray, N. S. (2009). Targeting cancer with small molecule kinase inhibitors. *Nature Reviews. Cancer*, *9*(1), 28–39. doi:10.1038/nrc2559